

UNIVERSITY of CALIFORNIA
Santa Barbara

Multi UAV Systems with Motion and Communication Constraints

A Dissertation submitted in partial satisfaction of the
requirements for the degree

Doctor of Philosophy

in

Electrical and Computer Engineering

by

Ketan D. Savla

Committee in charge:

Professor Francesco Bullo, Chair

Professor Emilio Frazzoli

Professor João Hespanha

Professor Bassam Bamieh

Professor Roy Smith

August 2007

The dissertation of Ketan D. Savla is approved.

Professor Emilio Frazzoli

Professor João Hespanha

Professor Bassam Bamieh

Professor Roy Smith

Professor Francesco Bullo, Committee Chair

June 2007

Multi UAV Systems with Motion and Communication Constraints

Copyright © 2007

by

Ketan D. Savla

To the memory of
my grandmother, *Hiruben Savla*
and my uncle, *Amratlal Kariya*

Acknowledgements

I am grateful to my advisors Francesco Bullo and Emilio Frazzoli for giving me utmost freedom. From them I have learned the importance of being organized and rigorous in research.

I would also like to thank Richard Murray and his group for the memorable summer at Caltech. Thanks also to Giuseppe and John for their collaboration during the course of my graduate studies.

I thank João Hespanha, Bassam Bamieh and Roy Smith for being in my committee.

I am thankful to my lab-mates for such a congenial work environment.

I thank Val (ECE) and Julie (ME) for their kind and immediate help in administrative issues.

I am indebted to all the professors and fellow students at IIT Bombay for the invaluable training and experience that I was exposed to.

I thank my grandfather, parents, brothers and other family members for their love and the sacrifices they have made for me. In the same league, I am indebted to Angelica for all that she has done for me.

Lastly, I am thankful to all my friends across the globe for their support and for their company in my non-academic activities.

Abstract

Multi UAV Systems with Motion and Communication Constraints

by

Ketan D. Savla

Unmanned Aerial Vehicle (UAV) technology holds great promise for various civilian and military applications. Cooperative control of a network of autonomous UAVs poses novel challenges because of the inherent constraints like non-holonomic motion, limited range communication, etc. In this dissertation, we present some recently-developed tools and strategies for motion coordination of UAVs. In particular, the focus is on algorithms for various coordination tasks such as vehicle routing to meet service demands, deployment over a region for surveillance and flying in flock-like formations.

We study minimum-time motion planning and routing problems for the Dubins vehicle, i.e., a nonholonomic vehicle that is constrained to move along planar paths of bounded curvature, without reversing direction. We consider the Traveling Salesperson Problem for the Dubins vehicle (DTSP): given n points on a plane, what is the shortest Dubins tour through these points and what is its length? We start by showing that the worst-case length of such a tour grows linearly with n and we propose a novel algorithm with worst-case performance within a constant factor approximation of the optimum. In doing this, we also obtain an upper bound on the optimal length in the classical point-to-point problem. We then study a stochastic version of the DTSP where the n targets are

randomly sampled from a uniform distribution. We show that the expected length of such a tour is of order at least $n^{2/3}$ and we propose a novel algorithm yielding a solution with length of order $n^{2/3}$ with high probability. We apply these results in a dynamic version of the DTSP: given a stochastic process that generates target points, is there a policy which guarantees that the number of unvisited points does not diverge over time? If such stable policies exist, what is the minimum expected time that a newly generated target waits before being visited by the vehicle? We propose a novel stabilizing algorithms such that the expected wait time is provably within a constant factor from the optimum. We obtain analogous results for \mathbb{R}^3 and extend various results to a double integrator vehicle model.

We also study a facility location problem for groups of Dubins vehicles, i.e., nonholonomic vehicles that are constrained to move along planar paths of bounded curvature, without reversing direction. Given a compact region and a group of Dubins vehicles, the coverage problem is to minimize the worst-case traveling time from any vehicle to any point in the region. Since the vehicles cannot hover, we assume that they fly along static closed curves called *loitering curves*. We present *circular loitering patterns* for a Dubins vehicle and for a group of Dubins vehicles that minimize the worst-case traveling time in sufficiently large regions. We do this by establishing an analogy to the disk covering problem.

Finally, we consider ad-hoc networks of robotic agents with double integrator dynamics. For such networks, the connectivity maintenance problems are: (i) do there exist control inputs for each agent to maintain network connectivity, and (ii) given desired controls for each agent, can one compute the closest connectivity-maintaining controls in a distributed fashion? The proposed solution is based on

three contributions. First, we define and characterize admissible sets for double integrators to remain inside disks. Second, we establish an existence theorem for the connectivity maintenance problem by introducing a novel state-dependent graph, called the *double-integrator disk graph*. Finally, we design a distributed “flow-control” algorithm to compute optimal connectivity-maintaining controls.

Contents

Acknowledgements	v
List of Figures	xii
1 Introduction	1
1.1 Background and related work	2
1.2 Summary of contributions	6
2 DTSP: The worst case	9
2.1 Problem setup: from the Euclidean to the Dubins Traveling Sales- person Problem	9
2.2 Lower bound for the DTSP	11
2.3 The Alternating Algorithm	14
2.4 Analysis of the algorithm	16
2.5 Summary	19
3 DTSP: The stochastic and the dynamic case	20
3.1 Lower bound for the stochastic DTSP	21
3.2 The basic geometric construction	22
3.3 The Recursive Bead-Tiling Algorithm	23
3.4 Analysis of the algorithm	25
3.5 The DTRP for a single vehicle	34
3.6 The DTRP for multiple vehicles	39

3.7	Summary	40
4	TSPs for a double integrator	42
4.1	Setup and worst-case DITSP	43
4.2	The stochastic DITSP	46
4.3	The DTRP for double integrator	59
4.4	Extension to the TSPs for the Dubins vehicle in \mathbb{R}^3	62
4.5	Summary	63
5	The coverage problem for loitering Dubins vehicles	64
5.1	Problem Setup and notations	65
5.2	Reachable set for the Dubins vehicle	68
5.3	The single vehicle case	72
5.4	The single team case	76
5.5	The multiple uniform team case	79
5.6	Summary	82
6	Maintaining limited-range connectivity among second-order agents	84
6.1	Preliminary developments	85
6.2	Connectivity constraints among second-order agents	96
6.3	Distributed computation of optimal controls	105
6.4	Simulations	108
6.5	Summary	110
7	Conclusions	111
	Bibliography	113
A	On the proof of Theorem 2.4	120
A.1	Dubins classification of optimal curves	120
A.2	Proof of Theorem 2.4	123
A.3	Numerical Results	132

B	Projected Jacobi method	133
C	On the Shostak's test	135
C.1	Shostak Theory	136
C.2	Satisfiability test	139

List of Figures

2.1	An application of the ALTERNATING ALGORITHM. Left figure: a graph representing the solution of ETSP over a given P . Right figure: a graph representing the solution given by the ALTERNATING ALGORITHM on P where the alternate segments of ETSP are retained.	16
3.1	Construction of the “bead” $\mathcal{B}_\rho(\ell)$. The figure shows how the upper half of the boundary is constructed, the bottom half is symmetric.	22
3.2	Sketch of “meta-beads” at successive phases in the recursive bead tiling algorithm. From left to right: phase 1, phase 2 and phase 3.	25
4.1	Construction of the “bead” $\mathcal{B}_\rho(\ell)$. The figure shows how the upper half of the boundary is constructed, the bottom half is symmetric. The figure shows the rectangle $efgh$ which is used to construct the “cylinder” $\mathcal{C}_\rho(\ell)$	51
4.2	A typical layer of cylinders formed by stacking rows of cylinders .	53
4.3	(a): Cross section of the arrangement of the layers of cylinders used for covering $\mathcal{Q} \subset \mathbb{R}^3$, (b): The relative position of the bigger cylinder relative to smaller ones of the prior phase during the phase transition.	53
4.4	From top left in the left-to-right, top-to bottom direction, sketch of projection of “meta-cylinders” on the corresponding side of $\mathcal{Q} \subset \mathbb{R}^3$ at second, third, fourth and fifth sub-phases of a phase in the recursive cylinder covering algorithm.	55
5.1	Reachable sets $\mathcal{R}_I(t)$ for the Dubins vehicle for $t = 3\rho, 5\rho$ and 7ρ .	70
5.2	Truncation of $\mathcal{R}_h(t)$ to form $\tilde{\mathcal{R}}_h(t)$	70

5.3	Finding the value $\lambda_1(5\rho)$	71
5.4	Finding the value $\lambda_1(7\rho)$	72
5.5	Finding the value $\lambda_4(7\rho)$	73
5.6	Plot of $\lambda_1(t)/\rho$ vs. t/ρ	73
5.7	Plot of $\lambda_2(t)/\rho$ vs. t/ρ	74
5.8	“Move-toward-the-circumcenter” algorithm for 16 disks in a convex polygonal domain. The left (respectively, right) figure illustrates the initial (respectively, final) locations and Voronoi partition. The central figure illustrates the network evolution. After 20 sec., the disk radius is approximately 0.43273 m. Simulations taken from [1].	80
6.1	The admissible set \mathcal{A}^1 for generic values of r_{pos} and r_{ctr}	92
6.2	The disk graph and the double-integrator disk graph in \mathbb{R}^2 for 20 agents with random positions and velocities.	95
6.3	Starting from p_i and p_j , the agents are restricted to move inside the disk centered at $\frac{p_i+p_j}{2}$ with radius $\frac{r_{\text{emm}}}{2}$	98
6.4	Velocity alignment and cohesiveness for 5 agents in the plane ($d = 2$)	109
A.1	<i>LRL</i> curves returning to the origin for $\psi \in [0, \pi]$	122
A.2	<i>LRL</i> curves returning to the origin for $\psi \in]\pi, 2\pi[$	122
A.3	A suboptimal path from $(0, 0, 0)$ to (d, θ, ψ) , $(d, \theta) = \text{polar}(x, y)$ for $(x, y) \in V_1^c(\psi)$	126
C.1	Snippet of the graph $G(\mathcal{L})$ for the system of inequalities in (C.2) .	137

Chapter 1

Introduction

A whole new generation of Unmanned Air Vehicles (UAVs) are emerging, using innovation and creative enterprise, which promise to transform both military and civilian aerospace operations, and airspace environments. The deployment of large group of UAVs is rapidly becoming possible because of technological advances in networking and miniaturization of electro-mechanical devices. The potential advantages of employing teams of vehicles are numerous. For instance, certain tasks are difficult, if not impossible, when performed by a single vehicle. UAVs are generally considered to offer benefits both in survivability and expendability, as well as being potentially more cost effective than manned systems. Further, a group of vehicles inherently provides robustness to failures of single vehicle or communication links.

Cooperative control of multi-agent systems has met a lot of success in the controls and robotics community. However, multi-UAV systems pose novel challenges because of the inherent constraints like non-holonomic motion, limited-range con-

nectivity, etc. Hence, there is a need to develop new tools and algorithms for cooperative control of multi-UAV systems. For the rest of this dissertation, we will use the terms UAVs, agents and robots interchangeably.

1.1 Background and related work

For motion planning purposes, the nominal behavior of UAVs with hover capabilities (e.g., helicopters) is usually captured by a simple double integrator model with bounded velocity and acceleration, e.g., see [2]. On the other hand, the Dubins vehicle is commonly accepted as a reasonably accurate kinematic model for fixed-wing aircraft motion planning problems, e.g., see [3], and its study is included in recent texts [4, 5]. Dubins vehicle is a nonholonomic vehicle that is constrained to move along paths of bounded curvature without reversing direction. In this dissertation, we develop novel tools and algorithms for various motion coordination tasks for these two models of UAVs.

In one part of the dissertation, we study a novel class of optimal motion planning problems for the Dubins vehicle required to visit collections of points in the plane. The objective is to find the shortest path for such vehicle through a given set of target points. Except for the nonholonomic constraint, this task is akin to the classic Traveling Salesperson Problem (TSP) and in particular to the Euclidean TSP (ETSP), in which the shortest path between any two target locations is a straight segment. Our focus is on the analysis and the algorithmic design of the TSP for the Dubins vehicle; we shall refer to this problem as to the Dubins TSP (DTSP).

A practical motivation to study the DTSP arises naturally in robotics and

uninhabited aerial vehicles (UAVs) applications like vehicle routing. We envision applying DTSP algorithms to the setting of a UAV monitoring a collection of spatially distributed points of interest. In one scenario, the location of the points of interests might be known and static. Additionally, UAV applications motivate the study of the Dynamic Traveling Repairperson Problem (DTRP), in which the UAV is required to visit a dynamically changing set of targets. Such problems are examples of distributed task allocation problems and are currently generating much interest; e.g., [6] discusses complexity issues related to UAVs assignments problems, [7] considers Dubins vehicles surveilling multiple mobile targets, [8] considers missions with dynamic threats, other relevant works include [9, 10, 11, 12].

The literature on the Dubins vehicle is very rich and includes contributions from researchers in multiple disciplines. The minimum-time point-to-point path planning problem with bounded curvature was originally introduced by Markov [13] and a first solution was given by Dubins [14]. Modern treatments on point-to-point planning exploit the Pontryagin Minimum Principle [15], carefully account for symmetries in the problem [16], and consider environments with obstacles [17].

The TSP and its variations continue to attract great interest from a wide range of fields, including operations research, mathematics and computer science. Tight bounds on the asymptotic dependence of the ETSP on the number of targets are given in the early work [18] and in the survey [19]. Exact algorithms, heuristics as well as polynomial-time constant factor approximation algorithms are available for the Euclidean TSP, see [20, 21, 22]. A variations of the TSP with potential robotic applications is the angular-metric problem studied in [23]. The DTRP (without nonholonomic constraints) was introduced in [24]. However, as with the

TSP, the study of the DTRP in context of the Dubins vehicle has eluded attention from the research community. Finally, it is worth remarking that, unlike other variations of the TSP, the Dubins TSP cannot be formulated as a problem on a finite-dimensional graph, thus preventing the use of well-established tools in combinatorial optimization.

To clarify our contributions to the DTSP, it is worthwhile to compare our results with the ones existing in literature. The DTSP was introduced in our early work [25], where a constant-factor approximation algorithm for the worst-case setting of the DTSP was proposed.

Subsequently, similar versions of this problem were also considered in [26] and [9]. A simplified version of the problem for a different but closely related kind of vehicle, the Reeds-Shepp vehicle, was considered in [27]. In [28], we introduced the stochastic DTSP and gave the first algorithm yielding, with high probability, a solution with a cost upper bounded by a strictly sub-linear function of the number n of target points. Specifically, it was shown that the lower bound on the stochastic DTSP was of order $n^{2/3}$ and that our algorithm performed asymptotically within a $(\log n)^{1/3}$ factor to this lower bound with high probability. This result was improved in [29] with an algorithm for the stochastic DTSP that asymptotically performs within any $\epsilon(n)$ factor of the optimal with high probability, where $\epsilon(n) \rightarrow +\infty$ as $n \rightarrow +\infty$. In [30] we designed the first algorithm that asymptotically achieves a constant factor approximation to the stochastic DTSP with high probability.

Another prototypical mission for UAVs that we consider, e.g., in environmental monitoring, security, or military setting, is wide-area surveillance. A low-altitude UAV in such a mission must provide coverage of a certain region

and investigate events of interest (“targets”) as they manifest themselves. In particular, we are interested in cases in which close-range information is required on targets detected by high-altitude aircraft, spacecraft, or ground spotters, and the UAVs must proceed to the location of the detected targets to gather on-site information.

Variations of problems falling in this class have been studied in a number of papers in the recent past, e.g., see [31, 8, 12, 11]. In these papers, the problem is set up in such a way that the location of targets is known a priori and a strategy is computed that attempts to optimize the coverage cost of servicing the known targets. Coordination algorithms for distributed sensing task were proposed and analyzed in [32]. A limitation of the results presented in [32] is the fact that omni-directional or locally controllable vehicles were considered in the problem formulation. Because of this assumption, the results are not applicable to many vehicles of interest, such as aircraft and car-like robots.

In contrast to *simpler* vehicles [32] which can wait at a single location while they are idle, Dubins vehicles have to *loiter* while they are waiting for targets to appear in the region. As a consequence, we need to characterize the configuration of the vehicles at the appearance of new targets in terms of Dubins paths, that we will call *loitering patterns*.

The motion coordination problem for groups of autonomous agents is a control problem in the presence of communication constraints. Typically, each agent makes decisions based only on partial information about the state of the entire network that is obtained via communication with its immediate neighbors. One important difficulty is that the topology of the communication network depends on the agents’ locations and, therefore, changes with the evolution of the net-

work. In order to ensure a desired emergent behavior for a group of agents, it is necessary that the group does not disintegrate into subgroups that are unable to communicate with each other. In other words, some restrictions must be applied on the movement of the agents to ensure *connectivity* among the members of the group. In terms of design, it is required to constrain the control input such that the resulting topology maintains connectivity throughout its course of evolution. In [33], a connectivity constraint was developed for a group of agents modeled as first-order discrete time dynamic systems. In [33] and in the related references [34, 35], this constraint is used to solve rendezvous problems. Connectivity constraints for line-of-sight communication are proposed in [36]. Another approach to connectivity maintenance for first-order systems is proposed in [37]. In [38], a centralized procedure to find the set of control inputs that maintain k -hop connectivity for a network of agents is given. However, there is no guarantee that the resulting set of feasible control inputs is non-empty. In this dissertation we fully characterize the set of admissible control inputs for a group of agents modeled as second order discrete time dynamic systems, which ensures connectivity of the group in the same spirit as described earlier.

1.2 Summary of contributions

The contributions of this dissertation are aimed at broadly three classes of coordination problems: (i) vehicle routing to meet service demands (ii) coverage by loitering Dubins vehicles and (iii) maintaining limited-range connectivity among second-order agents.

In the context of the vehicle routing problem our contributions, as presented in

Chapters 2 and 3, are threefold. First, we propose an algorithm for the worst-case DTSP through a point set P , called the ALTERNATING ALGORITHM. This algorithm is based on the solution to the ETSP over P and on an alternating heuristic to assign target orientations at each target point. This algorithm performs within a constant factor of the optimal in the worst case. As an intermediate step in the analysis of the algorithm, we provide an upper bound on the point-to-point minimum length of Dubins optimal paths. Second, we propose an algorithm for the stochastic DTSP, called the RECURSIVE BEAD-TILING ALGORITHM. This algorithm is based on a geometric tiling of the plane, tuned to the Dubins vehicle dynamics, and on a strategy for the vehicle to service targets from each tile. The RECURSIVE BEAD-TILING ALGORITHM is the first algorithm providing a provable constant-factor approximation to the DTSP optimal solution with high probability. Third, we propose an algorithm for the DTRP in the heavy load case, called the BEAD-TILING ALGORITHM, based on a fixed-resolution version of the RECURSIVE BEAD-TILING ALGORITHM. We show that the performance guarantees for the stochastic DTSP translate into stability guarantees for the average performance of the DTRP for the Dubins vehicle in heavy load case. Specifically, we show that the performance of BEAD-TILING ALGORITHM is within a constant factor from the theoretical optimum. Similar results for a double integrator vehicle are obtained in Chapter 4.

The main contributions to the coverage problem, as presented in Chapter 5 are as follows. First, we study the reachable set of Dubins vehicle and characterize some of its properties that are particularly useful for the problem at hand. Most importantly, we introduce a certain “covering problem” where a circle or a sector with given parameters is to be contained in the Dubins reachable set

of minimal time. Second, we characterize optimal circular loitering for a single Dubins vehicle by exploiting the rotational symmetry of the problem and the simple-connectedness of the Dubins reachable set. Third, we design efficient circular loitering patterns for a single team of multiple Dubins vehicle and provide a bound on the achievable performance for sufficiently large environments. Finally, we consider the case of multiple teams composed of the same number of vehicles. We propose a computational approach to computing loitering patterns based on (1) partitioning the environment into Voronoi partitions generated by virtual centers, (2) moving the virtual centers in such a way as to solve a minimum-radius disk-covering problem, and (3) designing efficient loitering patterns for each team in its corresponding Voronoi cell.

For the connectivity maintenance problem, as exposed in Chapter 6, the contributions are threefold. First, we consider a control system consisting of a double integrator with bounded control inputs. For such a system, we define and characterize the admissible set that allows the double integrator to remain inside disks. Second, we define a novel state-dependent graph – the *double-integrator disk graph* – and give an existence theorem for the connectivity maintenance problem for networks of second order agents with respect to an appropriate version of this new graph. Finally, we consider a relevant optimization problem, where given a set of desired control inputs for all the agents it is required to find the optimal set of connectivity-maintaining control inputs. We cast this problem into a standard quadratic programming problem and provide a distributed “flow-control” algorithm to solve it.

Chapter 2

DTSP: The worst case

In this chapter we study the length of optimal paths for Dubins vehicle. First, we obtain an upper bound on the optimal length in the point-to-point problem. Next, we consider the corresponding Traveling Salesperson Problem (TSP). We provide an algorithm with worst-case performance within a constant factor approximation of the optimum. We also establish an asymptotic bound on the worst-case length of the Dubins TSP.

2.1 Problem setup: from the Euclidean to the Dubins Traveling Salesperson Problem

In this section we setup the main problem and basic notations for this and the next chapter. A *Dubins vehicle* is a planar vehicle that is constrained to move along paths of bounded curvature, without reversing direction and maintaining a constant speed. Accordingly, we define a *feasible curve for the Dubins vehicle*

or a *Dubins path*, as a curve $\gamma : [0, T] \rightarrow \mathbb{R}^2$ that is twice differentiable almost everywhere, and such that the magnitude of its curvature is bounded above by $1/\rho$, where $\rho > 0$ is the minimum turning radius. We also let $\text{Length}(\gamma) = \int_0^T \|\gamma'(t)\| dt$ be the length of a differentiable curve $\gamma : [0, T] \rightarrow \mathbb{R}^2$. We represent the vehicle configuration by the triplet $(x, y, \psi) \in \text{SE}(2)$, where (x, y) are the Cartesian coordinates of the vehicle and ψ is its heading.

Let $P = \{p_1, \dots, p_n\}$ be a set of n points in a compact region $\mathcal{Q} \subset \mathbb{R}^2$ and \mathcal{P}_n be the collection of all point sets $P \subset \mathcal{Q}$ with cardinality n . Let $\text{ETSP}(P)$ denote the cost of the Euclidean TSP over P , i.e., the length of the shortest closed path through all points in P . Correspondingly, let $\text{DTSP}_\rho(P)$ denote the cost of the Dubins TSP over P , i.e., the length of the shortest closed Dubins path through all points in P with minimum turning radius ρ .

We conclude this section with some notation that is the standard concise way to state asymptotic properties. For $f, g : \mathbb{N} \rightarrow \mathbb{R}$, we say that $f \in O(g)$ (respectively, $f \in \Omega(g)$) if there exist $N_0 \in \mathbb{N}$ and $k \in \mathbb{R}_+$ such that $|f(N)| \leq k|g(N)|$ for all $N \geq N_0$ (respectively, $|f(N)| \geq k|g(N)|$ for all $N \geq N_0$). If $f \in O(g)$ and $f \in \Omega(g)$, then we use the notation $f \in \Theta(g)$. Finally, we say that $f \in o(g)$ as $N \rightarrow +\infty$ if $\lim_{N \rightarrow +\infty} f(N)/g(N) = 0$ or, for functions $f, g : \mathbb{R} \rightarrow \mathbb{R}$, we say that $f \in o(g)$ as $x \rightarrow 0$ if $\lim_{x \rightarrow 0} f(x)/g(x) = 0$.

The key objective is the design of an algorithm that provides a provably good approximation to the optimal solution of the Dubins TSP. To establish what a “good approximation” might be, let us recall what is known about the ETSP. First, given a compact set \mathcal{Q} , there exists [19] a finite constant $\alpha(\mathcal{Q})$ such that, for all $P \in \mathcal{P}_n$,

$$\text{ETSP}(P) \leq \alpha(\mathcal{Q})\sqrt{n}. \tag{2.1}$$

This upper bound is constructive in the sense that there exist [19] algorithms that generate closed paths through the points P with length of order \sqrt{n} . In the stochastic case, where the n points in P are independently chosen from a distribution φ with compact support $\mathcal{Q} \subset \mathbb{R}^2$, the following deterministic limit holds [18]:

$$\lim_{n \rightarrow +\infty} \frac{\text{ETSP}(P)}{\sqrt{n}} = \beta \int_{\mathcal{Q}} \sqrt{\bar{\varphi}(q)} dq, \quad \text{with probability 1,}$$

where $\bar{\varphi}$ is a probability density function corresponding to the absolutely continuous part of φ , and β is a constant, which has been evaluated as $\beta = 0.712 \pm 0.0001$, e.g., see [39]. The fact that the dependence of the ETSP is sub-linear in n is very important in the study of the DTRP, i.e., the problem in which new locations are continuously added to the set of outstanding points P ; see Section 3.5 in Chapter 3.

Motivated by the Euclidean case, in this chapter we show that the DTSP grows with n in the worst case (as both lower and upper bounds). Additionally, we propose a novel algorithm for the DTSP in the worst-case setting, whose performance is within a constant factor of the optimal solution in the asymptotic limit as $n \rightarrow +\infty$.

2.2 Lower bound for the DTSP

We first give a lower bound on $\text{DTSP}_\rho(P)$ in the worst case. Given any point set $P \in \mathcal{P}_n$ with $n \geq 2$ and $\rho > 0$, it is immediate to see that $\text{DTSP}_\rho(P) \geq \text{ETSP}(P)$. This bound is improved in the following theorem, whose proof is reported in Appendix A.

Theorem 2.1 (*Worst-case lower bound on the TSP for the Dubins vehicle*)

Given $\rho > 0$, there exists a point set $P \in \mathcal{P}_n$, $n \geq 2$, such that

$$\text{DTSP}_\rho(P) \geq \text{ETSP}(P) + 2 \left\lfloor \frac{n}{2} \right\rfloor \pi \rho.$$

Proof. We first describe the construction of the set $P \in \mathcal{P}_n$ for which the statement holds true. Let C_r be a circle of radius $r < \rho$ with center at the origin. For $i \in \{1, \dots, n\}$, define the i^{th} point b_i by

$$b_i = (r \cos(2\pi i/n), r \sin(2\pi i/n)).$$

This definition ensures that $b_i \neq b_j$ for $i \neq j$. Let $P(r) = \{b_1, \dots, b_n\}$. Let $E = (e_1, \dots, e_n)$ be an ordered set defined as follows: $\{e_1, \dots, e_n\} = P(r)$ and (e_1, \dots, e_n) are in clockwise order along the circle C_r . It is easy to see that in this case, the cost of the Euclidean TSP over these n points is given by

$$\text{ETSP}(P(r)) = \|e_n - e_1\| + \sum_{i=1}^{n-1} \|e_i - e_{i+1}\|. \quad (2.2)$$

Let $F = (f_1, \dots, f_n)$ be the (possibly, suboptimal) order of points which the Dubins vehicle will go through while executing any algorithm (not necessarily the optimal algorithm) over $P(r)$. Let τ denote the closed path followed by the Dubins vehicle, let $(s_i, s_{i+1})_\tau$ be the part of the path τ between the points s_i and s_{i+1} for $i \in \{1, \dots, n-1\}$, and let $(s_n, s_1)_\tau$ be the part of the path τ between the points s_n and s_1 . Let D_r be a closed disk of radius r with center at the origin. Let $G = (g_1, \dots, g_u) \subseteq E$ be an ordered set of all points for which $(g_{2a-1}, g_{2a})_\tau \subset D_r$ for $a \in \{1, \dots, \frac{u}{2}\}$. Let $H = (h_1, \dots, h_v)$ be an ordered set of points (possibly with repetition of points) for which $(h_{2a-1}, h_{2a})_\tau$ is not a subset of D_r for $a \in \{1, \dots, \frac{v}{2}\}$. If we let $L_{\text{ANY}}(P(r), r)$ denote the total length of τ , then

$$L_{\text{ANY}}(P(r), r) = \sum_{i=1}^{n-1} \text{Length}((f_i, f_{i+1})_\tau) + \text{Length}((f_n, f_1)_\tau).$$

Splitting the terms which represent the part of τ lying inside and outside of D_r , we compute

$$L_{\text{ANY}}(P(r), r) = \sum_{a=1}^{u/2} \text{Length}((g_{2a-1}, g_{2a})_\tau) + \sum_{a=1}^{\frac{v}{2}} \text{Length}((h_{2a-1}, h_{2a})_\tau). \quad (2.3)$$

Since the segment joining any two points is the shortest path between those two points, we have

$$\sum_{a=1}^{u/2} \text{Length}((g_{2a-1}, g_{2a})_\tau) \geq \sum_{a=1}^{u/2} \|g_{2a-1} - g_{2a}\|. \quad (2.4)$$

Noting that the ordered set F is the union of the ordered sets G and H , we have

$$\sum_{a=1}^{u/2} \|g_{2a-1} - g_{2a}\| = \sum_{i=1}^{n-1} \|f_i - f_{i+1}\| + \|f_n - f_1\| - \sum_{a=1}^{\frac{v}{2}} \|h_i - h_{i+1}\|.$$

Because the longest length of any segment lying entirely in D_r is $2r$, the last equation can be written as

$$\sum_{a=1}^{u/2} \|g_{2a-1} - g_{2a}\| \geq \sum_{i=1}^{n-1} \|f_i - f_{i+1}\| + \|f_n - f_1\| - vr. \quad (2.5)$$

From equations (2.3), (2.4) and (2.5), we get

$$L_{\text{ANY}}(P(r), r) \geq \sum_{i=1}^{n-1} \|f_i - f_{i+1}\| + \|f_n - f_1\| + \sum_{a=1}^{\frac{v}{2}} \text{Length}((h_{2a-1}, h_{2a})_\tau) - vr. \quad (2.6)$$

However, considering that the set E is the optimal order of points for Euclidean TSP over $P(r)$, we have

$$\sum_{i=1}^{n-1} \|f_i - f_{i+1}\| + \|f_n - f_1\| \geq \sum_{i=1}^{n-1} \|e_i - e_{i+1}\| + \|e_n - e_1\| \quad (2.7)$$

From equations (2.2), (2.6) and (2.7), it follows that

$$L_{\text{ANY}}(P(r), r) \geq \text{ETSP}(P(r)) + \sum_{a=1}^{\frac{v}{2}} \text{Length}((h_{2a-1}, h_{2a})_\tau) - vr. \quad (2.8)$$

From [14] it follows that under the minimum radius of curvature constraint, for its optimality, any $(h_{2a-1}, h_{2a})_\tau$ is composed of line segments and arcs of circle of radius r . Let $\zeta_{h_{2a-1}, h_{2a}}$ denote the angular displacement of the vehicle as it travels along the optimal path $(h_{2a-1}, h_{2a})_\tau$. Then,

$$\sum_{a=1}^{v/2} \text{Length}((h_{2a-1}, h_{2a})_\tau) \geq \sum_{a=1}^{v/2} \zeta_{h_{2a-1}, h_{2a}} r. \quad (2.9)$$

From (2.8) and (2.9) it follows that

$$L_{\text{ANY}}(P(r), r) \geq \text{ETSP}(P(r)) + \sum_{a=1}^{v/2} \zeta_{h_{2a-1}, h_{2a}} r - vr. \quad (2.10)$$

Now, we use the fact that as $r \rightarrow 0$, $\zeta_{h_{2a-1}, h_{2a}} \rightarrow 2\pi$ for all a . By taking the limit in (2.10) as $r \rightarrow 0^+$, we obtain

$$L_{\text{ANY}}(P(r), r) \geq \text{ETSP}(P(r)) + v\pi r. \quad (2.11)$$

The inequality (2.11) holds true for *any* algorithm over the set P . Therefore, it holds true for the optimal algorithm when v attains its minimum value of $2\lfloor n/2 \rfloor$. Substituting this value of v in (2.11) we obtain the desired lower bound. ■

Remark 2.2 *Theorem 2.1 implies that, for $P \in \mathcal{P}_n$ and in the worst case, $\text{DTSP}_\rho(P) \in \Omega(n)$.* □

2.3 The Alternating Algorithm

Here we propose a novel algorithm, the ALTERNATING ALGORITHM, that approximates the solution of the DTSP. The underlying principle of the algorithm is the following observation: since the optimal Dubins path between two configurations has been characterized in [14], a solution for the DTSP consists of (i)

determining the order in which the Dubins vehicle visits the given set of points, and (ii) assigning headings for the Dubins vehicle at the points. The algorithm builds on the knowledge of the optimal solution of the ETSP for the same point set, and provides a sub-optimal DTSP tour.

The ALTERNATING ALGORITHM works as follows. Compute an optimal ETSP tour of P and label the edges on the tour in order with consecutive integers. A DTSP tour can be constructed by retaining all odd-numbered (except n^{th}) edges, and replacing all even-numbered edges with minimum-length Dubins paths preserving the point ordering. In other words, the algorithm consists of the following steps:

- (i) set $(a_1, \dots, a_n) :=$ optimal ETSP ordering of P
- (ii) set $\psi_1 :=$ orientation of segment from a_1 to a_2
- (iii) for $i \in \{2, \dots, n-1\}$, do
 - if i is even, then set $\psi_i := \psi_{i-1}$, else set $\psi_i :=$ orientation of segment from a_i to a_{i+1}
- (iv) if n is even, then set $\psi_n := \psi_{n-1}$, else set $\psi_n :=$ orientation of segment from a_n to a_1
- (v) return the sequence of configurations $\{(a_i, \psi_i)\}_{i \in \{1, \dots, n\}}$.

We illustrate the output of the ALTERNATING ALGORITHM in Figure 2.1.

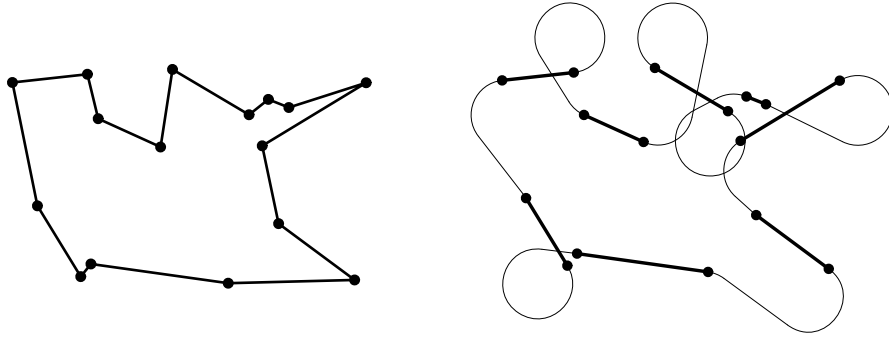


Figure 2.1: An application of the ALTERNATING ALGORITHM. Left figure: a graph representing the solution of ETSP over a given P . Right figure: a graph representing the solution given by the ALTERNATING ALGORITHM on P where the alternate segments of ETSP are retained.

2.4 Analysis of the algorithm

In this section we analyze the performance of the ALTERNATING ALGORITHM to obtain an upper bound on $\text{DTSP}_\rho(P)$ and then show that the algorithm performs within a constant factor of the optimal in the worst case. To obtain an upper bound on the length of the Dubins vehicle while executing the ALTERNATING ALGORITHM, we first obtain an upper bound on the optimal point-to-point problem for the Dubins vehicle.

Problem 2.3 *Given an initial configuration $(x_{\text{initial}}, y_{\text{initial}}, \psi_{\text{initial}})$ and a final configuration $(x_{\text{final}}, y_{\text{final}}, \psi_{\text{final}})$, find an upper bound on the length of the shortest Dubins path going from initial to final configuration. \square*

To tackle this problem, we introduce some preliminary definitions. Without loss of generality, we assume $(x_{\text{initial}}, y_{\text{initial}}, \psi_{\text{initial}}) = (0, 0, 0)$. Let $\mathcal{C}_\rho : \text{SE}(2) \rightarrow$

$\overline{\mathbb{R}}_+$ associate to a configuration (x, y, ψ) the length of the shortest Dubins path from $(0, 0, 0)$ to (x, y, ψ) . Define $F_0 :]0, \pi[\times]0, \pi[\rightarrow]0, \pi[$, $F_1 :]0, \pi[\rightarrow \mathbb{R}$ and $F_2 :]0, \pi[\rightarrow \mathbb{R}$ by

$$\begin{aligned} F_0(\psi, \theta) &= 2 \tan^{-1} \left(\frac{\sin(\psi/2) - 2 \sin(\psi/2 - \theta)}{\cos(\psi/2) + 2 \cos(\psi/2 - \theta)} \right), \\ F_1(\psi) &= \psi + \sin \left(\frac{F_0(\psi, \psi/2 - \alpha(\psi))}{2} \right) + 4 \cos^{-1} \left(\frac{\sin((\psi - F_0(\psi, \psi/2 - \alpha(\psi)))/2)}{2} \right), \\ F_2(\psi) &= 2\pi - \psi + 4 \cos^{-1} \left(\frac{\sin(\psi/2)}{2} \right), \end{aligned}$$

where $\alpha(\psi) = \pi/2 - \cos^{-1}(\frac{\sin(\psi/2)}{2})$. The proof of the following result is postponed to the appendix.

Theorem 2.4 (Upper bound on optimal point-to-point length) *For $\psi \in [0, 2\pi[$, $(x, y) \in \mathbb{R}^2$, and $\rho > 0$,*

$$\mathcal{C}_\rho(x, y, \psi) \leq \sqrt{x^2 + y^2} + \kappa\pi\rho,$$

where $\kappa \in [2.657, 2.658]$ is defined by $\kappa = \frac{1}{\pi} \max\{F_2(\pi), \sup_{\psi \in]0, \pi[} \min\{F_1(\psi), F_2(\psi)\}\}$.

The proof of this result requires new geometric constructions and is presented in Appendix.

Next, we let $L_{AA,\rho}(P)$ denote the length of Dubins path as given by the ALTERNATING ALGORITHM for a point set P . The following lemma is an immediate consequence of Theorem 2.4.

Lemma 2.1 (Upper bound on the performance of the ALTERNATING ALGORITHM) *For any $P \in \mathcal{P}_n$ and $\rho > 0$,*

$$L_{AA,\rho}(P) \leq \text{ETSP}(P) + \kappa \left\lceil \frac{n}{2} \right\rceil \pi\rho.$$

Having established bounds on the performance of the ALTERNATING ALGORITHM, we now show that it performs within a constant factor of the optimal in the worst case. To that effect, we first state the following result concerning the performance of the optimal algorithm.

Lemma 2.2 (*Bounds on the TSP for the Dubins vehicle*) For any point set $P \in \mathcal{P}_n$ with $n \geq 2$ and $\rho > 0$,

$$\text{ETSP}(P) \leq \text{DTSP}_\rho(P) \leq \text{ETSP}(P) + \kappa \left\lceil \frac{n}{2} \right\rceil \pi \rho.$$

Furthermore, given $\rho > 0$, there exists a point set $P \in \mathcal{P}_n$ such that

$$\text{ETSP}(P) + 2 \left\lceil \frac{n}{2} \right\rceil \pi \rho \leq \text{DTSP}_\rho(P) \leq \text{ETSP}(P) + \kappa \left\lceil \frac{n}{2} \right\rceil \pi \rho.$$

Proof. It is immediate that, for any point set P , $\text{ETSP}(P) \leq \text{DTSP}_\rho(P) \leq \text{L}_{\text{AA},\rho}(P)$. The first statement is therefore a consequence of Lemma 2.1. The second statement follows from Theorem 2.1. ■

Theorem 2.5 (*Worst-case performance of the ALTERNATING ALGORITHM*) For $n \geq 2$ and $\rho > 0$,

$$\sup_{P \in \mathcal{P}_n} \text{DTSP}_\rho(P) \leq \sup_{P \in \mathcal{P}_n} \text{L}_{\text{AA},\rho}(P) \leq \frac{\text{ETSP}(P) + \kappa \lceil n/2 \rceil \pi \rho}{\text{ETSP}(P) + 2 \lceil n/2 \rceil \pi \rho} \sup_{P \in \mathcal{P}_n} \text{DTSP}_\rho(P).$$

Furthermore, as $n \rightarrow +\infty$,

$$\sup_{P \in \mathcal{P}_n} \text{DTSP}_\rho(P) \leq \sup_{P \in \mathcal{P}_n} \text{L}_{\text{AA},\rho}(P) \leq \frac{\kappa}{2} \sup_{P \in \mathcal{P}_n} \text{DTSP}_\rho(P).$$

Proof. The first statement follows from the simple fact that $\text{L}_{\text{AA},\rho}(P) \geq \text{DTSP}_\rho(P)$, and from the results in Lemma 2.1 and Theorem 2.1. To prove the second statement, we take the limit as $n \rightarrow +\infty$ in the first statement and we use the bound in equation (2.1). ■

Remark 2.6 (i) Lemma 2.1 implies that $L_{AA,\rho}(P)$ belongs to $O(n)$ and Theorem 2.5 implies that in the worst case, $DTSP_\rho(P)$ belongs to $\Theta(n)$. This establishes that the ALTERNATING ALGORITHM performs within a constant factor of the optimal in the worst case.

(ii) The following fact is a consequence of Lemma 2.2: given a point set, for small enough ρ , the order of points in the optimal path for the Euclidean TSP is the same as in the optimal path for the Dubins TSP. \square

2.5 Summary

In this chapter, we have formulated and studied the TSP for vehicles that follow paths of bounded curvature in the plane. For the worst-case setting, we have obtained an upper bound that is within a constant factor of the lower bound; the upper bound is constructive in the sense that it is achieved by a novel algorithm. It is interesting to compare our results with the Euclidean setting (i.e., the setting in which vehicle paths do not have curvature constraints). For a given compact set and a point set P of n points, it is known [18, 19] that the ETSP(P) belongs to $\Theta(\sqrt{n})$. This is true for both stochastic and worst-case settings. In this paper, we showed that, given a fixed $\rho > 0$, the $DTSP_\rho(P)$ in the *worst case* belongs to $\Theta(n)$. In the next chapter, we study stochastic DTSP and DTRP.

Chapter 3

DTSP: The stochastic and the dynamic case

The discussion in the previous chapter showed that the ALTERNATING ALGORITHM performs well when the points to be visited by the tour are chosen in an adversarial manner. However, this algorithm is not a constant-factor approximation algorithm in the general case. Moreover, this algorithm might not perform very well when dealing with a random distribution of the target points. In this chapter we study a stochastic version of the DTSP where the n targets are randomly sampled from a uniform distribution. We show that the expected length of such a tour is of order at least $n^{2/3}$ and we propose a novel algorithm yielding a solution with length of order $n^{2/3}$ with high probability. Additionally, we study a dynamic version of the DTSP: given a stochastic process that generates target points, is there a policy which guarantees that the number of unvisited points does not diverge over time? If such stable policies exist, what is the minimum

expected time that a newly generated target waits before being visited by the vehicle? We propose a novel stabilizing algorithm such that the expected wait time is provably within a constant factor from the optimum.

We make the following assumptions: \mathcal{Q} is a rectangle of width W and height H with $W \geq H$; different choices for the shape of \mathcal{Q} affect our conclusions only by a constant. The two axes of the reference frame are parallel to the sides of \mathcal{Q} .

3.1 Lower bound for the stochastic DTSP

For the stochastic DTSP, we assume that the points $P = (p_1, \dots, p_n)$ are randomly generated according to a uniform distribution in \mathcal{Q} .

We begin with a result from [40] that provides a lower bound on the expected length of the stochastic DTSP.

Theorem 3.1 (Lower bound on stochastic DTSP) *For all $\rho > 0$, the expected cost of the DTSP for a set P of n uniformly-randomly-generated points in a rectangle of width W and height H satisfies*

$$\lim_{n \rightarrow +\infty} \frac{\mathbb{E}[\text{DTSP}_\rho(P)]}{n^{2/3}} \geq \frac{3}{4} \sqrt[3]{3\rho WH}.$$

Remark 3.2 *Theorem 3.1 implies that $\mathbb{E}[\text{DTSP}_\rho(P)]$ belongs to $\Omega(n^{2/3})$. \square*

3.2 The basic geometric construction

Here we define a useful geometric object and study its properties. Consider two points p_- and p_+ on the plane, with $\ell = \|p_+ - p_-\|_2 \leq 4\rho$, and construct the region $\mathcal{B}_\rho(\ell)$ as detailed in Figure 3.1. We refer to such a region as a *bead* of length

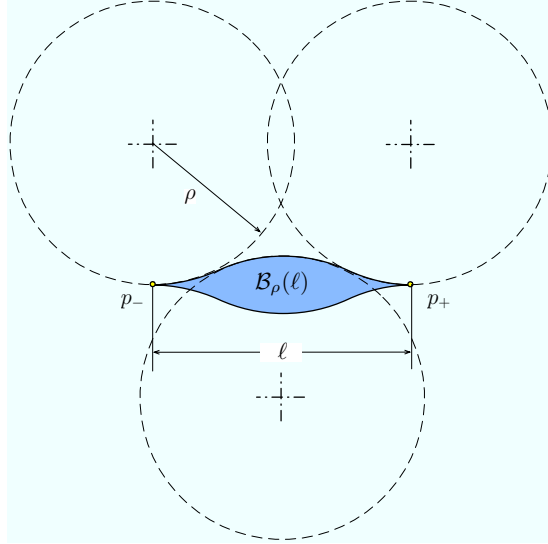


Figure 3.1: Construction of the “bead” $\mathcal{B}_\rho(\ell)$. The figure shows how the upper half of the boundary is constructed, the bottom half is symmetric.

ℓ . The region $\mathcal{B}_\rho(\ell)$ enjoys the following asymptotic properties as $(\ell/\rho) \rightarrow 0^+$:

(P1) Its maximum “thickness” is

$$w(\ell) = 4\rho \left(1 - \sqrt{1 - \frac{\ell^2}{16\rho^2}} \right) = \frac{\ell^2}{8\rho} + \rho \cdot o\left(\frac{\ell^3}{\rho^3}\right).$$

(P2) Its area is

$$\text{Area}(\mathcal{B}_\rho(\ell)) = \frac{\ell w(\ell)}{2} = \frac{\ell^3}{16\rho} + \rho^2 \cdot o\left(\frac{\ell^4}{\rho^4}\right).$$

(P3) For any $p \in \mathcal{B}_\rho(\ell)$, there is at least one Dubins path γ_p through the points $\{p_-, p, p_+\}$, entirely contained within $\mathcal{B}_\rho(\ell)$. The length of any such path

satisfies

$$\text{Length}(\gamma_p) \leq 4\rho \arcsin\left(\frac{\ell}{4\rho}\right) = \ell + \rho \cdot o\left(\frac{\ell^3}{\rho^3}\right).$$

These facts are verified using elementary planar geometry. Finally, the bead has the property that the plane can be periodically tiled¹ by identical copies of $\mathcal{B}_\rho(\ell)$, for any $\ell \in]0, 4\rho]$. This fact is illustrated in Figure 3.2 below.

Next, we study the probability of targets belonging to a given bead. Consider a bead B entirely contained in \mathcal{Q} and assume n points are uniformly randomly generated in \mathcal{Q} . The probability that the i^{th} point is sampled in B is

$$\mu(\ell) = \frac{\text{Area}(\mathcal{B}_\rho(\ell))}{\text{Area}(\mathcal{Q})}.$$

Furthermore, the probability that exactly k out of the n points are sampled in B has a binomial distribution, i.e., indicating with n_B the total number of points sampled in B ,

$$\Pr[n_B = k | n \text{ samples}] = \binom{n}{k} \mu^k (1 - \mu)^{n-k}.$$

If the bead length ℓ is chosen as a function of n in such a way that $\nu = n \cdot \mu(\ell(n))$ is a constant, then the limit for large n of the binomial distribution is [41] the Poisson distribution of mean ν , that is,

$$\lim_{n \rightarrow +\infty} \Pr[n_B = k | n \text{ samples}] = \frac{\nu^k}{k!} e^{-\nu}.$$

3.3 The Recursive Bead-Tiling Algorithm

In this section, we design a novel algorithm that computes a Dubins path through a point set in \mathcal{Q} . The proposed algorithm consists of a sequence of phases;

¹A tiling of the plane is a collection of sets whose intersection has measure zero and whose union covers the plane.

during each phase, a Dubins tour (i.e., a closed path with bounded curvature) is constructed that “sweeps” the set \mathcal{Q} . We begin by considering a tiling of the plane such that $\text{Area}(\mathcal{B}_\rho(\ell)) = WH/(2n)$; in such a case, $\mu(\ell(n)) = 1/(2n)$, $\nu = 1/2$, and

$$\ell(n) = 2\left(\frac{\rho WH}{n}\right)^{\frac{1}{3}} + o(n^{-\frac{1}{3}}), \quad (n \rightarrow +\infty).$$

(Note that this implies that n must be large enough in order that $\ell \leq 4\rho$.) Furthermore, the tiling is chosen in such a way that it is aligned with the sides of \mathcal{Q} , see Figure 3.2. In the first phase of the algorithm, a Dubins tour is constructed with the following properties:

- (i) it visits all non-empty beads once,
- (ii) it visits all rows² in sequence top-to-down, alternating between left-to-right and right-to-left passes, and visiting all non-empty beads in a row,
- (iii) when visiting a non-empty bead, it services at least one target in it.

In order to visit the targets outstanding after the first phase, a second phase is initiated. Instead of considering single beads, we now consider “meta-beads” composed of two beads each, as shown in Figure 3.2, and proceed in a way similar to the first phase, i.e., a Dubins tour is constructed with the following properties:

- (i) the tour visits all non-empty meta-beads once,
- (ii) it visits all (meta-bead) rows in sequence top-to-down, alternating between left-to-right and right-to-left passes, and visiting all non-empty meta-beads in a row,

²A row is a maximal sequence of horizontally-aligned beads with non-empty intersection with \mathcal{Q} .

(iii) when visiting a non-empty meta-bead, it services at least one target in it.

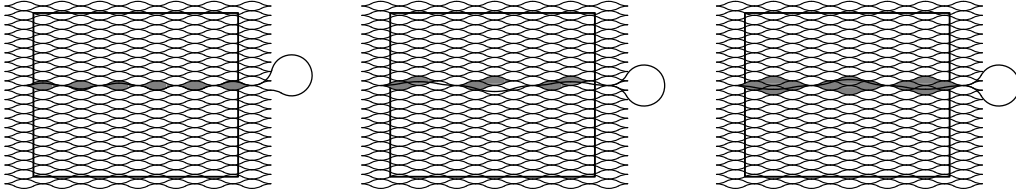


Figure 3.2: Sketch of “meta-beads” at successive phases in the recursive bead tiling algorithm. From left to right: phase 1, phase 2 and phase 3.

This process is iterated $\lceil \log_2 n \rceil$ times, and at each phase, meta-beads composed of two neighboring meta-beads from the previous phase are considered; in other words, the meta-beads at the i^{th} phase are composed of 2^{i-1} neighboring beads. After the last recursive phase, the leftover targets are visited using the **ALTERNATING ALGORITHM**.

3.4 Analysis of the algorithm

In this section, we calculate an upper bound on the length of Dubins path as given by the **RECURSIVE BEAD-TILING ALGORITHM**. By comparing this upper bound with the lower bound established earlier, we will conclude that the algorithm provides a constant factor approximation to the optimal stochastic DTSP with high probability. We begin with a key result about the number of outstanding targets after the execution of the $\lceil \log_2 n \rceil$ recursive phases; the proof of this result is based upon techniques similar to those developed in [42].

Theorem 3.3 (Targets remaining after recursive phases) *Let $P \in \mathcal{P}_n$ be uniformly randomly generated in \mathcal{Q} . The number of unvisited targets after the*

last recursive phase of the RECURSIVE BEAD-TILING ALGORITHM over P is less than $24 \log_2 n$ with high probability, i.e., with probability approaching one as $n \rightarrow +\infty$.

Proof. Associate a unique identifier to each bead, let $b(t)$ be the identifier of the bead in which the t^{th} target is sampled, and let $h(t) \in \mathbb{N}$ be the phase at which the t^{th} target is visited. Without loss of generality, assume that targets within a single bead are visited in the same order in which they are generated, i.e., if $b(t_1) = b(t_2)$ and $t_1 < t_2$, then $h(t_1) < h(t_2)$. Let $v_i(t)$ be the number of beads that contain unvisited targets at the inception of the i^{th} phase, computed after the insertion of the t^{th} target. Furthermore, let m_i be the number of i^{th} phase meta-beads (i.e., meta-beads containing 2^{i-1} neighboring beads) with a non-empty intersection with \mathcal{Q} . Clearly, $v_i(t) \leq v_i(n)$, $m_i \leq 2m_{i+1}$, and $v_1(n) \leq n \leq m_1/2$ with certainty. The t^{th} target will not be visited during the first phase if it is sampled in a bead that already contains other targets. In other words,

$$\Pr [h(t) \geq 2 \mid v_1(t)] = \frac{v_1(t)}{m_1} \leq \frac{v_1(n)}{2n} \leq \frac{1}{2}.$$

Similarly, the t^{th} target will not be visited during the i^{th} phase if (i) it has not been visited before the i^{th} pass, and (ii) it belongs to a meta-bead that already contains other targets not visited before the i^{th} phase:

$$\begin{aligned} & \Pr [h(t) \geq i + 1 \mid (v_i(t-1), v_{i-1}(t-1), v_1(t-1))] \\ &= \Pr [h(t) \geq i + 1 \mid h(t) \geq i, v_i(t-1)] \cdot \Pr [h(t) \geq i \mid (v_{i-1}(t-1), \dots, v_1(t-1))] \\ &\leq \frac{v_i(t-1)}{m_i} \Pr [h(t) \geq i \mid (v_{i-1}(t-1), \dots, v_1(t-1))] \\ &= \prod_{j=1}^i \frac{v_j(t-1)}{m_j} \leq \prod_{j=1}^i \frac{2^{j-1} v_j(n)}{2n} = \left(\frac{2^{\frac{i-3}{2}}}{n} \right)^i \prod_{j=1}^i v_j(n). \end{aligned}$$

Given a sequence $\{\beta_i\}_{i \in \mathbb{N}} \subset \mathbb{R}_+$ and given a fixed $i \geq 1$, define a sequence of binary random variables

$$Y_t = \begin{cases} 1, & \text{if } h(t) \geq i + 1 \text{ and } v_i(t-1) \leq \beta_i n, \\ 0, & \text{otherwise.} \end{cases}$$

In other words, $Y_t = 1$ if the t^{th} target is not visited during the first i phases even though the number of beads still containing unvisited targets at the inception of the i^{th} phase is less than $\beta_i n$. Even though the random variable Y_t depends on the targets generated before the t^{th} target, the probability that it takes the value 1 is bounded by

$$\Pr[Y_t = 1 \mid b(1), b(2), \dots, b(t-1)] \leq 2^{\frac{i(i-3)}{2}} \prod_{j=1}^i \beta_j =: q_i,$$

regardless of the actual values of $b(1), \dots, b(t-1)$. It is known [42] that if the random variables Y_t satisfy such a condition, the sum $\sum_t Y_t$ is stochastically dominated by a binomially distributed random variable, namely,

$$\Pr \left[\sum_{t=1}^n Y_t > k \right] \leq \Pr[B(n, q_i) > k].$$

In particular,

$$\Pr \left[\sum_{t=1}^n Y_t > 2nq_i \right] \leq \Pr[B(n, q_i) > 2np_i] < 2^{-nq_i/3}, \quad (3.1)$$

where the last inequality follows from Chernoff's Bound [41]. Now, it is convenient to define $\{\beta_i\}_{i \in \mathbb{N}}$ by

$$\beta_1 = 1, \quad \beta_{i+1} = 2q_i = 2^{\frac{i(i-3)}{2}+1} \prod_{j=1}^i \beta_j = 2^{i-2} \beta_i^2,$$

which leads to $\beta_i = 2^{1-i}$. In turn, this implies that equation (3.1) can be rewritten as

$$\Pr \left[\sum_{t=1}^n Y_t > \beta_{i+1} n \right] < 2^{-\beta_{i+1} n/6} = 2^{-\frac{n}{3 \cdot 2^i}},$$

which is less than $1/n^2$ for $i \leq i^*(n) := \lfloor \log_2 n - \log_2 \log_2 n - \log_2 6 \rfloor \leq \log_2 n$. Note that $\beta_i \leq 12 \frac{\log_2 n}{n}$, for all $i > i^*(n)$.

Let \mathcal{E}_i be the event that $v_i(n) \leq \beta_i n$. Note that if \mathcal{E}_i is true, then $v_{i+1}(n) \leq \sum_{t=1}^n Y_t$: the right hand side represents the number of targets that will be visited after the i^{th} phase, whereas the left hand side counts the number of beads containing such targets. We have, for all $i \leq i^*(n)$:

$$\Pr [v_{i+1} > \beta_{i+1} n \mid \mathcal{E}_i] \cdot \Pr[\mathcal{E}_i] \leq \Pr \left[\sum_{t=1}^n Y_t > \beta_{i+1} n \right] \leq \frac{1}{n^2},$$

that is, $\Pr [\neg \mathcal{E}_{i+1} \mid \mathcal{E}_i] \leq \frac{1}{n^2 \Pr[\mathcal{E}_i]}$, and thus (recall that \mathcal{E}_1 is true with certainty):

$$\Pr [\neg \mathcal{E}_{i+1}] \leq \frac{1}{n^2} + \Pr[\neg \mathcal{E}_i] \leq \frac{i}{n^2}.$$

In other words, for all $i \leq i^*(n)$, $v_i(n) \leq \beta_i n$ with high probability.

Let us now turn our attention to the phases such that $i > i^*(n)$. The total number of targets visited after the $(i^*)^{\text{th}}$ phase is dominated by a binomial variable $B(n, 12 \log_2 n/n)$; in particular,

$$\begin{aligned} \Pr [v_{i^*+1} > 24 \log_2 n \mid \mathcal{E}_{i^*}] \cdot \Pr[\mathcal{E}_{i^*}] &\leq \Pr \left[\sum_{t=1}^n Y_t > 24 \log_2 n \right] \\ &\leq \Pr [B(n, 12 \log_2 n/n) > 24 \log_2 n] \leq 2^{-12 \log_2 n}. \end{aligned}$$

Dealing with conditioning as before, we obtain

$$\Pr [v_{i^*+1} > 24 \log_2 n] \leq \frac{1}{n^{12}} + \Pr[\neg \mathcal{E}_{i^*}] \leq \frac{1}{n^{12}} + \frac{\log_2 n}{n^2}.$$

In other words, the number of targets that are left unvisited after the $(i^*)^{\text{th}}$ phase is bounded by a logarithmic function of n with high probability. ■

In summary, Theorem 3.3 says that after a sufficiently large number of phases, almost all targets will be visited, with high probability. The second key point

is to recognize that (i) the length of the first phase is of order $n^{2/3}$ and (ii) the length of each phase is decreasing at such a rate that the sum of the lengths of the $\lceil \log_2 n \rceil$ recursive phases remains bounded and proportional to the length of the first phase. (Since we are considering the asymptotic case in which the number of targets is very large, the length of the beads will be very small; in the remainder of this section we will tacitly consider the asymptotic behavior as $\ell/\rho \rightarrow 0^+$.)

Lemma 3.1 (Path length for the first phase) *Consider a tiling of the plane with beads of length ℓ . For any $\rho > 0$ and for any set of target points, the length L_1 of a path visiting once and only once each bead with a non-empty intersection with a rectangle \mathcal{Q} of width W and length H satisfies*

$$L_1 \leq \frac{16\rho WH}{\ell^2} \left(1 + \frac{7}{3}\pi \frac{\rho}{W} \right) + \rho \cdot o\left(\frac{\rho}{\ell}\right).$$

Proof. A path visiting each bead once can be constructed by a sequence of passes, during which all beads in a row are visited in a left-to-right or right-to-left order. In each row, there are at most $\lceil W/\ell \rceil + 1$ beads with a non-empty intersection with \mathcal{Q} . Hence, the cost of each pass is at most:

$$L_1^{\text{pass}} \leq W + 2\ell + \rho \cdot o\left(\frac{\ell^2}{\rho^2}\right).$$

Two passes are connected by a U-turn maneuver, in which the direction of travel is reversed, and the path moves to the next row, at distance equal to one half the width of a bead. Since the length of the shortest path to reverse the heading of a Dubins vehicle with co-located initial and final points is $(7/3)\pi\rho$, the length of the U-turn satisfies

$$L_1^{\text{U-turn}} \leq \frac{7}{3}\pi\rho + \frac{1}{2}w(\ell) \leq \frac{7}{3}\pi\rho + \frac{\ell^2}{16\rho} + \rho \cdot o\left(\frac{\ell^3}{\rho^3}\right).$$

The total number of passes, i.e., the total number of rows of beads with non-empty intersection with \mathcal{Q} , satisfies

$$N_1^{\text{pass}} \leq \left\lceil \frac{2H}{w(\ell)} \right\rceil + 1 \leq \frac{16\rho H}{\ell^2} + 2 + o\left(\frac{\rho}{\ell}\right).$$

A simple upper bound on the cost of closing the tour is given by

$$L_1^{\text{close}} \leq (W + 2\ell) + (H + 2w(\ell)) + 2\pi\rho = W + H + 2\pi\rho + 2\ell + \rho \cdot o(\ell/\rho).$$

In summary, the total length of the path followed during the first phase is

$$\begin{aligned} L_1 &\leq N_1^{\text{pass}} (L_1^{\text{pass}} + L_1^{\text{U-turn}}) + L_1^{\text{close}} \\ &\leq \left(\frac{16\rho H}{\ell^2} + 2 + o\left(\frac{\rho}{\ell}\right) \right) \left(W + 2\ell + \frac{7}{3}\pi\rho + \frac{\ell^2}{16\rho} + \rho \cdot o\left(\frac{\ell^2}{\rho^2}\right) \right) \\ &\quad + W + H + 2\pi\rho + 2\ell + \rho \cdot o(\ell/\rho) \\ &\leq \frac{16\rho WH}{\ell^2} \left(1 + \frac{7}{3}\pi \frac{\rho}{W} \right) + \rho \cdot o\left(\frac{\rho}{\ell}\right). \end{aligned}$$

■

Based on this calculation, we can estimate the length of the paths in generic phases of the algorithm. Since the total number of phases in the algorithm depends on the number of targets n , as does the length of the beads ℓ , we will retain explicitly the dependency on the phase number.

Lemma 3.2 (Path length at odd-numbered phases) *Consider a tiling of the plane with beads of length ℓ . For any $\rho > 0$ and for any set of target points, the length L_{2j-1} of a path visiting once and only once each meta-bead with a non-empty intersection with a rectangle \mathcal{Q} of width W and length H at phase number $(2j - 1)$, $j \in \mathbb{N}$ satisfies*

$$L_{2j-1} \leq 2^{5-j} \left[\frac{\rho WH}{\ell^2} \left(1 + \frac{7}{3}\pi \frac{\rho}{W} \right) + \rho \cdot o\left(\frac{\rho}{\ell}\right) \right] + 32 \frac{\rho H}{\ell} + \rho \cdot o\left(\frac{\rho}{\ell}\right) + 2^j \left[3\ell + \rho \cdot o\left(\frac{\ell}{\rho}\right) \right].$$

Proof. During odd-numbered phases, the number of beads in a meta-bead is a perfect square and the considerations made in the proof of Lemma 3.1 can be readily adapted. The length of each pass satisfies

$$L_{2j-1}^{\text{pass}} \leq (W + 2^j \ell) \left[1 + o\left(\frac{\ell}{\rho}\right) \right].$$

The length of each U-turn maneuver is bounded as

$$L_{2j-1}^{\text{U-turn}} \leq \frac{7}{3}\pi\rho + 2^{j-2}w(\ell) \leq \frac{7}{3}\pi\rho + 2^{j-2} \left[\frac{\ell^2}{8\rho} + \rho \cdot o\left(\frac{\ell^3}{\rho^3}\right) \right],$$

from which

$$L_{2j-1}^{\text{pass}} + L_{2j-1}^{\text{U-turn}} = W + \frac{7}{3}\pi\rho + o\left(\frac{\ell}{\rho}\right) + 2^j \left[\ell + \rho \cdot o\left(\frac{\ell}{\rho}\right) \right].$$

The number of passes satisfies:

$$N_{2j-1}^{\text{pass}} \leq 2^{5-j} \left[\frac{\rho H}{\ell^2} + o\left(\frac{\rho}{\ell}\right) \right] + 2.$$

Finally, the cost of closing the tour is bounded by

$$L_{2j-1}^{\text{close}} \leq W + H + 2\pi\rho + 2^j [\ell + \rho \cdot o(\ell/\rho)].$$

Therefore, a bound on the total length of the path is

$$\begin{aligned} L_{2j-1} &= N_{2j-1}^{\text{pass}}(L_{2j-1}^{\text{pass}} + L_{2j-1}^{\text{U-turn}}) + L_{2j-1}^{\text{close}} \\ &\leq 2^{5-j} \left[\frac{\rho W H}{\ell^2} \left(1 + \frac{7\pi\rho}{3W} \right) + \rho \cdot o\left(\frac{\rho}{\ell}\right) \right] + 32\frac{\rho H}{\ell} + \rho \cdot o\left(\frac{\rho}{\ell}\right) + 2^j \left[3\ell + \rho \cdot o\left(\frac{\ell}{\rho}\right) \right]. \end{aligned}$$

■

Lemma 3.3 (Path length at even-numbered phases) *Consider a tiling of the plane with beads of length ℓ . For any $\rho > 0$, a rectangle \mathcal{Q} of width W and length H and any set of target points, paths in each phase of the algorithm can be chosen such that $L_{2j} \leq 2L_{2j+1}$, for all $j \in \mathbb{N}$.*

Proof. Consider a generic meta-bead B_{2j+1} traversed in the $(2j+1)^{\text{th}}$ phase, and let l_3 be the length of the path segment within B_{2j+1} . The same meta-bead is traversed at most twice during the $(2j)^{\text{th}}$ phase; let l_1, l_2 be the lengths of the two path segments of the $(2j)^{\text{th}}$ phase within B_{2j+1} . By convention, for $i \in \{1, 2, 3\}$, we let $l_i = 0$ if the i^{th} path does not intersect B_{2j+1} . Without loss of generality, the order of target points can be chosen in such a way that $l_1 \leq l_2 \leq l_3$, and hence $l_1 + l_2 \leq 2l_3$. Repeating the same argument for all non-empty meta-beads, we prove the claim. \blacksquare

Finally, we can summarize these intermediate bounds into the main result of this section. We let $L_{\text{RBTA},\rho}(P)$ denote the length of the Dubins path computed by the RECURSIVE BEAD-TILING ALGORITHM for a point set P .

Theorem 3.4 (Path length for the Recursive Bead-Tiling Algorithm) *Let $P \in \mathcal{P}_n$ be uniformly randomly generated in the rectangle of width W and height H . For any $\rho > 0$, with high probability*

$$\lim_{n \rightarrow +\infty} \frac{\text{DTSP}_\rho(P)}{n^{2/3}} \leq \lim_{n \rightarrow +\infty} \frac{L_{\text{RBTA},\rho}(P)}{n^{2/3}} \leq 24 \sqrt[3]{\rho W H} \left(1 + \frac{7}{3} \pi \frac{\rho}{W} \right).$$

Proof. For simplicity we let $L_{\text{RBTA},\rho}(P) = L_{\text{RBTA}}$. Clearly, $L_{\text{RBTA}} = L'_{\text{RBTA}} + L''_{\text{RBTA}}$, where L'_{RBTA} is the path length of the first $\lceil \log_2 n \rceil$ phases of the algorithm and L''_{RBTA} is the length of the path required to visit all remaining targets. An immediate consequence of Lemma 3.3, is that

$$L'_{\text{RBTA}} = \sum_{i=1}^{\lceil \log_2(n) \rceil} L_i \leq 3 \sum_{j=1}^{\lceil \log_2(n)/2 \rceil} L_{2j-1}.$$

The summation on the right hand side of this equation can be expanded using Lemma 3.2, yielding

$$L'_{\text{RBTA}} \leq 3 \left\{ \left[\frac{\rho W H}{\ell^2} \left(1 + \frac{7 \pi \rho}{3 W} \right) + \rho \cdot o \left(\frac{\rho^2}{\ell^2} \right) \right] \sum_{j=1}^{\lceil \log_2(n)/2 \rceil} 2^{5-j} \right. \\ \left. + \left(32 \frac{\rho H}{\ell} + \rho \cdot o \left(\frac{\rho}{\ell} \right) \right) \left\lceil \frac{\log_2 n}{2} \right\rceil + [3\ell + \rho \cdot o(\ell/\rho)] \sum_{j=1}^{\lceil \log_2(n)/2 \rceil} 2^j \right\}.$$

Since $\sum_{j=1}^k 2^{-j} \leq \sum_{j=1}^{+\infty} 2^{-j} = 1$, and $\sum_{j=1}^k 2^j = 2^{k+1} - 2 \leq 2^{k+1}$, the previous equation can be simplified to

$$L'_{\text{RBTA}} \leq 3 \left\{ 32 \left[\frac{\rho W H}{\ell^2} \left(1 + \frac{7 \pi \rho}{3 W} \right) + \rho \cdot o \left(\frac{\rho}{\ell} \right) \right] \right. \\ \left. + \left(32 \frac{\rho H}{\ell} + \rho \cdot o \left(\frac{\ell}{\rho} \right) \right) \left\lceil \frac{\log_2 n}{2} \right\rceil + [3\ell + \rho \cdot o(\ell/\rho)] \cdot (4\sqrt{n}) \right\}.$$

Recalling that $\ell = 2(\rho W H/n)^{1/3} + o(n^{-1/3})$ for large n , the above can be rewritten as

$$L'_{\text{RBTA}} \leq 24 \sqrt[3]{\rho W H n^2} \left(1 + \frac{7}{3} \pi \frac{\rho}{W} \right) + o(n^{2/3}).$$

Now it suffices to show that L''_{RBTA} is negligible with respect to L'_{RBTA} for large n with high probability. From Theorem 3.3, we know that with high probability there will be at most $24 \log_2 n$ unvisited targets after the $\lceil \log_2 n \rceil$ recursive phases. From Lemma 2.1 we know that, with high probability, the length of a **ALTERNATING ALGORITHM** tour through these points satisfies

$$L''_{\text{RBTA}} \leq \kappa \lceil 12 \log_2 n \rceil \pi \rho + o(\log_2 n).$$

■

Remark 3.5 *Theorems 3.1 and 3.4 imply that, with high probability, the **RECURSIVE BEAD-TILING ALGORITHM** is a constant factor approximation (with*

respect to n) to the optimal DTSP and that $\text{DTSP}_\rho(P)$ belongs to $\Theta(n^{2/3})$. The computational complexity of the RECURSIVE BEAD-TILING ALGORITHM is of order n . \square

3.5 The DTRP for a single vehicle

We now turn our attention to the Dynamic Traveling Repairperson Problem (DTRP) that was introduced by Bertsimas and van Ryzin in [24]. When compared with previous work, the novel feature of the following work is the focus on the Dubins vehicle.

3.5.1 Model and problem statement

In this subsection we describe the vehicle and sensing model and the DTRP definition. The key aspect of the DTRP is that the Dubins vehicle is required to visit a dynamically growing set of targets, generated by some stochastic process. We assume that the Dubins vehicle has unlimited range and target-servicing capacity and that it moves at a unit speed with minimum turning radius $\rho > 0$.

Information about the outstanding targets representing the demand at time t is described by a finite set of positions $D(t) \subset \mathcal{Q}$, with $n(t) := \text{card}(D(t))$. Targets are generated, and inserted into D , according to a homogeneous (i.e., time-invariant) spatio-temporal Poisson process, with time intensity $\lambda > 0$, and uniform spatial density inside the rectangle \mathcal{Q} of width W and height H . In other words, given a set $\mathcal{S} \subseteq \mathcal{Q}$, the expected number of targets generated in \mathcal{S} within

the time interval $[t, t']$ is

$$\mathbb{E} [\text{card}(D(t') \cap \mathcal{S}) - \text{card}(D(t) \cap \mathcal{S})] = \lambda(t' - t) \text{Area}(\mathcal{S}).$$

(Strictly speaking, the above equation holds when targets are not being removed from the queue D .) Servicing of a target and its removal from the set D , is achieved when the Dubins vehicle moves to the target position.

A feedback control policy for the Dubins vehicle is a map Φ assigning a control input to the vehicle as a function of its configuration and of the current outstanding targets. We also consider policies that compute a control input based on a snapshot of the outstanding target configurations at certain time sequences. Let $\mathcal{T}_\Phi = \{t_k\}_{k \in \mathbb{N}}$ be a strictly increasing sequence of times at which such computations are started: with some abuse of terminology, we will say that Φ is a receding horizon strategy if it is based on the most recent target data $D_{\text{rh}}(t)$, where

$$D_{\text{rh}}(t) = D(\max\{t_{\text{rh}} \in \mathcal{T}_\Phi \mid t_{\text{rh}} \leq t\}).$$

The (receding horizon) policy Φ is a stable policy for the DTRP if, under its action

$$n_\Phi = \lim_{t \rightarrow +\infty} \mathbb{E}[n(t) \mid \dot{p} = \Phi(p, D_{\text{rh}})] < +\infty,$$

that is, if the Dubins vehicle is able to service targets at a rate that is, on average, at least as fast as the rate at which new targets are generated. Let T_j be the time that the j^{th} target spends within the set D , i.e., the time elapsed from the time the j^{th} target is generated to the time it is serviced. If the system is stable, then we can write the balance equation (known as Little's formula [43]):

$$n_\Phi = \lambda T_\Phi,$$

where $T_\Phi := \lim_{j \rightarrow +\infty} \mathbb{E}[T_j]$ is the steady-state system time for the DTRP under the policy Φ . Our objective is to minimize the steady-state system time, over all possible feedback control policies, i.e.,

$$T_{\text{DTRP}} = \inf\{T_\Phi \mid \Phi \text{ is a stable control policy}\}.$$

3.5.2 Lower and constructive upper bounds

In what follows, we design a control policy that provides a constant-factor approximation of the optimal achievable performance. Consistently with the theme of the chapter, we consider the case of *heavy load*, i.e., the problem as the time intensity $\lambda \rightarrow +\infty$. We first review from [40] a lower bound for the system time, and then present a novel approximation algorithm providing an upper bound on the performance.

Theorem 3.6 (*Lower bound on the system time for single-vehicle DTRP*) For any $\rho > 0$, the system time T_{DTRP} for the DTRP in a rectangle of width W and height H satisfies

$$\lim_{\lambda \rightarrow +\infty} \frac{T_{\text{DTRP}}}{\lambda^2} \geq \frac{81}{64} \rho W H.$$

Remark 3.7 *Theorem 3.6 implies that the system time for the Dubins vehicle depends quadratically on the time intensity λ , whereas in the Euclidean case it depends only linearly on it, e.g., see [24].* □

We now propose a simple strategy, the BEAD-TILING ALGORITHM, based on the concepts introduced in the previous section. The strategy consists of the following steps:

(i) Tile the plane with beads of length $\ell := \min\{C_{\text{BTA}}/\lambda, 4\rho\}$, where

$$C_{\text{BTA}} = \frac{7 - \sqrt{17}}{4} \left(1 + \frac{7}{3}\pi\frac{\rho}{W}\right)^{-1}. \quad (3.2)$$

(ii) Traverse all non-empty beads once, visiting one target per non-empty bead.

(iii) Repeat step (ii).

The following result characterizes the system time for the closed loop system induced by this algorithm and is based on the bound derived in Lemma 3.1.

Theorem 3.8 (*System time for the BEAD-TILING ALGORITHM*) *For any $\rho > 0$ and $\lambda > 0$, the BEAD-TILING ALGORITHM is a stable policy for the DTRP and the resulting system time T_{BTA} satisfies:*

$$\lim_{\lambda \rightarrow +\infty} \frac{T_{\text{DTRP}}}{\lambda^2} \leq \lim_{\lambda \rightarrow +\infty} \frac{T_{\text{BTA}}}{\lambda^2} \leq 70.5464 \rho W H \left(1 + \frac{7}{3}\pi\frac{\rho}{W}\right)^3.$$

Proof. Consider a generic bead B , with non-empty intersection with \mathcal{Q} . Target points within B will be generated according to a Poisson process with rate λ_B satisfying

$$\lambda_B = \lambda \frac{\text{Area}(B \cap \mathcal{Q})}{WH} \leq \lambda \frac{\text{Area}(B)}{WH} = \frac{C_{\text{BTA}}^3}{16\rho WH \lambda^2} + o\left(\frac{1}{\lambda^2}\right).$$

The vehicle will visit B at least once every L_1 time units, where L_1 is the bound on the length of a path through all beads, as computed in Lemma 3.1. As a consequence, targets in B will be visited at a rate no smaller than

$$\mu_B = \frac{C_{\text{BTA}}^2}{16\rho WH \lambda^2} \left(1 + \frac{7}{3}\pi\frac{\rho}{W}\right)^{-1} + o\left(\frac{1}{\lambda^2}\right).$$

In summary, the expected time T_B between the appearance of a target in B and its servicing by the vehicle is no more than the system time in a queue with

Poisson arrivals at rate λ_B , and deterministic service rate μ_B . Such a queue is called a $M/D/1$ queue in the literature [43], and its system time is known to be

$$T_{M/D/1} = \frac{1}{\mu_B} \left(1 + \frac{1}{2} \frac{\lambda_B}{\mu_B - \lambda_B} \right).$$

Using the computed bounds on λ_B and μ_B , and taking the limit as $\lambda \rightarrow +\infty$, we obtain

$$\lim_{\lambda \rightarrow +\infty} \frac{T_B}{\lambda^2} \leq \lim_{\lambda \rightarrow +\infty} \frac{T_{M/D/1}}{\lambda^2} \leq \frac{16\rho WH}{C_{\text{BTA}}^2 \left(1 + \frac{7}{3}\pi \frac{\rho}{W}\right)^{-1}} \left(1 + \frac{1}{2} \frac{C_{\text{BTA}}}{\left(1 + \frac{7}{3}\pi \frac{\rho}{W}\right)^{-1} - C_{\text{BTA}}} \right). \quad (3.3)$$

Since equation (3.3) holds for *any* bead intersecting \mathcal{Q} , the bound derived for T_B holds for all targets and is therefore a bound on T_{BTA} . The expression on the right hand side of (3.3) is a constant that depends on problem parameters ρ , W , and H , and on the design parameter C_{BTA} , as defined in equation (3.2). Stability of the queue is established by noting that $C_{\text{BTA}} < \left(1 + \frac{7}{3}\pi \rho/W\right)^{-1}$. Additionally, the choice of C_{BTA} in equation (3.2) minimizes the right hand side of (3.3) yielding the numerical bound in the statement. ■

Remark 3.9 *The achievable performance of the BEAD-TILING ALGORITHM provides a constant-factor approximation to the lower bound established in Theorem 3.6. Also, there exists no stable policy for the DTRP when the targets are generated in an adversarial worst-case fashion with $\lambda \geq (\pi\rho)^{-1}$. This fact is a consequence of the linear lower bound on the worst-case DTSP derived in Theorem 2.1.* □

3.6 The DTRP for multiple vehicles

The DTRP problem that was introduced in the earlier section for a single vehicle can be easily extended to the multiple vehicle case. In this section, We first obtain a lower bound for the system time for m homogeneous Dubins vehicles, and then present a novel strategy providing an upper bound on the performance.

Theorem 3.10 (*Lower bound on the system time for single-vehicle DTRP*) For any $\rho > 0$, the system time $T_{\text{DTRP},m}$ for the DTRP for m vehicles in a rectangle of width W and height H satisfies

$$\lim_{\lambda \rightarrow +\infty} \frac{T_{\text{DTRP},m}}{\lambda^2} \geq \frac{81}{64} \frac{\rho W H}{m^3}.$$

Proof. Let us assume that a stabilizing policy is available. In such a case, the number of outstanding targets approaches a finite steady-state value, n^* , related to the system time by Little's formula, i.e., $n^* = \lambda T_{\text{DTRP},m}$. In order for the policy to be stabilizing, the time needed, on average, to service m targets must be no greater than the average time interval in which m new targets are generated. Since there are m vehicles, the average time needed for them to service one target each, in parallel, is no greater than the expected minimum distance (in the Dubins' sense) from an arbitrarily placed vehicle to the closest target; in other words, we can write the stability condition $E[\delta^*(n^*)] \leq m/\lambda$. A bound on the expected value of δ^* has been computed in [40], yielding

$$\frac{3}{4} \left(\frac{3\rho W H}{n^*} \right)^{1/3} \leq E[\delta^*(n^*)] \leq m\lambda.$$

Using Little's formula $n^* = \lambda T_{\text{DTRP},m}$, and rearranging, we get the desired result. ■

From Theorem 3.8, one can infer that the system time depends on (i) the area of the region assigned to a vehicle, and (ii) on the shape of the region. In particular, the system time is minimized, for a given area, when one of its dimensions is maximized. This suggest the following strategy for partitioning the environment \mathcal{Q} , that we call the STRIP-TILING ALGORITHM. Partition \mathcal{Q} into m strips of width W and height H/m and assign each strip to a vehicle. Tile each strip with beads of length $\ell := \min\{mC_{\text{BTA}}/\lambda, 4\rho\}$, where C_{BTA} is given by eq. (3.2). Let each vehicle execute the BEAD-TILING ALGORITHM inside the assigned strip. Then, the following holds:

Theorem 3.11 (*System time for the STRIP-TILING ALGORITHM*) For any $\rho > 0$, $\lambda > 0$ and $m > 0$, the STRIP-TILING ALGORITHM is a stable policy for the DTRP and the resulting system time T_{STA} satisfies:

$$\lim_{\lambda \rightarrow +\infty} \frac{T_{\text{DTRP},m}}{\lambda^2} \leq \lim_{\lambda \rightarrow +\infty} \frac{T_{\text{BTA}}}{\lambda^2} \leq 70.5464 \frac{\rho W H}{m^3} \left(1 + \frac{7}{3}\pi \frac{\rho}{W}\right)^3.$$

Remark 3.12 *The achievable performance of the STRIP-TILING ALGORITHM provides a constant-factor approximation to the lower bound established in Theorem 3.10.* □

3.7 Summary

In this chapter, we have studied the DTSP in the stochastic setting, and obtained upper bounds that are within a constant factor of the lower bound; the upper bounds are constructive in the sense that they are achieved by novel

algorithms. We showed that, given a fixed $\rho > 0$, the *stochastic* $\text{DTSP}_\rho(P)$ belongs to $\Theta(n^{2/3})$ with high probability.

Remarkably, the differences between these various bounds play a crucial role when studying the DTRP; e.g., stable policies exist only when the TSP cost grows strictly sub-linearly with n . For the DTRP we have proposed the novel policy and shown its stability for a uniform target-generation process with intensity λ . It is known [40] that the system time for the DTRP for the Dubins vehicle belongs to $\Omega(\lambda^2)$; the policy proposed in this chapter shows that the system time belongs to $O(\lambda^2)$. Thus, the system time of the DTRP for the Dubins vehicle belongs to $\Theta(\lambda^2)$. This result differs from the result in the Euclidean case, where it is known [24] that the system time belongs to $\Theta(\lambda)$. Therefore, our analysis rigorously establishes the following intuitive fact: bounded-curvature constraints make the system much more sensitive to increases in the target generation rate.

In the next chapter, we extend the analysis of this chapter to other vehicle models and to the three-dimensional space.

Chapter 4

TSPs for a double integrator

In this chapter, we study path planning strategies for a double integrator with bounded velocity and bounded control inputs. First, we study the following version of the Traveling Salesperson Problem (TSP): given a set of points in \mathbb{R}^d , find the fastest tour over the point set for a double integrator. We first give asymptotic bounds on the time taken to complete such a tour in the worst-case. Then, we study a stochastic version of the TSP for double integrator where the points are randomly sampled from a uniform distribution in a compact environment in \mathbb{R}^2 and \mathbb{R}^3 . Lastly, we study the DTRP for a double integrator in \mathbb{R}^2 as well as \mathbb{R}^3 .

This work completes the generalization of the known combinatorial results on the ETSP and DTRP (applicable to systems with single integrator dynamics) to double integrators and Dubins vehicle models. It is interesting to compare our results with the setting where the vehicle is modeled by a single integrator or the so-called Euclidean case in combinatorial optimization. The results are

summarized as follows:

	Single integrator	Double integrator	Dubins vehicle
Min. time for TSP tour (worst-case)	$\Theta(n^{1-\frac{1}{d}})$ [19]	$\Omega(n^{1-\frac{1}{d}}),$ $O(n^{1-\frac{1}{2d}})$	$\Theta(n)$ [25] ($d = 2, 3$)
Exp. min. time for TSP tour (stochastic)	$\Theta(n^{1-\frac{1}{d}})$ [19]	$\Theta(n^{1-\frac{1}{2d-1}})$ w.h.p. ($d = 2, 3$)	$\Theta(n^{1-\frac{1}{2d-1}})$ w.h.p. ($d = 2, 3$)
System time for DTRP	$\Theta(\lambda^{d-1})$ [24] ($d = 1$)	$\Theta(\lambda^{2(d-1)})$ ($d = 2, 3$)	$\Theta(\lambda^{2(d-1)})$ ($d = 2, 3$)

4.1 Setup and worst-case DITSP

For $d \in \mathbb{N}$, consider a vehicle with double integrator dynamics:

$$\ddot{p}(t) = u(t), \quad \|u(t)\| \leq r_{\text{ctr}}, \quad \|\dot{p}(t)\| \leq r_{\text{vel}}, \quad (4.1)$$

where $p \in \mathbb{R}^d$ and $u \in \mathbb{R}^d$ are the position and control input of the vehicle, $r_{\text{vel}} \in \mathbb{R}_+$ and $r_{\text{ctr}} \in \mathbb{R}_+$ are the bounds on the attainable speed and control inputs. Let $\mathcal{Q} \subset \mathbb{R}^d$ be a unit hypercube. Let $P = \{q_1, \dots, q_n\}$ be a set of n points in \mathcal{Q} and \mathcal{P}_n be the collection of all point sets $P \subset \mathcal{Q}$ with cardinality n . Let $\text{ETSP}(P)$ denote the cost of the Euclidean TSP over P and let $\text{DITSP}(P)$ denote the cost of the TSP for double integrator over P , i.e., the time taken to traverse the fastest closed path for a double integrator through all points in P . We assume r_{vel} and r_{ctr} to be constant and we study the dependence of $\text{DITSP}: \mathcal{P}_n \rightarrow \mathbb{R}_+$ on n . Without loss of generality, we assume the vehicle starts traversing the TSP tour at $t = 0$ with initial position q_1 .

Lemma 4.1 (*Worst-case Lower Bound on the TSP for Double Integrator*) For $r_{\text{vel}}, r_{\text{ctr}} \in \mathbb{R}_+$ and $d \in \mathbb{N}$, there exists a point set $P \in \mathcal{P}_n$ in $\mathcal{Q} \subset \mathbb{R}^d$ such that $\text{DITSP}(P)$ belongs to $\Omega(n^{1-\frac{1}{d}})$.

Proof. We consider the class of point sets that give rise to the worst case scenario for the ETSP; we refer the reader to [19]. It suffice to note that, for such a point set of cardinality n in \mathbb{R}^d , the minimum distance between any two points belongs to $\Omega(n^{-\frac{1}{d}})$. The minimum time required for a double integrator with initial speed \tilde{v} to go from one point to another at a distance $\tilde{\delta}$ is lower bounded by $\sqrt{(\tilde{v}/r_{\text{ctr}})^2 + 2(\tilde{\delta}/r_{\text{ctr}})} - \tilde{v}/r_{\text{ctr}}$. However, $\tilde{v} \leq r_{\text{vel}}$ and for the point set under consideration, $\tilde{\delta}$ belongs to $\Omega(n^{-\frac{1}{d}})$. This implies that the minimum time required for a double integrator to travel between two points of the given point set belongs to $\Omega(n^{-\frac{1}{d}})$. Hence, the minimum time required for the vehicle to complete the tour over this point set belongs to $n\Omega(n^{-\frac{1}{d}})$, i.e., $\Omega(n^{1-\frac{1}{d}})$. ■

We now propose a simple strategy for the DITSP and analyze its performance. The STOP-GO-STOP strategy can be described as follows: The vehicle visits the points in the same order as in the optimal ETSP tour over the same set of points. Between any pair of points, the vehicle starts at the initial point at rest, follows the shortest-time path to reach the final point with zero velocity.

Theorem 4.1 (*Upper Bound on the TSP for Double Integrator*) For any point set $P \in \mathcal{P}_n$ in $\mathcal{Q} \subset \mathbb{R}^d$ and $r_{\text{ctr}} > 0$, $r_{\text{vel}} > 0$ and $d \in \mathbb{N}$, $\text{DITSP}(P)$ belongs to $O(n^{1-\frac{1}{2d}})$.

Proof. Without any loss of generality, let (q_1, \dots, q_n, q_1) be the optimal order of points for the Euclidean TSP over P . For $1 \leq i \leq n - 1$, let $\delta_i = \|q_i - q_{i+1}\|$

and $\delta_n = \|q_n - q_1\|$. If δ_i is the distance between a set of points, then the time t_i required to traverse that distance by a double integrator following the STOP-GO-STOP strategy is given by:

$$t_i = \begin{cases} 2\sqrt{\frac{\delta_i}{r_{\text{ctr}}}}, & \text{if } \delta_i \leq \frac{r_{\text{vel}}^2}{r_{\text{ctr}}}, \\ \frac{r_{\text{vel}}}{r_{\text{ctr}}} + \frac{\delta_i}{r_{\text{vel}}}, & \text{otherwise.} \end{cases}$$

Let $\mathcal{I} = \{1 \leq i \leq n \mid \delta_i \leq r_{\text{vel}}^2/r_{\text{ctr}}\}$ and $\mathcal{I}^c = \{1, \dots, n\} \setminus \mathcal{I}$. Also, let $n_{\mathcal{I}}$ be the cardinality of the set \mathcal{I} and let $n_{\mathcal{I}^c} = n - n_{\mathcal{I}}$. Therefore, an upper bound on the minimum time taken to complete the tour as obtained from this strategy is

$$\begin{aligned} \text{DITSP}(P) &\leq \sum_{i=1}^n t_i = \sum_{i \in \mathcal{I}} t_i + \sum_{i \in \mathcal{I}^c} t_i = \frac{2}{\sqrt{r_{\text{ctr}}}} \sum_{i \in \mathcal{I}} \sqrt{\delta_i} + n_{\mathcal{I}^c} \frac{r_{\text{vel}}}{r_{\text{ctr}}} + \frac{1}{r_{\text{vel}}} \sum_{i \in \mathcal{I}^c} \delta_i \\ &\leq \frac{2}{\sqrt{r_{\text{ctr}}}} \sum_{i \in \mathcal{I}} \sqrt{\delta_i} + n_{\mathcal{I}^c} \left(\frac{r_{\text{vel}}}{r_{\text{ctr}}} + \frac{\text{diam}(\mathcal{Q})}{r_{\text{vel}}} \right), \end{aligned} \tag{4.2}$$

where $\text{diam}(\mathcal{Q})$ is the length of the largest segment lying completely inside \mathcal{Q} . From the well known upper bound [19] on the tour length of optimal ETSP, there exists a constant $\beta(\mathcal{Q})$ such that $\sum_{i \in \mathcal{I}} \delta_i \leq \sum_{i=1}^n \delta_i \leq \beta(\mathcal{Q})n^{1-\frac{1}{d}}$. Hence an upper bound on the term $\sum_{i \in \mathcal{I}} \sqrt{\delta_i}$ in eqn. (4.2) can be obtained by solving the following optimization problem:

$$\text{maximize } \sum_{i \in \mathcal{I}} \sqrt{\delta_i}, \quad \text{subj. to } \sum_{i \in \mathcal{I}} \delta_i \leq \beta(\mathcal{Q})n^{1-\frac{1}{d}}.$$

By employing the method of Lagrange multipliers, one can see that the maximum is achieved when $\delta_i = \beta(\mathcal{Q}) \frac{n^{1-\frac{1}{d}}}{n_{\mathcal{I}}} \quad \forall i \in \mathcal{I}$. Hence $\sum_{i \in \mathcal{I}} \sqrt{\delta_i} \leq \sqrt{\beta(\mathcal{Q})} \sqrt{n_{\mathcal{I}} n^{1-\frac{1}{d}}}$. Substituting this in eqn. (4.2), we get that

$$\text{DITSP}(P) \leq \frac{2\sqrt{\beta(\mathcal{Q})}}{\sqrt{r_{\text{ctr}}}} \sqrt{n_{\mathcal{I}} n^{\frac{1}{2}-\frac{1}{2d}}} + n_{\mathcal{I}^c} \left(\frac{r_{\text{vel}}}{r_{\text{ctr}}} + \frac{\text{diam}(\mathcal{Q})}{r_{\text{vel}}} \right). \tag{4.3}$$

However, $n_{\mathcal{I}} \leq n$ and Lemma 4.2 implies that $n_{\mathcal{I}^c}$ belongs to $O(n^{1-\frac{1}{d}})$. Incorporating these facts into eqn. (4.3), one arrives at the final result. ■

The above theorem relies on the following key result.

Lemma 4.2 *Given any point set $P \in \mathcal{P}_n$ in $\mathcal{Q} \subset \mathbb{R}^d$, if $(q_1, q_2, \dots, q_n, q_1)$ is the order of points for the optimal ETSP tour over P , then for any $\eta \in \mathbb{R}_+$, the cardinality of the set $\{q_i \in P \mid \|q_i - q_{i+1}\| > \eta\}$ belongs to $O(n^{1-\frac{1}{d}})$.*

Proof. By contradiction, assume there exists $\tilde{\eta} \in \mathbb{R}_+$ such that the cardinality of $\{p_i \in P \mid \|q_i - q_{i+1}\| > \tilde{\eta}\}$ belongs to $\Omega(n^{1-\frac{1}{d}+\epsilon})$ for some $\epsilon > 0$. This implies that $\text{ETSP}(P)$ belongs to $\tilde{\eta} \times \Omega(n^{1-\frac{1}{d}+\epsilon}) = \Omega(n^{1-\frac{1}{d}+\epsilon})$. However, we know from [19] that $\text{ETSP}(P) \in O(n^{1-\frac{1}{d}})$. ■

4.2 The stochastic DITSP

The results in the previous section showed that based on a simple strategy, the STOP-GO-STOP strategy, we are already guaranteed to have sub-linear cost for the DITSP when the point sets are considered on an individual basis. However, it is reasonable to argue that there might be better algorithms when one is concerned with *average* performance. In particular, one can expect that when n target points are stochastically generated in \mathcal{Q} according to a uniform probability distribution function, the cost of DITSP should be lower than the one given by the STOP-GO-STOP strategy. We shall refer to the problem of studying the average performance of DITSP over this class of point sets as *stochastic* DITSP. In this section, we present novel algorithms for stochastic DITSP and then establish bounds on their performances.

We make the following assumptions: in \mathbb{R}^2 , \mathcal{Q} is a rectangle of width W and height H with $W \geq H$; in \mathbb{R}^3 , \mathcal{Q} is a rectangular box of width W , height H and depth D with $W \geq H \geq D$. Different choices for the shape of \mathcal{Q} affect our conclusions only by a constant. The axes of the reference frame are parallel to the sides of \mathcal{Q} . The points $P = (p_1, \dots, p_n)$ are randomly generated according to a uniform distribution in \mathcal{Q} .

4.2.1 Lower bounds

First we provide lower bounds on the expected length of stochastic DITSP for the 2 and 3 dimensional case.

Theorem 4.2 (*Lower bounds on stochastic DITSP*) For all $r_{\text{vel}} > 0$ and $r_{\text{ctr}} > 0$, the expected cost of a stochastic DITSP visiting a set of n uniformly-randomly-generated points satisfies the following inequalities:

$$\begin{aligned} \lim_{n \rightarrow +\infty} \frac{\mathbb{E}[\text{DITSP}(P \subset \mathcal{Q} \subset \mathbb{R}^2)]}{n^{2/3}} &\geq \frac{3}{4} \left(\frac{6WH}{r_{\text{vel}} r_{\text{ctr}}} \right)^{1/3} \quad \text{and} \\ \lim_{n \rightarrow +\infty} \frac{\mathbb{E}[\text{DITSP}(P \subset \mathcal{Q} \subset \mathbb{R}^3)]}{n^{4/5}} &\geq \frac{5}{6} \left(\frac{20WHD}{\pi r_{\text{vel}} r_{\text{ctr}}^2} \right)^{1/5}. \end{aligned}$$

Proof. We first prove the first inequality. Choose a random point $q_i \in P$ as the initial position and v_i as the initial speed of the vehicle on the tour, and choose the heading randomly. We would like to compute a bound on the expected time to the closest next point in the tour; let us call such a time t^* . To this purpose, consider the set R_t of points that are reachable by a second order vehicle within time t . It can be verified that the area of such a set can be bounded, as $t \rightarrow 0^+$, by

$$\text{Area}(R_t) \leq \frac{r_{\text{ctr}} v_i t^3}{6} + o(t^3) \leq \frac{r_{\text{ctr}} r_{\text{vel}} t^3}{6} + o(t^3). \quad (4.4)$$

Given time t , the probability that $t^* > t$ is no less than the probability that there is no other target reachable within a time at most t ; in other words,

$$\Pr[t^* > t] \geq 1 - n \frac{\text{Area}(R_t)}{\text{Area}(\mathcal{Q})} \geq 1 - n \frac{r_{\text{ctr}} r_{\text{vel}} t^3}{6WH} - o(t^3).$$

In terms of expectation, defining $c = \frac{nr_{\text{ctr}}r_{\text{vel}}}{6WH}$,

$$\begin{aligned} \mathbb{E}[t^*] &= \int_0^{+\infty} \Pr(t^* > \xi) d\xi \\ &\geq \int_0^{+\infty} \max\left\{0, 1 - \frac{nr_{\text{ctr}}r_{\text{vel}}}{6WH} \xi^3 - o(\xi^3)\right\} d\xi \\ &\geq \int_0^{c^{-1/3}} (1 - c\xi^3) d\xi - n \int_0^{c^{-1/3}} o(\xi^3) d\xi \\ &= \frac{3}{4} \left(\frac{6WH}{r_{\text{vel}}r_{\text{ctr}}n} \right)^{1/3} - o(n^{-1/3}). \end{aligned}$$

The expected total tour time will be no smaller than n times the expected shortest time between two points, i.e.,

$$\mathbb{E}[\text{DITSP}(P)_{r_{\text{vel}}, r_{\text{ctr}}2}] \geq \frac{3}{4} \left(\frac{6n^2WH}{r_{\text{vel}}r_{\text{ctr}}} \right)^{1/3} - o(n^{2/3}).$$

Dividing both sides by $n^{2/3}$ and taking the limit as $n \rightarrow +\infty$, we get the first result.

We now prove the second inequality. Choose a random point $q_i \in P$ as the initial position and v_i as the initial speed of the vehicle on the tour, and choose the heading randomly. We would like to compute a bound on the expected time to the closest next point in the tour; let us call such a time t^* . To this purpose, consider the set R_t of points that are reachable by a second order vehicle within time t . It can be verified that the volume of such a set can be bounded, as $t \rightarrow 0^+$, by

$$\text{Volume}(R_t) \leq \frac{\pi r_{\text{ctr}}^2 v_i t^5}{20} + o(t^5) \leq \frac{\pi r_{\text{ctr}}^2 r_{\text{vel}} t^5}{20} + o(t^5). \quad (4.5)$$

Given time t , the probability that $t^* > t$ is no less than the probability that there is no other target reachable within a time at most t ; in other words,

$$\Pr[t^* > t] \geq 1 - n \frac{\text{Volume}(R_t)}{\text{Volume}(\mathcal{Q})} \geq 1 - n \frac{\pi r_{\text{ctr}}^2 r_{\text{vel}} t^5}{20WHD} - o(t^5).$$

In terms of expectation, defining $c = \frac{n\pi r_{\text{ctr}}^2 r_{\text{vel}}}{20WHD}$,

$$\begin{aligned} \mathbb{E}[t^*] &= \int_0^{+\infty} \Pr(t^* > \xi) d\xi \\ &\geq \int_0^{+\infty} \max \left\{ 0, 1 - \frac{n\pi r_{\text{ctr}}^2 r_{\text{vel}}}{20WHD} \xi^5 - o(\xi^5) \right\} d\xi \\ &\geq \int_0^{c^{-1/5}} (1 - c\xi^5) d\xi - n \int_0^{c^{-1/5}} o(\xi^5) d\xi \\ &= \frac{5}{6} \left(\frac{20WHD}{r_{\text{vel}} r_{\text{ctr}}^2 n} \right)^{1/5} - o(n^{-1/5}). \end{aligned}$$

The expected total tour time will be no smaller than n times the expected shortest time between two points, i.e.,

$$\mathbb{E}[\text{DITSP}(P)_{r_{\text{vel}}, r_{\text{ctr}}} 3] \geq \frac{5}{6} \left(\frac{20n^4WHD}{r_{\text{vel}} r_{\text{ctr}}^2} \right)^{1/5} - o(n^{4/5}).$$

Dividing both sides by $n^{4/5}$ and taking the limit as $n \rightarrow +\infty$, we get the second result. ■

4.2.2 Relation with the Dubins vehicle

In Chapter 3, we studied stochastic versions of TSP for a Dubins vehicle. Though conventionally a Dubins vehicle is restricted to be a *planar* vehicle, one can easily generalize the model even for the three (and higher) dimensional case. Correspondingly, a Dubins vehicle can be defined as a vehicle that is constrained

to move with a constant speed along paths of bounded curvature, without reversing direction. Accordingly, a *feasible curve for a Dubins vehicle* or a *Dubins path* is defined as a curve that is twice differentiable almost everywhere, and such that the magnitude of its curvature is bounded above by $1/\rho$, where $\rho > 0$ is the minimum turn radius. Based on this, one can immediately come up with the following analogy between feasible curves for a Dubins vehicle and a double integrator.

Lemma 4.3 (*Trajectories of Dubins vehicles and double integrators*) *For all $\rho > 0$ such that $\sqrt{\rho r_{\text{ctr}}} \leq r_{\text{vel}}$, a feasible curve for a Dubins vehicle with minimum turn radius ρ is a feasible curve for a double integrator (modeled in eqn. (4.1)) moving with a constant speed $\sqrt{\rho r_{\text{ctr}}}$. Conversely, a feasible curve for a double integrator moving with a constant speed $s \leq r_{\text{vel}}$ is a feasible curve for Dubins vehicle with minimum turn radius s^2/r_{ctr} .*

In Chapter 3, we proposed a novel algorithm, the RECURSIVE BEAD-TILING ALGORITHM (RECBTA) for the stochastic version of the Dubins TSP (DTSP) in \mathbb{R}^2 ; we showed that this algorithm performed within a constant factor of the optimal with high probability. In this section, taking inspiration from those ideas, we propose an algorithm to compute feasible curves for a double integrator moving with constant speed r_{vel} . Note that moving at the maximum speed r_{vel} is not necessarily the best strategy since it restricts the maneuvering capability of the vehicle. Nonetheless, this strategy leads to efficient algorithms. We adopt the RECBTA for the stochastic DITSP in \mathbb{R}^2 and based on the same ideas, we propose the RECURSIVE CYLINDER-COVERING ALGORITHM (RECCCA) for stochastic DITSP in \mathbb{R}^3 . We prove that these algorithms perform within a constant factor

of the optimal with high probability.

4.2.3 The basic geometric construction

Here we define useful geometric objects and study their properties. Given the constant speed r_{vel} for the double integrator let $\rho = \frac{r_{\text{vel}}^2}{r_{\text{ctr}}}$; from Lemma 4.3 this constant corresponds to the minimum turning radius of the *analogous* Dubins vehicle. Consider two points p_- and p_+ on the plane, with $\ell = \|p_+ - p_-\|_2 \leq 4\rho$, and construct the bead $\mathcal{B}_\rho(\ell)$ as detailed in Figure 4.1.

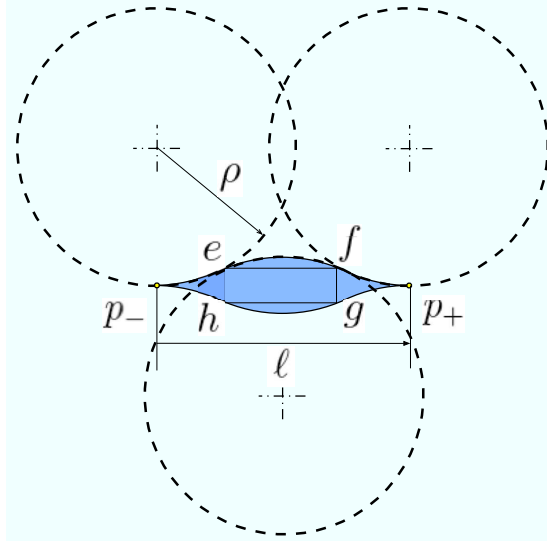


Figure 4.1: Construction of the “bead” $\mathcal{B}_\rho(\ell)$. The figure shows how the upper half of the boundary is constructed, the bottom half is symmetric. The figure shows the rectangle $efgh$ which is used to construct the “cylinder” $\mathcal{C}_\rho(\ell)$.

Associated with the bead is also the rectangle $efgh$. Rotating this rectangle about the line passing through p_- and p_+ gives rise to a cylinder $\mathcal{C}_\rho(\ell)$. $\mathcal{C}_\rho(\ell)$ enjoys the following asymptotic properties as $(l/\rho) \rightarrow 0^+$ (properties of the bead, $\mathcal{B}_\rho(\ell)$ are listed in Chapter 3:

(P1) The length of $\mathcal{C}_\rho(\ell)$ is ℓ and its radius of cross-section is $w(\ell)/4$, where $w(\ell)$ is the maximum *thickness* of the bead $\mathcal{B}_\rho(\ell)$ and it is equal to

$$w(\ell) = 4\rho \left(1 - \sqrt{1 - \frac{\ell^2}{16\rho^2}} \right) = \frac{\ell^2}{8\rho} + \rho \cdot o\left(\frac{\ell^3}{\rho^3}\right).$$

(P2) The volume of $\mathcal{C}_\rho(\ell)$ is equal to

$$\text{Volume}[\mathcal{C}_\rho(\ell)] = \pi \left(\frac{w(\ell)}{4} \right)^2 \frac{\ell}{2} = \frac{\pi \ell^5}{2048\rho^2} + \rho^3 \cdot o\left(\frac{\ell^6}{\rho^6}\right).$$

(P3) For any $p \in \mathcal{C}_\rho$, there is at least one feasible curve γ_p through the points $\{p_-, p, p_+\}$, entirely contained within the region obtained by rotating $\mathcal{B}_\rho(\ell)$ about the line passing through p_- and p_+ . The length of any such path is at most

$$\text{Length}(\gamma_p) \leq 4\rho \arcsin\left(\frac{\ell}{4\rho}\right) = \ell + \rho \cdot o\left(\frac{\ell^3}{\rho^3}\right).$$

The geometric shapes introduced above can be used to cover \mathbb{R}^2 and \mathbb{R}^3 in an *organized* way. The plane can be periodically *tiled*¹ by identical copies of $\mathcal{B}_\rho(\ell)$, for any $\ell \in]0, 4\rho]$. The cylinder, however does not enjoy any such special property. For our purpose, we consider a particular covering of \mathbb{R}^3 by cylinders described as follows.

A *row of cylinders* is formed by joining cylinders end to end along their length. A layer of cylinders is formed by placing rows of cylinders parallel and on top of each other as shown in Figure 4.2. For covering \mathbb{R}^3 , these layers are arranged next to each other and with offsets as shown in Figure 4.3(a), where the cross section of this arrangement is shown. We refer to this construction as the *covering of \mathbb{R}^3* .

¹A tiling of the plane is a collection of sets whose intersection has measure zero and whose union covers the plane.

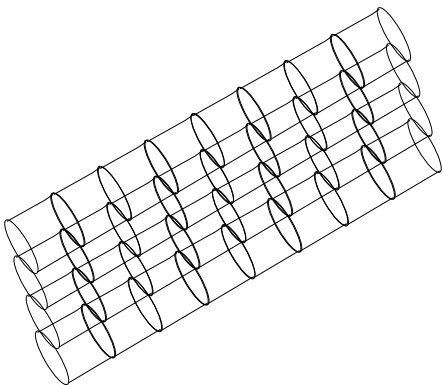


Figure 4.2: A typical layer of cylinders formed by stacking rows of cylinders

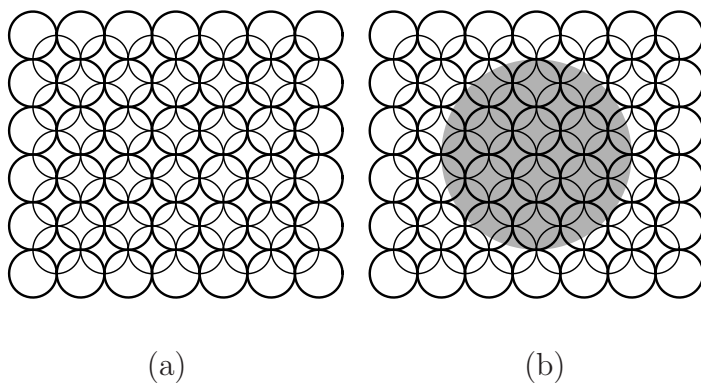


Figure 4.3: (a): Cross section of the arrangement of the layers of cylinders used for covering $\mathcal{Q} \subset \mathbb{R}^3$, (b): The relative position of the bigger cylinder relative to smaller ones of the prior phase during the phase transition.

4.2.4 The algorithm

We adopt the RECURSIVE BEAD-TILING ALGORITHM (RECBTA) (Chapter 3) for the stochastic DITSP in \mathbb{R}^2 . Let $\mathcal{T}_{\text{RecBTA}}$ be the time taken by a double integrator to traverse a stochastic DITSP tour according to the RECBTA. The RECBTA performance is analyzed as follows.

Theorem 4.3 (*Upper bound on the total time in \mathbb{R}^2*) *Let $P \in \mathcal{P}_n$ be uniformly randomly generated in the rectangle of width W and height H . For any double integrator (4.1), with high probability,*

$$\lim_{n \rightarrow +\infty} \frac{\mathcal{T}_{\text{RecBTA}}}{n^{2/3}} \leq 24 \left(\frac{WH}{r_{\text{vel}} r_{\text{ctr}}} \right)^{1/3} \left(1 + \frac{7\pi r_{\text{vel}}^2}{3W r_{\text{ctr}}} \right).$$

Remark 4.4 *Theorems 4.2 and 4.3 imply that, with high probability, the RECBTA is a $\frac{32}{\sqrt[3]{6}} \left(1 + \frac{7\pi r_{\text{vel}}^2}{3W r_{\text{ctr}}} \right)$ -factor approximation (with respect to n) to the optimal stochastic DITSP in \mathbb{R}^2 and that $\mathbb{E}[\text{DITSP}(P \subset \mathcal{Q} \subset \mathbb{R}^2)]$ belongs to $\Theta(n^{2/3})$.*

Taking inspiration from the RECBTA, we now propose the RECURSIVE CYLINDER-COVERING ALGORITHM (RECCCA) for the stochastic DITSP in \mathbb{R}^3 . Consider a covering of $\mathcal{Q} \in \mathbb{R}^3$ by cylinders such that $\text{Volume}[\mathcal{C}_\rho(\ell)] = \text{Volume}[\mathcal{Q} \subset \mathbb{R}^3]/(4n) = WHD/(4n)$ (assuming that n is sufficiently large). Furthermore, the covering is chosen in such a way that it is aligned with the sides of $\mathcal{Q} \subset \mathbb{R}^3$.

The proposed algorithm will consist of a sequence of phases; each phase will consist of five sub-phases, all similar in nature. For the first sub-phase of the first phase, a feasible curve is constructed with the following properties:

- (i) it visits all non-empty cylinders once,

- (ii) it visits all rows of cylinders in a layer in sequence top-to-down in a layer, alternating between left-to-right and right-to-left passes, and visiting all non-empty cylinders in a row,
- (iii) it visits all layers in sequence from one end of the region to the other,
- (iv) when visiting a non-empty cylinder, it services at least one target in it.

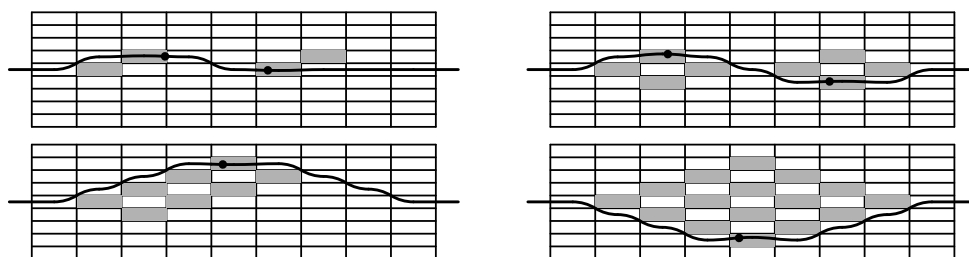


Figure 4.4: From top left in the left-to-right, top-to bottom direction, sketch of projection of “meta-cylinders” on the corresponding side of $\mathcal{Q} \subset \mathbb{R}^3$ at second, third, fourth and fifth sub-phases of a phase in the recursive cylinder covering algorithm.

In subsequent sub-phases, instead of considering single cylinders, we will consider “meta-cylinders” composed of 2, 4, 8 and 16 beads each for the remaining four sub-phases, as shown in Figure 4.4, and proceed in a similar way as the first sub-phase, i.e., a feasible curve is constructed with the following properties:

- (i) the curve visits all non-empty meta-cylinders once,
- (ii) it visits all (meta-cylinder) rows in sequence top-to-down in a (meta-cylinder) layer, alternating between left-to-right and right-to-left passes, and visiting all non-empty meta-cylinders in a row,

- (iii) it visits all (meta-cylinder) layers in sequence from one end of the region to the other,
- (iv) when visiting a non-empty meta-cylinder, it services at least one target in it.

A meta-cylinder at the end of the fifth sub-phase, and hence at the end of the first phase will consist of 16 nearby cylinders. After this phase, the transitioning to the next phase will involve enlarging the cylinder to 32 times its current size by increasing the radius of its cross section by a factor of 4 and doubling its length as outlined in Figure 4.3(b). It is easy to see that this bigger cylinder will contain the union of 32 nearby smaller cylinders. In other words, we are forming the object $\mathcal{C}_\rho(2\ell)$ using a conglomeration of 32 $\mathcal{C}_\rho(\ell)$ objects. This whole process is repeated at most $\log_2 n + 2$ times. After the last phase, the leftover targets will be visited using, for example, a greedy strategy. We have the following result for the leftover targets after the last phase which is similar to the result for RECBTA (Chapter 3).

Theorem 4.5 (Targets remaining after recursive phases) *Let $P \in \mathcal{P}_n$ be uniformly randomly generated in $\mathcal{Q} \subset \mathbb{R}^3$. The number of unvisited targets after the last phase of the RECURSIVE CYLINDER-COVERING ALGORITHM over P is less than $24 \log_2 n$ with high probability.*

We now give a bound on the path length required to execute the first sub-phase.

Lemma 4.4 (Path length for the first sub phase) *Consider a covering of the space with cylinders $\mathcal{C}_\rho(\ell)$. For any $\rho > 0$ and for any set of target points, the*

length L_I of a path executing the first sub-phase of the RECURSIVE CYLINDER-COVERING ALGORITHM in a rectangular box \mathcal{Q} of width W , height H and depth D satisfies

$$L_I \leq \frac{1024\rho^2WHD}{\ell^4} \left(1 + \frac{7\pi\rho}{3W}\right) + \rho \cdot o\left(\frac{\rho^3}{\ell^3}\right).$$

Proof. We first derive bounds on the length of paths required to *sweep* a row of cylinders from one end to the other and to make a *u-turn* when going from one row to another. The results follows from counting the total number of rows required to cover the domain \mathcal{Q} . ■

Similar calculations give the following bounds for the path lengths in subsequent sub-phases.

$$\begin{aligned} L_{II} &\leq \frac{1024\rho^2WHD}{\ell^4} \left(1 + \frac{7\pi\rho}{3W}\right) + \rho \cdot o\left(\frac{\rho^3}{\ell^3}\right), \\ L_{III} &\leq \frac{512\rho^2WHD}{\ell^4} \left(1 + \frac{7\pi\rho}{3W}\right) + \rho \cdot o\left(\frac{\rho^3}{\ell^3}\right), \\ L_{IV} &\leq \frac{512\rho^2WHD}{\ell^4} \left(1 + \frac{7\pi\rho}{3W}\right) + \rho \cdot o\left(\frac{\rho^3}{\ell^3}\right), \\ L_V &\leq \frac{256\rho^2WHD}{\ell^4} \left(1 + \frac{7\pi\rho}{3W}\right) + \rho \cdot o\left(\frac{\rho^3}{\ell^3}\right). \end{aligned}$$

The path length for the first phase is then the sum of the path lengths for the five sub-phases.

Lemma 4.5 (Path length for the first phase) *Consider a covering of the space with cylinders $\mathcal{C}_\rho(\ell)$. For any $\rho > 0$ and for any set of target points, the length L_1 of a path visiting once and only once each cylinder with a non-empty intersection with a rectangular box \mathcal{Q} of width W , height H and depth D satisfies*

$$L_1 \leq \frac{3328\rho^2WHD}{\ell^4} \left(1 + \frac{7\pi\rho}{3W}\right) + \rho \cdot o\left(\frac{\rho^3}{\ell^3}\right).$$

Since we increase the length of cylinders by a factor of two while doing the phase transition from one phase to the another, the length of path for the subsequent i^{th} phase is given by:

$$L_i \leq \frac{3328\rho^2 WHD}{16^i \ell^4} \left(1 + \frac{7\pi\rho}{3W}\right) + \rho \cdot o\left(\frac{\rho^3}{\ell^3}\right).$$

We now state the following result which characterizes the total path length for the RECCCA, which we denote as $L_{\text{RCFA},\rho}(P)$.

Theorem 4.6 (*Path length for the RECURSIVE CYLINDER-COVERING ALGORITHM*) *Let $P \in \mathcal{P}_n$ be uniformly randomly generated in the rectangle of width W , height H and depth D . For any $\rho > 0$, with high probability*

$$\begin{aligned} \lim_{n \rightarrow +\infty} \frac{\text{DITSP}(P \subset \mathcal{Q} \subset \mathbb{R}^3)}{n^{4/5}} &\leq \lim_{n \rightarrow +\infty} \frac{L_{\text{RCFA},\rho}(P)}{n^{4/5}} \\ &\leq \frac{3328}{15} \left(\frac{\pi}{16}\right)^{4/5} (\rho^2 WHD)^{1/5} \left(1 + \frac{7\pi\rho}{3W}\right). \end{aligned}$$

Proof. There are at most $\log_2 n + 2$ phases. By summing the expression for the path length for the i^{th} phase, L_i , over $\log_2 n + 2$ phases and expressing ℓ in terms of the other parameters, we get the desired result. ■

In order to obtain an upper bound on the $\text{DITSP}(P)$ in \mathbb{R}^3 , we derive the expression for time taken, $\mathcal{T}_{\text{RecCCA}}$, by the RECCCA to execute the path of length $L_{\text{RCFA},\rho}(P)$.

Theorem 4.7 (*Upper bound on the total time in \mathbb{R}^3*) *Let $P \in \mathcal{P}_n$ be uniformly randomly generated in the rectangular box of width W , height H and depth D . For any double integrator (4.1), with high probability,*

$$\lim_{n \rightarrow +\infty} \frac{\mathcal{T}_{\text{RecCCA}}}{n^{4/5}} \leq 61 \left(\frac{WHD}{r_{\text{ctr}}^2 r_{\text{vel}}}\right)^{1/5} \left(1 + \frac{7\pi r_{\text{vel}}^2}{3W r_{\text{ctr}}}\right).$$

Proof. We substitute $\rho = \frac{r_{\text{vel}}^2}{r_{\text{ctr}}}$ in the bound for $L_{\text{RCFA},\rho}(P)$ given by Theorem 4.6 and evaluate the time required to traverse the total path of length $L_{\text{RCFA},\rho}(P)$ at speed r_{vel} . ■

Remark 4.8 *Theorems 4.2 and 4.7 imply that, with high probability, the REC-CCA is a $50 \left(1 + \frac{7\pi r_{\text{vel}}^2}{3W r_{\text{ctr}}}\right)$ -factor approximation (with respect to n) to the optimal stochastic DITSP in \mathbb{R}^3 and that $E[\text{DITSP}(P \subset \mathcal{Q} \subset \mathbb{R}^3)]$ belongs to $\Theta(n^{4/5})$.*

4.3 The DTRP for double integrator

We now turn our attention to the Dynamic Traveling Repairperson Problem (DTRP) for the double integrator modeled in eqn. (4.1). In the DTRP, the double integrator is required to visit a dynamically growing set of targets, generated by some stochastic process. We assume that the double integrator has unlimited range and target-servicing capacity. We let $\mathcal{D}(t)$ denote the set of $n(t)$ outstanding target positions representing the demand at time t . Targets are generated and inserted into \mathcal{D} according to a time-invariant spatio-temporal Poisson process with time intensity $\lambda > 0$ and with uniform spatial density inside the region \mathcal{Q} . As before, \mathcal{Q} is a rectangle in two dimensions and a rectangular box in three dimensions. Servicing of a target and its removal from the set \mathcal{D} is achieved when the double integrator moves to the target position. A control policy Φ for the DTRP assigns a control input to the vehicle as a function of its configuration and of the current outstanding targets. The policy Φ is a stable policy for the DTRP if, under its action

$$n_{\Phi} = \lim_{t \rightarrow +\infty} E[n(t) | \dot{p} = \Phi(p, \mathcal{D})] < +\infty,$$

i.e., if the double integrator is able to service targets at a rate that is, on average, at least as large as the target generation rate λ . Let T_j be the time elapsed from the time the j^{th} target is generated to the time it is serviced and let $T_\Phi := \lim_{j \rightarrow +\infty} \mathbb{E}[T_j]$ be the steady-state system time for the DTRP under the policy Φ . (If the system is stable, then it is known [43] that $n_\Phi = \lambda T_\Phi$.)

In what follows, we design a control policy Φ whose system time T_Φ is within a constant-factor approximation of the optimal achievable performance. Consistently with the theme of the chapter, we consider the case of *heavy load*, i.e., the problem as the time intensity $\lambda \rightarrow +\infty$. We first provide lower bounds for the system time, and then present novel approximation algorithms providing upper bound on the performance.

Theorem 4.9 (Lower bound on the DTRP system time) *For a double integrator (4.1), the system time $T_{\text{DTRP},2}$ and $T_{\text{DTRP},3}$ for the DTRP in two and three dimensions satisfy*

$$\lim_{\lambda \rightarrow \infty} \frac{T_{\text{DTRP},2}}{\lambda^2} \geq \frac{81}{32} \frac{WH}{r_{\text{vel}} r_{\text{ctr}}}, \quad \lim_{\lambda \rightarrow \infty} \frac{T_{\text{DTRP},3}}{\lambda^4} \geq \frac{7813}{972} \frac{WHD}{r_{\text{vel}} r_{\text{ctr}}^2}.$$

Proof. For a stable policy, the average time, $t^*(n^*)$, needed to service a target must be no greater than the average time interval in which a new target is generated, i.e., $\mathbb{E}[t^*(n^*)] \leq 1/\lambda$, where n^* is the average number of outstanding targets. This gives a bound on n^* . Using Little's formula [43], one obtains the result. ■

In Chapter 3, we proposed a simple strategy, the BEAD-TILING ALGORITHM (BTA) for the DTRP for Dubins vehicle in \mathbb{R}^2 . We adapt the BTA for the DTRP problem for a double integrator in \mathbb{R}^2 and based on those ideas, we propose the

CYLINDER COVERING ALGORITHM (CCA) for \mathbb{R}^3 . The BTA strategy consists of the following steps:

- (i) Tile the plane with beads of length $\ell := \min\{C_{\text{BTA}}/\lambda, 4\rho\}$, where $C_{\text{BTA}} = 0.5241r_{\text{vel}} \left(1 + \frac{7\pi\rho}{3W}\right)^{-1}$.
- (ii) Traverse all non-empty beads once, visiting one target per bead. Repeat this step.

The CCA strategy is akin to the BTA, where the region is covered with cylinders constructed from beads of length $\ell := \min\{C_{\text{CFA}}/\lambda, 4\rho\}$, where $C_{\text{CCA}} = 0.1615r_{\text{vel}} \left(1 + \frac{7\pi\rho}{3W}\right)^{-1}$. The policy is then to traverse all non-empty cylinders once, visiting one target per cylinder. The following result characterizes the system time for the closed loop system induced by these algorithms and is based on the bounds derived to arrive at Theorems 4.3 and 4.7.

Theorem 4.10 (Upper bound on the DTRP system time) *For a double integrator (4.1) and $\lambda > 0$, the BTA and the CCA are stable policies for the DTRP and the resulting system times T_{BTA} and T_{CFA} satisfy:*

$$\begin{aligned} \lim_{\lambda \rightarrow \infty} \frac{T_{\text{DTRP},2}}{\lambda^2} &\leq \lim_{\lambda \rightarrow \infty} \frac{T_{\text{BTA}}}{\lambda^2} \leq 70.5 \frac{WH}{r_{\text{vel}}r_{\text{ctr}}} \left(1 + \frac{7\pi r_{\text{vel}}^2}{3Wr_{\text{ctr}}}\right)^3, \\ \lim_{\lambda \rightarrow \infty} \frac{T_{\text{DTRP},3}}{\lambda^4} &\leq \lim_{\lambda \rightarrow \infty} \frac{T_{\text{CFA}}}{\lambda^4} \leq 2 \cdot 10^7 \frac{WHD}{r_{\text{vel}}r_{\text{ctr}}^2} \left(1 + \frac{7\pi r_{\text{vel}}^2}{3r_{\text{ctr}}}\right)^5. \end{aligned}$$

Proof. For the given policies, we derive bounds on the target generation rate and servicing rate for a bead/cylinder. The bead/cylinder is then modeled as a standard $M/D/1$ queue and we use the known result [43] for the system time for such a queue. ■

Remark 4.11 *Note that the achievable performances of the BTA and the CCA provide a constant-factor approximation to the lower bounds established in Theorem 4.9.*

4.4 Extension to the TSPs for the Dubins vehicle in \mathbb{R}^3

In Chapter 3, we have studied the Dubins Traveling Salesperson Problem (DTSP) for the planar case. In that chapter, we proposed an algorithm that gave a constant factor approximation to the optimal stochastic DTSP with high probability. This naturally led to a stable policy for the DTRP problem for the Dubins vehicle in \mathbb{R}^2 which also performed within a constant factor of the optimal with high probability. The RECCA developed in this chapter can naturally be extended to apply to the stochastic DTSP in \mathbb{R}^3 . It follows directly from Lemma 4.3 that in order to use the RECCA for a Dubins vehicle with minimum turning radius ρ , one has to simply compute feasible curves for double integrator moving with a constant speed $\sqrt{\rho r_{\text{ctr}}}$. Hence the results stated in Theorem 4.7 and Theorem 4.10 also hold true for the Dubins vehicle.

This equivalence between trajectories makes the RECCA the first known strategy with a strictly sub-linear asymptotic minimum time for the stochastic DTSP in \mathbb{R}^3 . Also novel is that the RECCA performs within a constant factor of the optimal with high probability and gives rise to a constant factor approximation and stabilizing policy for DTRP for Dubins vehicle in \mathbb{R}^3 .

4.5 Summary

In this chapter we have proposed novel algorithms for various TSP problems for vehicles with double integrator dynamics. We showed that the $\text{DITSP}(P)$ belongs to $O(n^{1-\frac{1}{2a}})$ and in the *worst case* also belongs to $\Omega(n^{1-\frac{1}{a}})$. We further proposed novel approximation algorithm and showed that the *stochastic* $\text{DITSP}(P)$ belongs to $\Theta(n^{2/3})$ in \mathbb{R}^2 and to $\Theta(n^{4/5})$ in \mathbb{R}^3 , both with high probability. The policy proposed in this chapter for the DTRP for a double integrator help in proving that the system time belongs to $\Theta(\lambda^2)$ in \mathbb{R}^2 and to $\Theta(\lambda^4)$ in \mathbb{R}^3 . Comparing our results with those for the single integrator [24], we argue that our analysis rigorously establishes the following intuitive fact: higher order dynamics make the system much more sensitive to increases in the target generation rate.

It is interesting to note that the results presented in the chapter hold true even in the presence of small damping in the double integrator dynamics: the lower bounds are the same because the damping only slows down the vehicle; the upper bounds also remain the same as long as the damping coefficient is *relatively small* as compared to r_{ctr} .

Chapter 5

The coverage problem for loitering Dubins vehicles

In this chapter we study a facility location problem for groups of Dubins vehicles, i.e., nonholonomic vehicles that are constrained to move along planar paths of bounded curvature, without reversing direction. Given a compact region and a group of Dubins vehicles, the coverage problem is to minimize the worst-case traveling time from any vehicle to any point in the region. Since the vehicles cannot hover, we assume that they fly along static closed curves called *loitering curves*. The chapter presents *circular loitering patterns* for a Dubins vehicle and for a group of Dubins vehicles that minimize the worst-case traveling time in sufficiently large regions. We do this by establishing an analogy to the disk covering problem.

5.1 Problem Setup and notations

In this section we setup the main problem of the chapter and review some basic required notation. A *Dubins vehicle* is a planar vehicle that is constrained to move along paths of bounded curvature, without reversing direction and maintaining a constant speed. We will design loitering patterns for n Dubins vehicle with unlimited sensing range in a compact region $\mathcal{Q} \subset \mathbb{R}^2$. Given a duration $T > 0$, let $\gamma : [0, T] \rightarrow \mathbb{R}^2$ be a *closed feasible curve for the Dubins vehicle* or a *closed Dubins path*, i.e., γ is a curve that is twice differentiable almost anywhere, $\|\gamma'(t)\| = 1$ for all $t \in [0, T]$, and the magnitude of the curvature of γ is bounded above by $1/\rho$, where $\rho > 0$ is the minimum turning radius and $\gamma(0) = \gamma(T)$. The configuration of the Dubins vehicle traversing the curve γ will be denoted by $g_\gamma(t)$, where $g_\gamma(t) = (\gamma(t), \text{ArcTan}(\gamma'(t))) \in \text{SE}(2)$, where $\text{SE}(2)$ is the special Euclidean group of dimension 2. Let $\Gamma_\rho = \{\gamma \mid \gamma \text{ is a closed Dubins path}\}$. The loitering curves that are designed in this chapter belong to Γ_ρ .

Given n vehicles, a *team composition* can be represented as $\{m_1, \dots, m_n\}$, where $m_i \in \mathbb{N} \cup \{0\}$ and $\sum_{i=1}^n m_i = n$, where \mathbb{N} is the set of all natural numbers. let $\mathcal{M}(n)$ denote the set of all such possible team compositions. In particular, if there are $\ell \leq n$ teams, then the team composition will be given by $\{m_1, \dots, m_\ell, 0, \dots, 0\}$. The idea is to partition \mathcal{Q} into ℓ sub-regions such that each team is responsible for one sub-region. Given ℓ teams, let $\Lambda = (\gamma_1, \dots, \gamma_\ell) \in \Gamma_\rho^\ell$ be a set of closed Dubins path for the teams. These curves will represent the *loitering curves* for the Dubins vehicle. In this chapter we will be concerned with minimizing the worst case traveling time by the *closest* Dubins vehicle to any arbitrary (unknown) target point in \mathcal{Q} . Since we constrain the vehicles to move

at constant (unit) speed along the curves, one can prove by symmetry that the vehicles that are part of the same team are equally spaced along their common loitering curve and move in the same direction (i.e., clockwise/counter-clockwise). Therefore, given a region \mathcal{Q} and a team composition $M = (m_1, \dots, m_\ell, 0, \dots, 0)$, Λ completely specifies the loitering *pattern*.

We now define the coverage cost associated with a given loitering pattern. Let $L_\rho : \text{SE}(2) \times \mathbb{R}^2 \rightarrow \mathbb{R}_+$ be the length of the shortest Dubins path from initial position and orientation described by an element of $\text{SE}(2)$ to a point $q \in \mathbb{R}^2$, where \mathbb{R} is the set of real numbers and \mathbb{R}_+ is the set of positive real numbers. Recall that L_ρ is continuous almost everywhere [44].

Definition 5.1 (Coverage cost) *Given a region \mathcal{Q} , a team composition M , and a loitering pattern $\Lambda = (\gamma_1, \dots, \gamma_\ell)$ with durations (T_1, \dots, T_ℓ) , define the coverage cost associated with the loitering pattern by*

$$\mathcal{T}_{\mathcal{Q},M}(\Lambda) := \sup_{q \in \mathcal{Q}} \min_{i \in \{1, \dots, \ell\}} \sup_{s \in [0, \frac{T_i}{m_i})} \min_{j \in \{1, \dots, m_i\}} L_\rho \left(g_{\gamma_i} \left(s + \frac{(j-1)T_i}{m_i} \right), q \right).$$

The coverage cost gives the worst-case traveling time from any vehicle to any point in the region. In the rest of the chapter, we will use coverage cost and cost interchangeably. The minimum cost associated with the given region \mathcal{Q} and team composition M is defined by

$$\mathcal{T}_{\mathcal{Q},M}^* := \inf_{\Lambda \in \Gamma_\rho^\ell} \mathcal{T}_{\mathcal{Q},M}(\Lambda).$$

Finally, the minimum cost associated with the given region \mathcal{Q} is defined as

$$\mathcal{T}_{\mathcal{Q}}^{**} := \min_{M \in \mathcal{M}(n)} \mathcal{T}_{\mathcal{Q},M}^*.$$

In general, the optimal loitering patterns will have to be computed based on the shape of the region \mathcal{Q} . However, we will concentrate on *circular loitering patterns*; the rationale for doing so is that it (simplifies the problem and) allows us to provide algorithms and bounds that are independent of the particular shape of the environment. Furthermore, it seems unlikely that UAVs in the field will be able to compute optimal loitering patterns as their assigned regions change in real time; on the other hand, determining the location of the center, and the radius of a circular loitering patterns are much easier tasks.

For a given center $c \in \mathbb{R}^2$, radius $r \in \mathbb{R}_+$, let $\mathcal{O}^+(c, r) : [0, T] \rightarrow \mathbb{R}^2$ represent a circular curve of radius r with center c with counter-clockwise orientation. Similarly let $\mathcal{O}^-(c, r)$ represent one with clockwise orientation. Since we will be concentrating only on circular curves, with a slight abuse of notation, we shall use Γ_ρ to denote the set the circular curves with radii greater than or equal to ρ , i.e.,

$$\Gamma_\rho = \{\mathcal{O}^+(c, r) \mid r \geq \rho\} \cup \{\mathcal{O}^-(c, r) \mid r \geq \rho\}.$$

Accordingly, define a *sub-minimum* cost associated with the given region \mathcal{Q} and team composition M as:

$$\tilde{\mathcal{T}}_{\mathcal{Q}, M}^* := \inf_{\Lambda \in \Gamma_\rho^\ell} \mathcal{T}_{\mathcal{Q}, M}(\Lambda), \quad (5.1)$$

where the set of loitering curves is now a set of circular curves with centers at c_1, \dots, c_ℓ and radii r_1, \dots, r_ℓ .

We are now ready to formulate the problem statement: Given n Dubins vehicles with known team composition, design circular loitering patterns that minimize the cost function given by eq. (5.1).

We need to define a few more notations and concepts. Consider a point $c \in \mathbb{R}^2$

and $r \in \mathbb{R}_+$, let $C(c, r)$ be the circle with center at c and of radius r . For a region $U \subset \mathbb{R}^2$, let $U^{2\pi}(c)$ be the annulus traced by U as it rotated through a 2π angle about the point c , i.e.,

$$U^{2\pi}(c) = \cup_{q \in U} C(c, \|q - c\|).$$

Let $B(r, c)$ be the closed ball of radius r and centered at c . Given a set of angles $\alpha \in [0, 2\pi)$, $\Delta\alpha \in [0, 2\pi]$, let $\mathcal{S}_c(r, \alpha, \Delta\alpha)$ be the sector traced by a segment of length r and fixed at c as it rotates from the angle α to the angle $\alpha + \Delta\alpha$ in the counter-clockwise direction. With this notation, $B(r, c) = \mathcal{S}_c(r, 0, 2\pi)$. Let $EB_c(U)$ be the minimum ball enclosing U centered at c , i.e., $EB_c(U) = B(\sup_{q \in U} \|q - c\|, c)$, where $\|\cdot\|$ represents the Euclidean norm. Let $REB_c(U) = \sup_{q \in U} \|q - c\|$ be the radius of the enclosing ball $EB_c(U)$. Since circumball is the smallest of all the enclosing balls, we will give it a special notation. Accordingly, for the region U , let $D(U)$ be the circumball, $R(U)$ be the circumradius and $C(U)$ be the circumcenter of U . Finally, the symbol $\mathbf{I} \in \text{SE}(2)$ will represent the identity element of the $\text{SE}(2)$ group. Specifically, \mathbf{I} will correspond to that state of the Dubins vehicle where it is positioned at the origin and its heading is aligned with the positive X axis.

5.2 Reachable set for the Dubins vehicle

In this section we state some properties of the Dubins *reachable set* which shall be useful in the due course of the chapter. Given $t \geq 0$ and the current configuration of the Dubins vehicle $h \in \text{SE}(2)$, let $\mathcal{R}_h(t)$ denote the reachable set

of the Dubins vehicle in time t starting with state h , i.e.,

$$\mathcal{R}_h(t) = \{q \in \mathbb{R}^2 \mid L_\rho(h, q) \leq t\}.$$

Reachable sets for the Dubins vehicle are shown in Fig. 5.1. The boundary of the reachable sets consist of arcs of circle involutes and arcs of epicycloids (for further details on these families of curves see, e.g., [45]). We shall also use a *slightly* truncated version of $\mathcal{R}_h(t)$ for *sufficiently large* t . We will denote this set by $\tilde{\mathcal{R}}_h(t)$. For the sake of clarity we explain the construction of $\tilde{\mathcal{R}}_h(t)$ from $\mathcal{R}_h(t)$ with the help of Fig. 5.2 as follows: Consider the axis that is perpendicular to the heading of the Dubins vehicle. Let this axis intersect the boundary of $\mathcal{R}_h(t)$ at $P_L(t)$ and $P_R(t)$. Let $P_B(t)$ be the furthest point that lies exactly *behind* the Dubins vehicle. Let $H_L(t)$ be the half-plane generated by the line passing through $P_L(t)$ and $P_B(t)$ that does not contain the origin. Similarly, let $H_R(t)$ be the half-plane generated by the line passing through $P_R(t)$ and $P_B(t)$ that does not contain the origin. Then $\tilde{\mathcal{R}}_h(t) = \mathcal{R}_h(t) \setminus (H_L(t) \cap H_R(t))$.

Using the definition of the reachable sets and planar geometry, one can prove that the following properties hold true for any $h \in \text{SE}(2)$.

(P1) $\mathcal{R}_h(t)$ is a monotonic function in t , i.e., $\mathcal{R}_h(t') \subseteq \mathcal{R}_h(t)$ for $t' \leq t$.

There exist constants $\kappa_1 \in [5.7, 5.8]$ and $\kappa_2 \in [6.5, 6.6]$ such that

(P2) $\mathcal{R}_h(t)$ is a simply connected set for all $t \in \mathbb{R}_+ \setminus [\kappa_1\rho, \kappa_2\rho]$.

(P3) For all $t \geq \kappa_2\rho$, $\tilde{\mathcal{R}}_h(t)$ is star-shaped¹ and the kernel² of $\tilde{\mathcal{R}}_h(t)$ is the set of

¹A region U is called star-shaped if there is a point $a \in U$ such that the line segment \bar{ab} is contained in U for all $b \in U$. Here $\bar{ab} = \{ta + (1-t)b \mid t \in [0, 1]\}$. We then say that U is star-shaped with respect to a .

²The kernel of a star-shaped region U is the set of points from which the entire set U is visible.

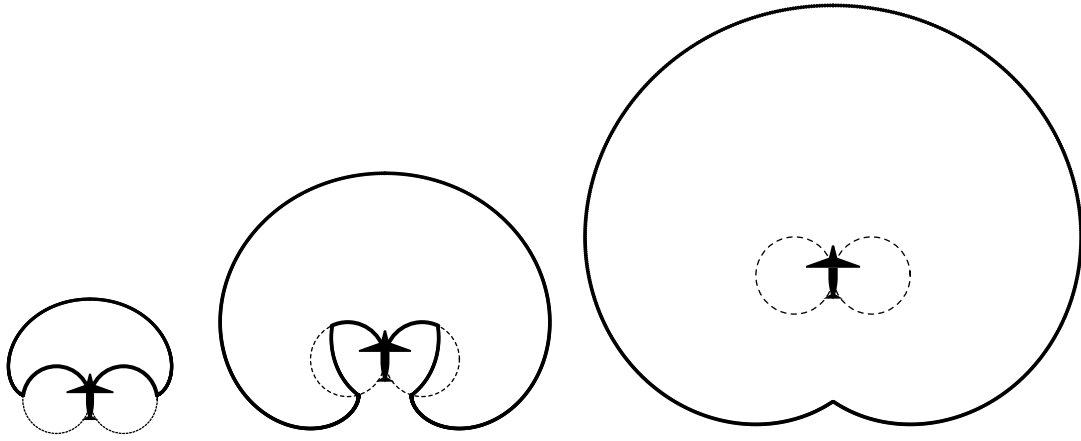


Figure 5.1: Reachable sets $\mathcal{R}_I(t)$ for the Dubins vehicle for $t = 3\rho$, 5ρ and 7ρ .

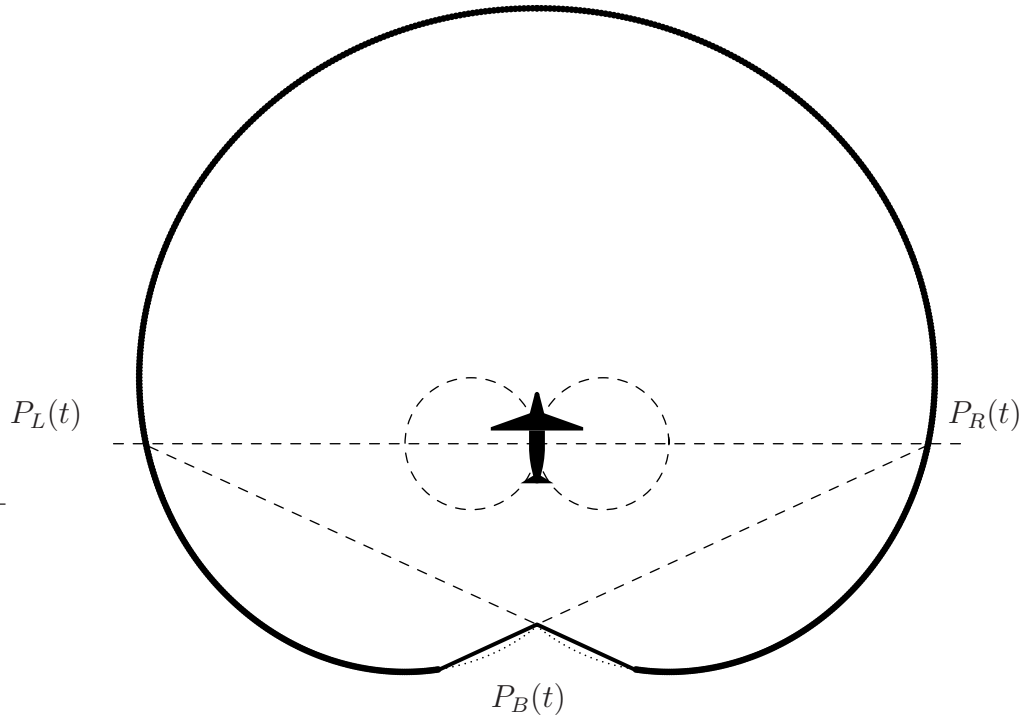


Figure 5.2: Truncation of $\mathcal{R}_h(t)$ to form $\tilde{\mathcal{R}}_h(t)$.

points that lie on the axis which is perpendicular to the heading direction of the vehicle at h .

Next, we introduce a “set covering problem” that will play a key role in the design of efficient loitering patterns. For $m > 0$, define a function $\lambda : \mathbb{R}_+ \rightarrow \mathbb{R}_+$ by

$$\lambda_m(t) := \max \left\{ r \in \mathbb{R}_+ \mid \exists y \geq \rho, \alpha \in [0, 2\pi) \text{ s.t. } \mathcal{S}_{(0,y)} \left(r, \alpha, \frac{2\pi}{m} \right) \subset \mathcal{R}_I(t) \right\}.$$

The function $t \mapsto \lambda_m(t)$ is the radius of the largest sector extending an angle $\frac{2\pi}{m}$ that is centered on the Y axis and away from the point $(0, \rho)$ and can be contained inside $\mathcal{R}_I(t)$. In particular, $\lambda_1(t)$ denotes the radius of the largest disk centered on the Y axis away from $(0, \rho)$ and contained inside $\mathcal{R}_I(t)$.

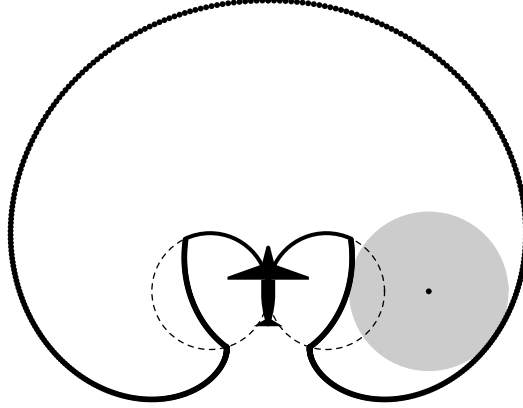


Figure 5.3: Finding the value $\lambda_1(5\rho)$.

One can show that, at fixed m , the function $t \mapsto \lambda_m(t)$ is a strictly increasing function in t . This can also be verified from Figs. 5.6 and 5.7 where we have plotted $\lambda_1(t)/\rho$ vs. t/ρ and $\lambda_2(t)/\rho$ vs. t/ρ respectively. Hence, the inverse function λ_m^{-1} is also well defined and satisfies

$$\lambda_m^{-1}(r) := \min \left\{ t \mid \exists y \geq \rho, \alpha \in [0, 2\pi) \text{ s.t. } \mathcal{S}_{(0,y)} \left(r, \alpha, \frac{2\pi}{m} \right) \subset \mathcal{R}_I(t) \right\}.$$

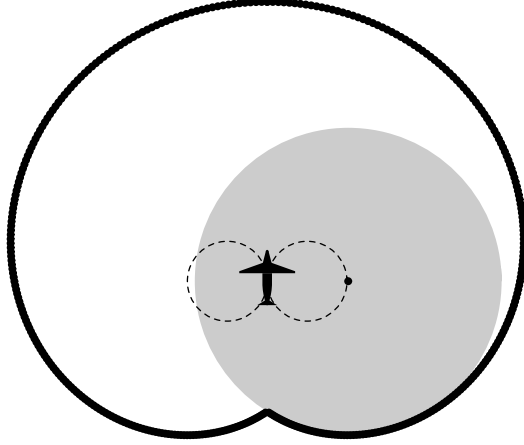


Figure 5.4: Finding the value $\lambda_1(7\rho)$.

For each $m > 0$, $\lambda_m(t)$ is associated with functions $\delta_m : \mathbb{R}_+ \rightarrow \mathbb{R}_+$ and $\beta_m : \mathbb{R}_+ \rightarrow [0, 2\pi)$ which are defined to satisfy the relation $\mathcal{S}_{(0, \delta_m(t))} \left(r, \beta_m(t), \frac{2\pi}{m} \right) \subset \mathcal{R}_I(t)$ for all $t \in \mathbb{R}_+$.

The functions δ_m and β_m can be computed numerically along with λ_m .

5.3 The single vehicle case

In this section we concentrate our attention on the case when $M = (1)$, i.e., only one vehicle is assigned the task to service the region \mathcal{Q} . It is easy to see that $\mathcal{T}_{\mathcal{Q},1}(\mathcal{O}^+(c, r)) = \mathcal{T}_{\mathcal{Q},1}(\mathcal{O}^-(c, r))$ for any region \mathcal{Q} . Hence, for the rest of the section, we shall omit the explicit mention of the direction of rotation for circular curves.

Lemma 5.1 (Equivalence by rotation) *For a region \mathcal{Q} , $\rho > 0$, $c \in \mathbb{R}^2$ and*

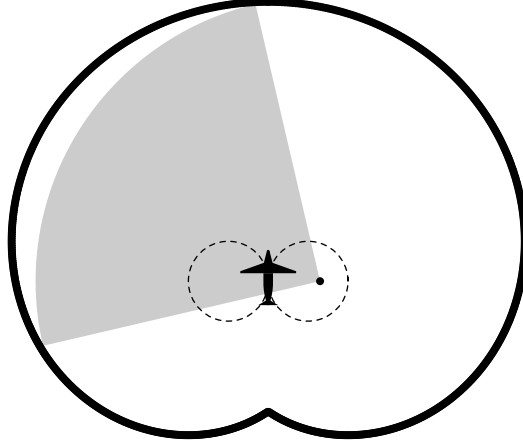


Figure 5.5: Finding the value $\lambda_4(7\rho)$.

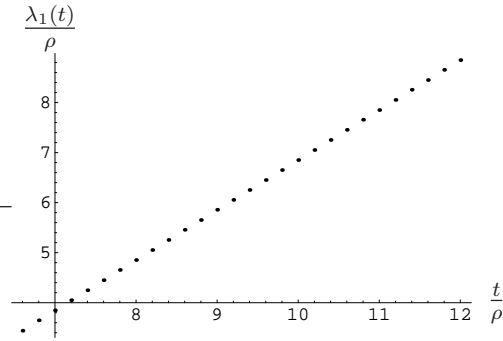


Figure 5.6: Plot of $\lambda_1(t)/\rho$ vs. t/ρ .

radius $r \geq \rho$,

$$\mathcal{T}_{\mathcal{Q},1}(\mathcal{O}(c,r)) = \mathcal{T}_{\mathcal{Q}^{2\pi(c),1}}(\mathcal{O}(c,r)).$$

Proof. For a point $q \in \mathcal{Q}$, define the function $\tau(q) = \sup_{s \in [0,T)} L_\rho(g_{\mathcal{O}(c,r)}(s), q)$. This definition implies that $\tau(q)$ is the minimum t such that q belongs to $\mathcal{R}_{g_{\mathcal{O}(c,r)}(s)}(t)$ for all $s \in [0, T)$. Consider any other point q' (not necessarily in \mathcal{Q}) such that $\|q' - c\| = \|q - c\|$. By rotational symmetry about the center c , given any $s \in [0, T)$, one can always find a $s' \in [0, T)$ such that $L_\rho(g_{\mathcal{O}(c,r)}(s'), q') = L_\rho(g_{\mathcal{O}(c,r)}(s), q)$,

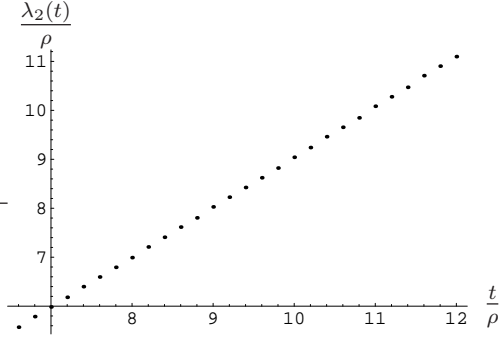


Figure 5.7: Plot of $\lambda_2(t)/\rho$ vs. t/ρ .

i.e., q' also belongs to $\mathcal{R}_{g_{\mathcal{O}(c,r)}(s')}(\tau(q))$ for all $s' \in [0, T)$. This implies that the circle of radius $\|c - q\|$ and centered at c belongs to $\mathcal{R}_{g_{\mathcal{O}(c,r)}(s)}(\tau(q))$ for all $s \in [0, T)$. Taking the union over all $q \in \mathcal{Q}$, one arrives at the lemma. \blacksquare

Lemma 5.2 For a region \mathcal{Q} , $\rho > 0$, $c \in \mathbb{R}^2$ and radius $r \geq \rho$,

$$\mathcal{T}_{\mathcal{Q},1}(\mathcal{O}(c, r)) = \min\{t \in \mathbb{R}_+ \mid \cup_{q \in \mathcal{Q}} C((0, r), \|c - q\|) \subset \mathcal{R}_I(t)\}.$$

Proof. Let $\mathcal{T}_{\mathcal{Q},1}(\mathcal{O}(c, r)) = t^*$. Lemma 5.1 implies that $\cup_{q \in \mathcal{Q}} C(c, \|c - q\|)$ belongs to $\mathcal{R}_{g_{\mathcal{O}(c,r)}(s)}(t^*)$ for all $s \in [0, T)$. This property when viewed in the reference frame attached to the Dubins vehicle gives the lemma. \blacksquare

Lemma 5.3 (Equivalence) For any region \mathcal{Q} , $\rho > 0$, $c \in \mathbb{R}^2$ and radius $r \geq \rho$, if $\mathcal{T}_{\mathcal{Q},1}(\mathcal{O}(c, r)) \in \mathbb{R}_+ \setminus [\kappa_1\rho, \kappa_2\rho]$, then

$$\mathcal{T}_{\mathcal{Q},1}(\mathcal{O}(c, r)) = \mathcal{T}_{EB_c(\mathcal{Q}),1}(\mathcal{O}(c, r)).$$

Proof. Let $\mathcal{T}_{\mathcal{Q},1}(\mathcal{O}(c, r)) = t^*$. Lemma 5.2 combined with the simply connectedness property (P2) of the reachable set implies that a disk of radius $\max_{q \in \mathcal{Q}} \|c - q\|$

centered at $(0, r)$ belongs to $\mathcal{R}_{\mathbf{I}}(t^*)$ if $t^* \in \mathbb{R}_+ \setminus [\kappa_1\rho, \kappa_2\rho]$. An equivalent statement is that for values of time in $\mathbb{R}_+ \setminus [\kappa_1\rho, \kappa_2\rho]$, t^* is the smallest t such that $EB_c(\mathcal{Q}) \subset \mathcal{R}_{g_{\mathcal{O}(c,r)}(s)}(t)$ for all $s \in [0, T)$, that is, $\mathcal{T}_{EB_c(\mathcal{Q}),1}(\mathcal{O}(c, r)) = t^* = \mathcal{T}_{\mathcal{Q},1}(\mathcal{O}(c, r))$. ■

We are now ready to state the main result of this section.

Theorem 5.1 (An optimal circular loitering) *Given a region \mathcal{Q} for which $R(\mathcal{Q}) \in \mathbb{R}_+ \setminus [\lambda_1(\kappa_1\rho), \lambda_1(\kappa_2\rho)]$, the circle of radius $\delta_1(\lambda_1^{-1}(R(\mathcal{Q})))$ with center at $C(\mathcal{Q})$ is an optimal circular loitering curve over \mathcal{Q} . Moreover,*

$$\tilde{\mathcal{T}}_{\mathcal{Q},1}^* = \lambda_1^{-1}(R(\mathcal{Q})) = \mathcal{T}_{\mathcal{Q},1}(\mathcal{O}(C(\mathcal{Q}), \delta_1(\lambda_1^{-1}(R(\mathcal{Q}))))).$$

Proof. We shall consider the case when $R(\mathcal{Q}) \geq \kappa_2\rho$. The proof for the case when $R(\mathcal{Q}) \leq \kappa_1\rho$ follows on similar lines. From the definition of λ_1 , $R(\mathcal{Q}) \geq \kappa_2\rho$ implies that

$$\min\{t \in \mathbb{R}_+ \mid B(R(\mathcal{Q}), (0, r)) \subset \mathcal{R}_{\mathbf{I}}(t)\} \geq \kappa_2\rho.$$

Since $D(\mathcal{Q})$ is the minimum of all the enclosing balls of \mathcal{Q} , we also have that

$$\min\{t \in \mathbb{R}_+ \mid EB_{(0,r)}(REB_c(\mathcal{Q})) \subset \mathcal{R}_{\mathbf{I}}(t)\} \geq \kappa_2\rho.$$

The closedness and the simply connectedness property of $\mathcal{R}_{\mathbf{I}}(t)$ for $t \geq \kappa_2\rho$ implies that

$$\min\{t \in \mathbb{R}_+ \mid C((0, r), REB_c(\mathcal{Q})) \subset \mathcal{R}_{\mathbf{I}}(t)\} \geq \kappa_2\rho.$$

This combined with Lemma 5.2 gives us that

$$\mathcal{T}_{\mathcal{Q},1}(\mathcal{O}(c, r)) = \min\{t \in \mathbb{R}_+ \mid \cup_{q \in \mathcal{Q}} C((0, r), \|c - q\|) \subset \mathcal{R}_{\mathbf{I}}(t)\} \geq \kappa_2\rho.$$

Since $\mathcal{T}_{\mathcal{Q},1}(\mathcal{O}(c, r)) \geq \kappa_2\rho$, the previous discussion combined with Lemma 5.3 implies that

$$\mathcal{T}_{\mathcal{Q},1}(\mathcal{O}(c, r)) = \mathcal{T}_{EB_c(\mathcal{Q}),1}(\mathcal{O}(c, r)) \geq \mathcal{T}_{D(\mathcal{Q}),1}(\mathcal{O}(C(\mathcal{Q}), r)).$$

This proves that the location of the center of rotation for an optimal circular loitering curve is at the circumcenter of \mathcal{Q} .

Therefore,

$$\begin{aligned}
\tilde{\mathcal{T}}_{\mathcal{Q},1}^* &= \min_{c \in \mathbb{R}^2, r \geq \rho} \mathcal{T}_{\mathcal{Q},1}(\mathcal{O}(c, r)) \\
&= \min_{r \geq \rho} \mathcal{T}_{\mathcal{D}(\mathcal{Q}),1}(\mathcal{O}(C(\mathcal{Q}), r)) \\
&= \min\{t \in \mathbb{R}_+ \mid B(R(\mathcal{Q}), (0, r)) \subset \mathcal{R}_{\mathbf{I}}(t) \text{ for some } r \geq \rho\} \\
&= \lambda_1^{-1}(R(\mathcal{Q})).
\end{aligned}$$

The fact that $\delta_1(\lambda_1^{-1}(R(\mathcal{Q})))$ is the radius of an optimal circular loitering curve follows from the definition of δ . This also proves the second equality in the theorem. ■

Remark 5.2 (Circular loitering patterns are optimal) *Although we have been restricting our attention on circular loitering curves, one can prove that, for the single vehicle case, an optimal circular loitering curve is also an optimal loitering curve, i.e.,*

$$\mathcal{T}_{\mathcal{Q},1}^* = \lambda_1^{-1}(R(\mathcal{Q})) = \mathcal{T}_{\mathcal{Q},1}(\mathcal{O}(C(\mathcal{Q}), \delta_1(\lambda_1^{-1}(R(\mathcal{Q}))))).$$

□

5.4 The single team case

In this section we design a loitering circle for a team of n Dubins vehicles servicing the region \mathcal{Q} , i.e., $M = (n, 0, \dots, 0)$. For brevity in notation, we shall

denote this team composition by $M = (n)$. By symmetry, the n vehicles will be placed at an angular distance of $\frac{2\pi}{n}$ from each other. Once again, the direction of the rotation on the curves does not matter. Hence, we shall continue to omit the mention of the direction of rotation for circular curves.

Lemma 5.4 (Equivalence by rotation) *For a region \mathcal{Q} and $n > 1$,*

$$\mathcal{T}_{\mathcal{Q},n}(\mathcal{O}(c,r)) = \mathcal{T}_{\mathcal{Q}^{2\pi(c),n}}(\mathcal{O}(c,r)).$$

Proof. For the sake of this proof we will interpret $\mathcal{T}_{\mathcal{Q},1}(\mathcal{O}(c,r))$ as the minimum t for which \mathcal{Q} belongs to $\cup_{j \in \{1, \dots, n\}} \mathcal{R}_{g_{\mathcal{O}(c,r)}(s+(j-1)\frac{T}{n})}(t)$ for all $s \in [0, \frac{T}{n})$. With a slight abuse of notation, for the fixed circular loitering curve $\mathcal{O}(c,r)$, define the function τ by $\tau(q) = \mathcal{T}_{q,n}(\mathcal{O}(c,r))$. This definition implies that $\tau(q)$ is the smallest t which satisfies the property that, given a $s \in [0, \frac{T}{n})$, there exists at least one vehicle $j \in \{1, \dots, n\}$ such that q belongs to $\mathcal{R}_{g_{\mathcal{O}(c,r)}(s+(j-1)\frac{T}{n})}(t)$. Consider any other point q' (not necessarily in \mathcal{Q}) such that $\|q' - c\| = \|q - c\|$. By rotational symmetry about the center c , one can find $j' \in \{1, \dots, n\}$ such that $L_\rho(g_{\mathcal{O}(c,r)}(s+(j'-1)\frac{T}{n}), q') = L_\rho(g_{\mathcal{O}(c,r)}(s+(j-1)\frac{T}{n}), q)$, i.e., q' also belongs to $\cup_{j \in \{1, \dots, n\}} \mathcal{R}_{g_{\mathcal{O}(c,r)}(s+(j-1)\frac{T}{n})}(t)$. This implies that the circle of radius $\|c - q\|$ and centered at c belongs to $\cup_{j \in \{1, \dots, n\}} \mathcal{R}_{g_{\mathcal{O}(c,r)}(s+(j-1)\frac{T}{n})}(t)$ for all $s \in [0, \frac{T}{n})$. Taking the union over all $q \in \mathcal{Q}$, one arrives at the lemma. ■

Given a set $\{g_1, \dots, g_n\} \subset \text{SE}(2)$ of n distinct positions and orientations, the *Dubins Voronoi partition* generated by $\{g_1, \dots, g_n\}$ is the collection of sets $\{V_1, \dots, V_n\}$ defined by

$$V_i = \{q \in \mathbb{R}^2 \mid L_\rho(g_i, q) \leq L_\rho(g_j, q) \text{ for all } j \in \{1, \dots, n\}\}.$$

We refer to V_i as the *Dubins Voronoi cell* of g_i . For our case, we shall denote the Voronoi partitions in a different way. Given n Dubins vehicles equally spaced along a circle of center c and radius r and all moving counterclockwise, let $\mathcal{V}(g_i, c, r, n) \subset \mathbb{R}^2$ be the Dubins Voronoi cell of the i th Dubins vehicle at state $g_i \in \text{SE}(2)$.

Lemma 5.5 *For a region \mathcal{Q} and $n > 1$,*

$$\mathcal{T}_{\mathcal{Q},n}(\mathcal{O}(c, r)) = \min\{t \in \mathbb{R}_+ \mid \mathcal{V}(g_{\mathcal{O}(c,r)}(s), c, r, n) \cap \mathcal{Q}^{2\pi}(c) \subset \mathcal{R}_{g_{\mathcal{O}(c,r)}(s)}(t)\},$$

for any $s \in [0, T)$.

Proof. Lemma 5.4 implies that $\mathcal{T}_{\mathcal{Q},n}(\mathcal{O}(c, r)) = \mathcal{T}_{\mathcal{Q}^{2\pi}(c),n}(\mathcal{O}(c, r))$. $\mathcal{T}_{\mathcal{Q}^{2\pi}(c),n}(\mathcal{O}(c, r))$ can be interpreted as the minimum t for which $\mathcal{Q}^{2\pi}(c)$ belongs to $\cup_{j \in \{1, \dots, n\}} \mathcal{R}_{g_{\mathcal{O}(c,r)}(s+(j-1)\frac{T}{n})}(t)$ for all $s \in [0, \frac{T}{n})$. The lemma then follows from the rotational symmetry about the center c and the definition of Dubins Voronoi partition. ■

Lemma 5.5 suggests how to compute the optimal circular trajectory for a team of Dubins vehicles by converting it into an optimization problem for a single vehicle. However, solving this optimization problem requires the knowledge of the shape of Dubins Voronoi partitions. Even though there is an element of rotational symmetry in our case, the shapes of the Dubins Voronoi partition are not easy enough to lend themselves to analysis. Hence, we shall approximate the Voronoi partitions by sectors. This approximation helps in deriving upper bounds on the cost function.

We are now ready to state the main result of the section.

Theorem 5.3 (*An upper bound on the coverage cost for a single team in large environments*) For $n > 1$ and for a region \mathcal{Q} with $R(\mathcal{Q}) \geq \lambda_n(\kappa_2\rho)$,

$$\tilde{\mathcal{T}}_{\mathcal{Q},n}^* \leq \lambda_n^{-1}(R(\mathcal{Q})) \leq \mathcal{T}_{\mathcal{Q},n}(\mathcal{O}(C(\mathcal{Q}), \delta_n(\lambda_n^{-1}(R(\mathcal{Q}))))).$$

Proof. In the interest of space, we will only sketch the proof here. Let $\tilde{\mathcal{T}}_{\mathcal{Q},n}^* = t^*$. On the lines similar to the proof of Theorem 5.1, one can show that $R(\mathcal{Q}) \geq \lambda_n(\kappa_2\rho)$ implies that $t^* > \kappa_2\rho$. Lemma 5.5 implies that

$$t^* = \min\{t \mid \mathcal{V}(g_{\mathcal{O}(c,r)}(s), c, r, n) \cap \mathcal{Q}^{2\pi}(c) \subset \mathcal{R}_{g_{\mathcal{O}(c,r)}(s)}(t)\},$$

for any $s \in [0, T)$. Changing the reference frame to the one attached to the Dubins vehicle and approximating the Dubins Voronoi partitions by sectors one can state that t^* is the minimum t such that $\mathcal{S}_{(0,r)}\left(REB_c(\mathcal{Q}), \alpha, \frac{2\pi}{n}\right) \setminus \mathcal{S}_{(0,r)}\left(\min_{q \in \mathcal{Q}} \|q - c\|, \alpha, \frac{2\pi}{n}\right) \subset \mathcal{R}_{\mathbf{I}}(t)$ for any $\alpha \in [0, 2\pi)$. Since $t^* > \kappa_2\rho$, $\tilde{\mathcal{R}}_{\mathbf{I}}(t)$ is star-shaped and simply connected for all $t > t^*$. Also $\tilde{\mathcal{R}}_{\mathbf{I}}(t)$ is an inner approximation of $\mathcal{R}_{\mathbf{I}}(t)$. Combining these observations with the definition of λ_n^{-1} , one arrives at the lemma. ■

Remark 5.4 *The bound obtained in Theorem 5.3 is tightest among the bounds possible by approximations of Dubins Voronoi partitions for vehicles moving along circular curves by sectors of circles.*

5.5 The multiple uniform team case

In this section we consider the multiple team case. We first concentrate on the case when the teams have *uniform* composition. A group of n vehicles comprising

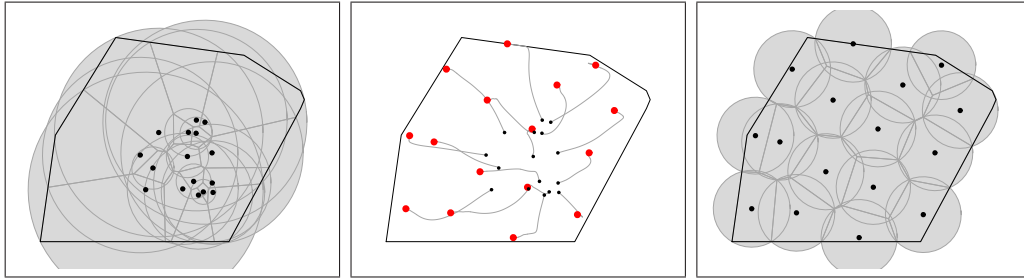


Figure 5.8: “Move-toward-the-circumcenter” algorithm for 16 disks in a convex polygonal domain. The left (respectively, right) figure illustrates the initial (respectively, final) locations and Voronoi partition. The central figure illustrates the network evolution. After 20 sec., the disk radius is approximately 0.43273 m. Simulations taken from [1].

of ℓ teams is said to have uniform team composition if n is a multiple of ℓ and the team composition is of the form $(\frac{n}{\ell}, \dots, \frac{n}{\ell}, 0, \dots, 0)$. We shall show that, for a *sufficiently large and convex* region \mathcal{Q} , an upper bound on the cost of coverage by the l team of loitering Dubins vehicles can be obtained by solving a related disk covering problem.

We first briefly describe the disk-covering problem or, more precisely, the version of the disk covering problem that is relevant for our purposes here. In our context, the disk covering problem can be stated as follows: given a convex region \mathcal{Q} and an integer ℓ , find the smallest real number $RDC_{\mathcal{Q}}(\ell)$ and a set of locations $\{c_1, \dots, c_{\ell}\}$ such that the ℓ disks, each of radius $RDC_{\mathcal{Q}}(\ell)$ and centered at $\{c_1, \dots, c_{\ell}\}$ cover \mathcal{Q} , that is, $\mathcal{Q} \subset \cup_{i \in \{1, \dots, \ell\}} B(RDC_{\mathcal{Q}}(\ell), c_i)$. We shall refer to $(RDC_{\mathcal{Q}}(\ell), \{c_1, \dots, c_{\ell}\})$ as the solution to the disk covering problem for \mathcal{Q} .

Disk covering problems have a long and beautiful history [46]. Many variants of the problem (e.g., geometric minimum disk cover problem) find their applica-

tions in numerous engineering applications (e.g., localization in sensor networks).

In [1] distributed algorithms were designed to solve the disk covering problem via a dynamical systems approach. Specifically, the chapter proposes the *move toward the furthest* and *move toward the circumcenter* algorithms for a group of ℓ mobile robots. In the *move toward the furthest* algorithm, each “disk center” moves towards the furthest vertex of its Voronoi cell (inside the Voronoi partition generated by all “disk centers”). In the *move toward the circumcenter* algorithm, each disk-center moves toward the circumcenter of its Voronoi cell. In both algorithms the Voronoi partition is continuously updated as the disk centers move. Asymptotically, an execution of one of these two algorithms computes a locally optimal solution to the disk covering problem in the sense that the location of these robots correspond to the centers c_1, \dots, c_ℓ and the largest of the circumradii of the Voronoi partitions corresponds to $RDC_{\mathcal{Q}}(\ell)$. Moreover, these distributed control laws can be implemented as local interactions between the disk centers. In our setting, this would imply that this would require interaction only between *neighboring* teams of vehicles, i.e., teams whose center of rotations are Voronoi neighbors. An execution of the *move toward the circumcenter* algorithm is illustrated in Figure 5.8.

We now state the following result which gives an upper bound on the coverage cost for multiple uniform teams of loitering Dubins vehicles.

Theorem 5.5 *Consider a group of n Dubins vehicles divided into ℓ teams of uniform composition loitering in a convex region \mathcal{Q} . Let $(RDC_{\mathcal{Q}}(\ell), \{c_1, \dots, c_\ell\})$ be the solution to the disk covering problem for \mathcal{Q} . If $\text{Area}(\mathcal{Q}) \geq \ell\pi\lambda_{\frac{n}{\ell}}^2(\kappa_2\rho)$, then*

$$\tilde{T}_{\mathcal{Q}, (\frac{n}{\ell}, \dots, \frac{n}{\ell}, 0, \dots, 0)}^* \leq \lambda_{\frac{n}{\ell}}^{-1}(RDC_{\mathcal{Q}}(\ell)).$$

Moreover, the loitering pattern which achieves this upper bound is the set of circular curves, each of radius $\delta_{\frac{n}{\ell}}(\lambda_{\frac{n}{\ell}}^{-1}(RDC_{\mathcal{Q}}(\ell)))$, and with centers at $\{c_1, \dots, c_{\ell}\}$.

Using the control algorithms from [1], one can design a computational approach to computing loitering patterns as follows:

- (i) Partition the environment into Voronoi partitions generated by virtual centers.
- (ii) Move the virtual centers in such a way as to solve a minimum-radius disk-covering problem
- (iii) Designing efficient loitering patterns for each team in its corresponding Voronoi cell.

5.6 Summary

In this chapter, we considered the coverage problem for loitering Dubins vehicles. We have characterized the configuration of the vehicles at the appearance of new targets in terms of Dubins paths, that we call *loitering patterns*. We defined the coverage cost to be the worst-case traveling time from any vehicle to any point in the region. Optimal circular loitering for a single vehicle and efficient circular loitering for a single team of vehicles were characterized. Finally, by establishing an analogy to the disk-covering problem, we proposed a computational approach to characterize efficient loitering patterns for multiple uniform teams.

This chapter leaves numerous important extensions open for further research. One needs to study the functions λ_n^{-1} to derive closed form expression for the

bounds derived in this chapter. It would be interesting to consider the coverage problem for other meaningful cost functions. The problem of multi *non-uniform* team of vehicles is also important. Determining the ideal team composition for a given region provides an exciting challenge too.

Chapter 6

Maintaining limited-range connectivity among second-order agents

In this chapter we consider ad-hoc networks of agents with double integrator dynamics. For such networks, the connectivity maintenance problems are: (i) do there exist control inputs for each agent to maintain network connectivity, and (ii) given desired controls for each agent, can one compute the closest connectivity-maintaining controls in a distributed fashion? The proposed solution is based on three contributions. First, we define and characterize admissible sets for double integrators to remain inside disks. Second, we establish an existence theorem for the connectivity maintenance problem by introducing a novel state-dependent graph, called the *double-integrator disk graph*. Finally, we design a distributed “flow-control” algorithm to compute optimal connectivity-maintaining controls.

6.1 Preliminary developments

We begin with some notations. We let \mathbb{N} , \mathbb{N}_0 , and \mathbb{R}_+ denote the natural numbers, the non-negative integer numbers, and the positive real numbers, respectively. For $d \in \mathbb{N}$, we let 0_d and 1_d denote the vectors in \mathbb{R}^d whose entries are all 0 and 1, respectively. We let $\|p\|$ denote the Euclidean norm of $p \in \mathbb{R}^d$. For $r \in \mathbb{R}_+$ and $p \in \mathbb{R}^d$, we let $B(p, r)$ denote the closed ball centered at p with radius r , i.e., $B(p, r) = \{q \in \mathbb{R}^d \mid \|p - q\| \leq r\}$. For $x, y \in \mathbb{R}^d$, we let $x \preceq y$ denote component-wise inequality, i.e., $x_k \leq y_k$ for $k \in \{1, \dots, d\}$. We let $f : A \rightrightarrows B$ denote a set-valued map; in other words, for each $a \in A$, $f(a)$ is a subset of B . We identify $\mathbb{R}^d \times \mathbb{R}^d$ with \mathbb{R}^{2d} .

6.1.1 Maintaining a double integrator inside a disk

For $t \in \mathbb{N}_0$, consider the discrete-time control system in \mathbb{R}^{2d}

$$\begin{aligned} p[t+1] &= p[t] + v[t], \\ v[t+1] &= v[t] + u[t], \end{aligned} \tag{6.1}$$

where the norm of the control is upper-bounded by $r_{\text{ctr}} \in \mathbb{R}_+$, i.e., $u[t] \in B(0_d, r_{\text{ctr}})$ for $t \in \mathbb{N}_0$. We refer to this control system as the *discrete-time double integrator* in \mathbb{R}^d or, more loosely, as a second-order system. Given $(p, v) \in \mathbb{R}^{2d}$ and $\{u_\tau\}_{\tau \in \mathbb{N}_0} \subseteq B(0_d, r_{\text{ctr}})$, let $\phi(t, (p, v), \{u_\tau\})$ denote the solution of (6.1) at time $t \in \mathbb{N}_0$ from initial condition (p, v) with inputs u_1, \dots, u_{t-1} .

In what follows we consider the following problem: assume that the initial position of (6.1) is inside a disk centered at 0_d , find inputs that keep it inside that disk. This task is impossible for general values of the initial velocity. In

what follows we identify assumptions on the initial velocity that render the task possible.

For $r_{\text{pos}} \in \mathbb{R}_+$, we define the *admissible set at time zero* by

$$\mathcal{A}_0^d(r_{\text{pos}}) = B(0_d, r_{\text{pos}}) \times \mathbb{R}^d.$$

For $r_{\text{pos}}, r_{\text{ctr}} \in \mathbb{R}_+$, we define the *admissible set for m time steps* by

$$\begin{aligned} \mathcal{A}_m^d(r_{\text{pos}}, r_{\text{ctr}}) &= \{(p, v) \in \mathbb{R}^{2d} \mid \exists \{u_\tau\}_{\tau \in [0, m-1]} \subseteq B(0_d, r_{\text{ctr}}) \\ &\quad \text{s.t. } \phi(t, (p, v), \{u_\tau\}) \in \mathcal{A}_0^d(r_{\text{pos}}) \ \forall t \in [0, m]\}, \end{aligned}$$

and the *admissible set* by

$$\begin{aligned} \mathcal{A}^d(r_{\text{pos}}, r_{\text{ctr}}) &= \{(p, v) \in \mathbb{R}^{2d} \mid \exists \{u_\tau\}_{\tau \in \mathbb{N}_0} \subseteq B(0_d, r_{\text{ctr}}) \\ &\quad \text{s.t. } \phi(t, (p, v), \{u_\tau\}) \in \mathcal{A}_0^d(r_{\text{pos}}), \ \forall t \in \mathbb{N}_0\}. \end{aligned}$$

With slight abuse of notation we shall sometimes suppress the arguments in the definitions of admissible sets. The following theorem establishes some important properties of the admissible sets.

Theorem 6.1 (Properties of the admissible sets) *For all $d \in \mathbb{N}$ and $r_{\text{pos}}, r_{\text{ctr}} \in \mathbb{R}_+$, the following statements hold:*

(i) *for all $m \in \mathbb{N}$, $\mathcal{A}_m^d(r_{\text{pos}}, r_{\text{ctr}}) \subseteq \mathcal{A}_{m-1}^d(r_{\text{pos}}, r_{\text{ctr}})$ and*

$$\mathcal{A}^d(r_{\text{pos}}, r_{\text{ctr}}) = \lim_{m \rightarrow +\infty} \mathcal{A}_m^d(r_{\text{pos}}, r_{\text{ctr}}) = \lim_{m \rightarrow +\infty} \bigcap_{k=1}^m \mathcal{A}_k^d(r_{\text{pos}}, r_{\text{ctr}});$$

(ii) *$\mathcal{A}^d(r_{\text{pos}}, r_{\text{ctr}})$ is a convex, compact set and is the largest controlled-invariant¹ subset of $\mathcal{A}_0^d(r_{\text{pos}})$;*

¹A set is controlled invariant for a control system if there exists a feedback law such that the set is positively invariant for the closed-loop system.

- (iii) $\mathcal{A}^d(r_{\text{pos}}, r_{\text{ctr}})$ is invariant under orthogonal transformations in the sense that, if $(p, v) \in \mathcal{A}^d(r_{\text{pos}}, r_{\text{ctr}})$, then also $(Rp, Rv) \in \mathcal{A}^d(r_{\text{pos}}, r_{\text{ctr}})$ for all orthogonal² matrices R in $\mathbb{R}^{d \times d}$;
- (iv) if $0 < r_1 < r_2$, then $\mathcal{A}^d(r_{\text{pos}}, r_1) \subset \mathcal{A}^d(r_{\text{pos}}, r_2)$ and $\mathcal{A}^d(r_1, r_{\text{ctr}}) \subset \mathcal{A}^d(r_2, r_{\text{ctr}})$.

Proof. The two facts in statement (i) are direct consequences of the definitions of \mathcal{A}_m^d and \mathcal{A}^d . Regarding statement (ii), each \mathcal{A}_m^d , $m \in \mathbb{N}$, is closed, the intersection of closed sets is closed, and, therefore, $\mathcal{A}^d = \lim_{m \rightarrow +\infty} \bigcap_{k=1}^m \mathcal{A}_k^d$ is closed. To show that \mathcal{A}^d is bounded it suffices to show that \mathcal{A}_1^d is bounded. Note that $(p, v) \in \mathcal{A}_1^d$ implies that there exists $u \in B(0_d, r_{\text{ctr}})$ such that $(p, v) \in \mathcal{A}_0^d$ and $(p+v, v+u) \in \mathcal{A}_0^d$. This, in turn, implies that $p \in B(0_d, r_{\text{pos}})$ and $p+v \in B(0_d, r_{\text{pos}})$. Therefore, \mathcal{A}_1^d is bounded. Next, we prove that \mathcal{A}_m^d is convex. Given (p_1, v_1) and (p_2, v_2) in \mathcal{A}_m^d , let u_1 and u_2 be controls that ensure that $\phi(t, (p_i, v_i), \{u_i\}) \in \mathcal{A}_0^d$, $t \in [0, m]$, $i \in \{1, 2\}$. For $\lambda \in [0, 1]$, consider the initial condition $(p_\lambda, v_\lambda) = (\lambda p_1 + (1 - \lambda)p_2, \lambda v_1 + (1 - \lambda)v_2)$ and the input $u_\lambda = \lambda u_1 + (1 - \lambda)u_2$, and note that, by linearity,

$$\phi(t, (p_\lambda, v_\lambda), u_\lambda) = \lambda \phi(t, (p_1, v_1), \{u_1\}) + (1 - \lambda) \phi(t, (p_2, v_2), \{u_2\}), \quad t \in [0, m].$$

Because $\phi(t, (p_1, v_1), \{u_1\})$ and $\phi(t, (p_2, v_2), \{u_2\})$ belong to the convex set \mathcal{A}_0^d , then also their convex combination does. Therefore, (p_λ, v_λ) belongs to \mathcal{A}_m^d , and \mathcal{A}_m^d is convex. Finally, \mathcal{A}^d is convex because the intersection of convex sets is convex.

Next, we show that \mathcal{A}^d is controlled invariant. Given $(p, v) \in \mathcal{A}^d$ (with corresponding control sequence $\{u_\tau\}_{\tau \in \mathbb{N}_0}$), we need to show that there exists a control

²A matrix $R \in \mathbb{R}^{d \times d}$ is orthogonal if $RR^T = R^T R = I_d$.

input $x \in B(0_d, r_{\text{ctr}})$ such that $\phi(1, (p, v), x) \in \mathcal{A}^d$. Such input can be chosen as $x = u_0$. Indeed, the control sequence $\{u_{\tau+1}\}_{\tau \in \mathbb{N}_0}$ keeps the trajectory starting from $\phi(1, (p, v), x)$ inside \mathcal{A}_0^d and, therefore, $\phi(1, (p, v), x) \in \mathcal{A}^d$. Additionally, it is easy to see that $\mathcal{A}^d \subset \mathcal{A}_0^d$. Finally, we need to prove that \mathcal{A}^d is the largest controlled-invariant subset of \mathcal{A}_0^d . Assume that there exists \mathcal{A}^{d*} with the same properties and larger than \mathcal{A}^d . This means that there exists $(p, v) \in \mathcal{A}^{d*} \setminus \mathcal{A}^d$. This is equivalent to saying that $\exists \tau^* \in \mathbb{N}_0$ such that, for every choice of the input u , $\phi(\tau^*, (p, v), u) \notin \mathcal{A}_0^d$. But, since $\mathcal{A}^{d*} \subset \mathcal{A}_0^d$, this leads to a contradiction.

Regarding statement (iii), observe that, if $(p, v) \in \mathcal{A}_0^d$, then $(Rp, Rv) \in \mathcal{A}_0^d$ and, if $u \in B(0, r_{\text{ctr}})$, then $Ru \in B(0, r_{\text{ctr}})$. Therefore, using again the linearity of the maps ϕ , the proof follows. Regarding statement (iv), the two results follow from the definition of $\mathcal{A}^d(r_{\text{pos}}, r_{\text{ctr}})$ and the facts that, for all $0 < r_1 < r_2$, $B(0, r_1) \subset B(0, r_2)$ and $\mathcal{A}_0^d(r_1) \subset \mathcal{A}_0^d(r_2)$. \blacksquare

Next, we study the set-valued map that associates to each state in $\mathcal{A}^d(r_{\text{pos}}, r_{\text{ctr}})$ the set of control inputs that keep the state inside $\mathcal{A}^d(r_{\text{pos}}, r_{\text{ctr}})$ in one step. We define the *admissible control set* $\mathcal{U}^d(r_{\text{pos}}, r_{\text{ctr}}) : \mathcal{A}^d(r_{\text{pos}}, r_{\text{ctr}}) \rightrightarrows B(0_d, r_{\text{ctr}})$ by

$$\mathcal{U}^d(r_{\text{pos}}, r_{\text{ctr}}) \cdot (p, v) = \{u \in B(0_d, r_{\text{ctr}}) \mid (p + v, v + u) \in \mathcal{A}^d(r_{\text{pos}}, r_{\text{ctr}})\},$$

or, equivalently,

$$\mathcal{U}^d(r_{\text{pos}}, r_{\text{ctr}}) \cdot (p, v) = B(0_d, r_{\text{ctr}}) \cap \{w - v \mid (p + v, w) \in \mathcal{A}^d(r_{\text{pos}}, r_{\text{ctr}})\}. \quad (6.2)$$

Lemma 6.1 (*Properties of the admissible control set*)

For all $(p, v) \in \mathcal{A}^d(r_{\text{pos}}, r_{\text{ctr}})$, the set $\mathcal{U}^d(r_{\text{pos}}, r_{\text{ctr}}) \cdot (p, v)$ is non-empty, convex and compact. For generic $(p, v) \in \mathcal{A}^d(r_{\text{pos}}, r_{\text{ctr}})$, the set $\mathcal{U}^d(r_{\text{pos}}, r_{\text{ctr}}) \cdot (p, v)$ does not contain 0_d .

Proof. The non-emptiness of the set $\mathcal{U}^d(r_{\text{pos}}, r_{\text{ctr}}) \cdot (p, v)$ derives directly from the definition of $\mathcal{A}^d(r_{\text{pos}}, r_{\text{ctr}})$. Clearly, from equation (6.2), $\mathcal{U}^d(r_{\text{pos}}, r_{\text{ctr}}) \cdot (p, v)$ is closed (it is the intersection of two closed sets). It is also bounded ($\mathcal{U}^d(r_{\text{pos}}, r_{\text{ctr}}) \cdot (p, v) \subset B(0_d, r_{\text{ctr}})$), hence it is compact. To prove that it is convex, we need to show the following: given $(p, v) \in \mathcal{A}^d(r_{\text{pos}}, r_{\text{ctr}})$, if there exist u_1 and u_2 in $\mathcal{U}^d(r_{\text{pos}}, r_{\text{ctr}}) \cdot (p, v)$ such that $\phi(1, (p, v), u_1)$ and $\phi(1, (p, v), u_2)$ belong to $\mathcal{A}^d(r_{\text{pos}}, r_{\text{ctr}})$, then $u_{12} = \lambda u_1 + (1 - \lambda)u_2$, $\lambda \in [0, 1]$, belongs to $\mathcal{U}^d(r_{\text{pos}}, r_{\text{ctr}}) \cdot (p, v)$, that is, $\phi(1, (p, v), u_{12}) \in \mathcal{A}^d(r_{\text{pos}}, r_{\text{ctr}})$. But this fact follows directly from the linearity of ϕ and the convexity of $\mathcal{A}^d(r_{\text{pos}}, r_{\text{ctr}})$. This proves that $\mathcal{U}^d(r_{\text{pos}}, r_{\text{ctr}}) \cdot (p, v)$ is convex. The fact that it does not necessarily contain the origin can be proven by contradiction as follows. Consider a $(p, v) \in \mathcal{A}^d(r_{\text{pos}}, r_{\text{ctr}})$ such that $v \neq 0_d$ and $\mathcal{U}^d(r_{\text{pos}}, r_{\text{ctr}}) \cdot (p, v)$ contains 0_d . This means that $(p + v, v)$ also belongs to $\mathcal{A}^d(r_{\text{pos}}, r_{\text{ctr}})$. Now, either $\mathcal{U}^d(r_{\text{pos}}, r_{\text{ctr}}) \cdot (p + v, v)$ does not contain 0_d , in which case we have proved the statement, or $\mathcal{A}^d(r_{\text{pos}}, r_{\text{ctr}})$ also contains $(p + 2v, v)$. Continuing along these lines, if it were true that $\mathcal{U}^d(r_{\text{pos}}, r_{\text{ctr}}) \cdot (p, v)$ contains the origin for all $(p, v) \in \mathcal{A}^d(r_{\text{pos}}, r_{\text{ctr}})$, then one could show that $(p + tv, v)$ belongs to $\mathcal{A}^d(r_{\text{pos}}, r_{\text{ctr}})$ for all $t \in \mathbb{N}$. However, $\mathcal{A}^d(r_{\text{pos}}, r_{\text{ctr}})$ is bounded by Theorem 6.1. Hence, one can always find a $t^* \in \mathbb{N}$ such that $(p + t^*v, v) \in \mathcal{A}^d(r_{\text{pos}}, r_{\text{ctr}})$ but $(p + (t^* + 1)v, v) \notin \mathcal{A}^d(r_{\text{pos}}, r_{\text{ctr}})$, thereby proving that $\mathcal{U}^d(r_{\text{pos}}, r_{\text{ctr}}) \cdot (p + t^*v, v)$ does not contain 0_d . ■

6.1.2 Computing admissible sets

We characterize \mathcal{A}^d for $d = 1$ in the following result and we illustrate the outcome in Figure 6.1.

Lemma 6.2 (Admissible set in 1 dimension) For $r_{\text{pos}}, r_{\text{ctr}} \in \mathbb{R}_+$, the following holds:

(i) $\mathcal{A}^1(r_{\text{pos}}, r_{\text{ctr}})$ is the polytope containing the points $(p, v) \in \mathbb{R}^2$ satisfying

$$-\frac{r_{\text{pos}}}{m} - \frac{m-1}{2}r_{\text{ctr}} \leq v + \frac{p}{m} \leq \frac{r_{\text{pos}}}{m} + \frac{m-1}{2}r_{\text{ctr}}, \quad (6.3)$$

for all $m \in \mathbb{N}$, and $p \in [-r_{\text{pos}}, r_{\text{pos}}]$;

(ii) If $\widehat{m}(r_{\text{pos}}, r_{\text{ctr}}) \in \mathbb{N}$ is defined by

$$\widehat{m}(r_{\text{pos}}, r_{\text{ctr}}) = \left\lceil -\frac{1}{2} + \sqrt{\frac{1}{4} + \frac{4r_{\text{pos}}}{r_{\text{ctr}}}} \right\rceil, \quad (6.4)$$

then $\mathcal{A}^1 = \mathcal{A}_m^1 = \mathcal{A}_{\widehat{m}(r_{\text{pos}}, r_{\text{ctr}})}^1$, for $m \geq \widehat{m}(r_{\text{pos}}, r_{\text{ctr}})$.

Proof. Regarding statement (i), it suffices to show that, for $m \in \mathbb{N}$, $\mathcal{A}_m^1(r_{\text{pos}}, r_{\text{ctr}})$ is the set of points in $\mathcal{A}_{m-1}^1(r_{\text{pos}}, r_{\text{ctr}})$ that satisfy equation (6.3). If we show that this property holds for all m , then we can use statement (i) of Theorem 6.1 to complete the proof. Consider the set of equations (6.1) for m consecutive time indices after t . The solution of the linear system can be written in terms of the state at instant t as

$$\begin{bmatrix} p[t+m] \\ v[t+m] \end{bmatrix} = \begin{bmatrix} 1 & m \\ 0 & 1 \end{bmatrix} \begin{bmatrix} p[t] \\ v[t] \end{bmatrix} + \sum_{\tau=0}^{m-1} \begin{bmatrix} 1 & (m-1-\tau) \\ 0 & 1 \end{bmatrix} \begin{bmatrix} 0 \\ 1 \end{bmatrix} u[t+\tau], \quad (6.5)$$

where we used the equality

$$A^\tau = \begin{bmatrix} 1 & 1 \\ 0 & 1 \end{bmatrix}^\tau = \begin{bmatrix} 1 & \tau \\ 0 & 1 \end{bmatrix}, \quad \tau \in \mathbb{N}.$$

It is clear that the points on the boundary of \mathcal{A}_m^1 have the property that the maximum control effort is needed to enforce the constraint. In other words we

look for the points $(p[t], v[t]) \in \mathcal{A}_0^1$ with $v[t] \geq 0$ (the case $v[t] \leq 0$ can be solved in a similar way) such that the points $p[t+m] \leq r_{\text{cmm}}$ are reached by using the maximum control effort $u[t+\tau] = -r_{\text{ctr}}$, $\tau \in \{0, \dots, m-1\}$.

Substituting the expression of the control in (6.5) we obtain

$$p[t+m] = p[t] + mv[t] - r_{\text{ctr}} \sum_{\tau=0}^{m-1} (m-1-\tau),$$

$$v[t+m] = v[t] - mr_{\text{ctr}},$$

and using the equality $\sum_{\tau=0}^{m-1} (m-1-\tau) = \frac{m(m-1)}{2}$, we have

$$p[t+m] = p[t] + mv[t] - r_{\text{ctr}} \frac{m(m-1)}{2},$$

$$v[t+m] = v[t] - mr_{\text{ctr}},$$
(6.6)

In order to belong to \mathcal{A}_m^1 , the point $(p[t], v[t])$ must satisfy the constraint $p[t+\tau] \leq r_{\text{cmm}}$, $\tau \in \{1, \dots, m\}$, or equivalently

$$v[t] \leq -\frac{p[t]}{\tau} + \frac{r_{\text{cmm}}}{\tau} + r_{\text{ctr}} \frac{(\tau-1)}{2}, \quad \tau \in \{1, \dots, m\}.$$

Using the same procedure for the points in the half plane $v[t] \leq 0$ (in this case the control is $u[t+\tau] = r_{\text{ctr}}$, $\tau \in \{0, \dots, m-1\}$), it turns out that \mathcal{A}_m^1 is equal to the set of all pairs $(p, v) \in \mathcal{A}_0^1$ satisfying

$$-\frac{p}{\tau} - \frac{r_{\text{cmm}}}{\tau} - \frac{\tau-1}{2} r_{\text{ctr}} \leq v \leq -\frac{p}{\tau} + \frac{r_{\text{cmm}}}{\tau} + \frac{\tau-1}{2} r_{\text{ctr}}, \quad \tau \in \{1, \dots, m\}.$$

By using statement (i) of Theorem 6.1 the proof is complete.

Regarding statement (ii), let us consider the case $v[t] \geq 0$ and evaluate the points on the boundary such that $(p[t+m], v[t+m]) = (r_{\text{cmm}}, 0)$, $m \in \mathbb{N}$. These points are obtained by substituting the above value of $(p[t+m], v[t+m])$ in (6.6). The points obtained are (p, v) such that

$$p = r_{\text{cmm}} - m \frac{(m+1)}{2} r_{\text{ctr}}, \quad m \in \mathbb{N}_0.$$

It is easy to see that $\widehat{m}(r_{\text{pos}}, r_{\text{ctr}})$, as defined in equation (6.4), is the lowest m such that $p \leq -r_{\text{cmm}}$. ■

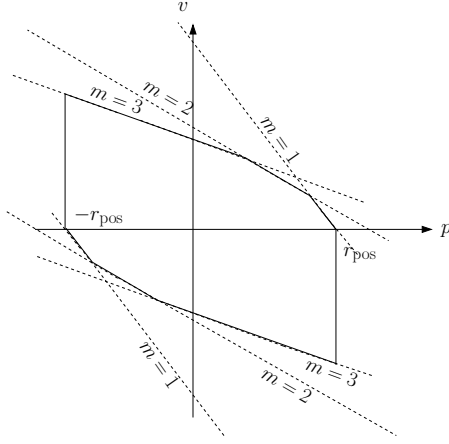


Figure 6.1: The admissible set \mathcal{A}^1 for generic values of r_{pos} and r_{ctr}

Remarks 6.2 (i) If $r_{\text{ctr}} \geq 2r_{\text{pos}}$, then $\mathcal{A}^1 = \mathcal{A}_1^1$, that is, for sufficiently large $r_{\text{ctr}}/r_{\text{pos}}$, the admissible set is equal to the admissible set in 1 time step.

(ii) The methodology for constructing $\mathcal{A}^1(r_{\text{pos}}, r_{\text{ctr}})$ is related to the procedure for constructing the so-called isochronic regions for discrete time optimal control of double integrators, as outlined in [47]. □

Next, we introduce some definitions useful to provide an inner approximation of \mathcal{A}^d when $d \geq 2$. Given $p \in \mathbb{R}^d$ and $v \in \mathbb{R}^d \setminus \{0_d\}$, define $p_{\parallel} \in \mathbb{R}$ and $p_{\perp} \in \mathbb{R}^d$ by

$$p = p_{\parallel} \frac{v}{\|v\|} + p_{\perp},$$

where $p_\perp \cdot v = 0$. For $r_{\text{pos}}, r_{\text{ctr}} \in \mathbb{R}_+$, define

$$\mathcal{A}_{\parallel}^d(r_{\text{pos}}, r_{\text{ctr}}) = \left\{ (p, v) \in B(0_d, r_{\text{pos}}) \times \mathbb{R}^d \mid v = 0_d \text{ or } (p_{\parallel}, \|v\|) \in \mathcal{A}^1(\sqrt{r_{\text{pos}}^2 - \|p_{\perp}\|^2}, r_{\text{ctr}}) \right\}. \quad (6.7)$$

Lemma 6.3 For $r_{\text{pos}}, r_{\text{ctr}} \in \mathbb{R}_+$, $\mathcal{A}_{\parallel}^d(r_{\text{pos}}, r_{\text{ctr}})$ is a compact subset of $\mathcal{A}^d(r_{\text{pos}}, r_{\text{ctr}})$.

Proof. We begin by showing that definition (6.7) is equivalent to

$$\begin{aligned} \mathcal{A}_{\parallel}^d(r_{\text{pos}}, r_{\text{ctr}}) = \{ & (p, v) \in \mathcal{A}_0^d \mid v = 0_d \text{ or } \exists \{u_{\parallel\tau}\}_{\tau \in \mathbb{N}_0} \subseteq [-r_{\text{ctr}}, r_{\text{ctr}}] \\ & \text{s.t. } \phi\left(t, (p, v), \{u_{\parallel\tau}\}_{\tau \in \mathbb{N}_0} \frac{v}{\|v\|}\right) \in \mathcal{A}_0^d(r_{\text{pos}}), \forall t \in \mathbb{N}_0 \}. \end{aligned} \quad (6.8)$$

To establish this equivalence, we use the definition of the set \mathcal{A}^1 . For $v \neq 0_d$, we rewrite the solution of the system as

$$\phi(t, (p, v), \{u_{\tau}\}) = \phi_{\parallel}(t, (p, v), \{u_{\tau}\}) \frac{v}{\|v\|} + \phi_{\perp}(t, (p, v), \{u_{\tau}\}),$$

where $\phi_{\perp}(t, (p, v), \{u_{\tau}\}) \cdot v = 0$ for all $t \in \mathbb{N}_0$. It is easy to see that, if $\{u_{\tau}\}_{\tau \in \mathbb{N}_0} = \{u_{\parallel\tau}\}_{\tau \in \mathbb{N}_0} \frac{v}{\|v\|}$, then $\phi_{\perp}(t, (p, v), \{u_{\tau}\}) = (p_{\perp}, 0_d)$ for all $t \in \mathbb{N}_0$. Therefore,

$$\phi(t, (p, v), \{u_{\tau}\}) = \phi_{\parallel}(t, (p, v), \{u_{\tau}\}) \frac{v}{\|v\|} + (p_{\perp}, 0_d).$$

Note that, if $p = p_{\parallel} \frac{v}{\|v\|} + p_{\perp}$, then $\|p\| \leq r_{\text{pos}}$ if and only if $p_{\parallel} \leq \sqrt{r_{\text{pos}}^2 - \|p_{\perp}\|^2}$. Therefore, the property $\phi\left(t, (p, v), \{u_{\parallel\tau}\}_{\tau \in \mathbb{N}_0} \frac{v}{\|v\|}\right) \in \mathcal{A}_0^d(r_{\text{pos}})$ is equivalent to

$$\phi_{\parallel}\left(t, (p, v), \{u_{\parallel\tau}\}_{\tau \in \mathbb{N}_0} \frac{v}{\|v\|}\right) \in \mathcal{A}_0^1\left(\sqrt{r_{\text{pos}}^2 - \|p_{\perp}\|^2}\right),$$

and, in turn, definitions (6.7) and (6.8) are equivalent. In order to prove that $\mathcal{A}_{\parallel}^d(r_{\text{pos}}, r_{\text{ctr}})$ is compact, we simply observe that it is a closed subset of the compact set $\mathcal{A}^d(r_{\text{pos}}, r_{\text{ctr}})$. ■

Remark 6.3 *In what follows we use our representation of $\mathcal{A}_{\parallel}^d$ to compute an inner approximation for the convex set \mathcal{A}^d , for $d \geq 2$. For example, for fixed $p \in B(0_d, r_{\text{pos}})$, we compute velocity vectors v such that $(p, v) \in \mathcal{A}^d$ by considering a sample of unit-length vectors $w \in \mathbb{R}^d$ and computing the maximum allowable velocity v parallel to w according to equation (6.7). Furthermore, we perform computations by adopting inner polytopic representations for the various compact convex sets. \square*

6.1.3 The double-integrator disk graph

Let us introduce some concepts about state dependent graphs and some useful examples. For a set X , let $\mathbb{F}(X)$ be the collection of finite subsets of X ; e.g., $\mathcal{P} \in \mathbb{F}(\mathbb{R}^d)$ is a set of points. For a finite set X , let $\mathbb{G}(X)$ be the set of undirected graphs whose vertices are elements of X , i.e., whose vertex set belongs to $\mathbb{F}(X)$. For a set X , a *state dependent graph on X* is a map $\mathcal{G} : \mathbb{F}(X) \rightarrow \mathbb{G}(X)$ that associates to a finite subset V of X an undirected graph with vertex set V and edge set $\mathcal{E}_{\mathcal{G}}(V)$ where $\mathcal{E}_{\mathcal{G}} : \mathbb{F}(X) \rightarrow \mathbb{F}(X \times X)$ satisfies $\mathcal{E}_{\mathcal{G}}(V) \subseteq V \times V$. In other words, what edges exist in $\mathcal{G}(V)$ depends on the elements of V that constitute the nodes.

The following three examples of state dependent graphs play an important role. First, given $r_{\text{pos}} \in \mathbb{R}_+$, the *disk graph* $\mathcal{G}_{\text{disk}}(r_{\text{pos}})$ is the state dependent graph on \mathbb{R}^d defined as follows: for $\{p_1, \dots, p_n\} \subset \mathbb{R}^d$, the pair (p_i, p_j) is an edge in $\mathcal{G}_{\text{disk}}(r_{\text{pos}}) \cdot (\{p_1, \dots, p_n\})$ if and only if

$$\|p_i - p_j\| \leq r_{\text{pos}} \iff p_i - p_j \in B(0_d, r_{\text{pos}}).$$

Second, given $r_{\text{pos}}, r_{\text{ctr}} \in \mathbb{R}_+$, the *double-integrator disk graph* $\mathcal{G}_{\text{di-disk}}(r_{\text{pos}}, r_{\text{ctr}})$ is the state dependent graph on \mathbb{R}^{2d} defined as follows: for $\{(p_1, v_1), \dots, (p_n, v_n)\} \subset \mathbb{R}^{2d}$, the pair $((p_i, v_i), (p_j, v_j))$ is an edge if and only if the relative positions and velocities satisfy

$$(p_i - p_j, v_i - v_j) \in \mathcal{A}^d(r_{\text{pos}}, r_{\text{ctr}}).$$

Third, it is convenient to define the disk graph also as a state dependent graph on \mathbb{R}^{2d} by stating that $((p_i, v_i), (p_j, v_j))$ is an edge if and only if (p_i, p_j) is an edge of the disk graph on \mathbb{R}^d . We illustrate the first two graphs in Figure 6.2.

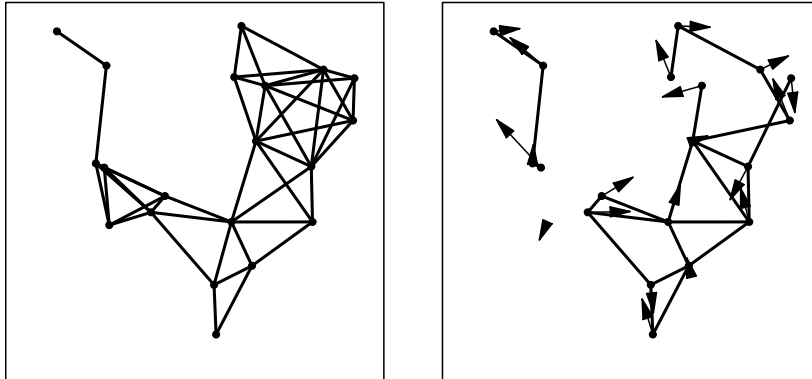


Figure 6.2: The disk graph and the double-integrator disk graph in \mathbb{R}^2 for 20 agents with random positions and velocities.

Remark 6.4 *As is well known, the disk graph is invariant under rigid transformations and reflections. Loosely speaking, the double integrator disk graph is invariant under the following class of transformations: position and velocities of the agents may be expressed with respect to any rotated and translated frame that is moving at constant linear velocity. These transformations are related to the classic Galilean transformations in geometric mechanics. \square*

6.2 Connectivity constraints among second-order agents

In this section we state the model, the notion of connectivity, and a sufficient condition that guarantees connectivity can be preserved.

6.2.1 Networks of robotic agents with second-order dynamics and the connectivity maintenance problem

We begin by introducing the notion of *network of robotic agents with second-order dynamics* in \mathbb{R}^d . Let n be the number of agents. Each agent has the following computation, motion control, and communication capabilities. For $i \in \{1, \dots, n\}$, the i th agent has a processor with the ability of allocating continuous and discrete states and performing operations on them. The i th agent occupies a location $p_i \in \mathbb{R}^d$, moves with velocity $v_i \in \mathbb{R}^d$, according to the discrete-time double integrator dynamics in (6.1), i.e.,

$$\begin{aligned} p_i[t+1] &= p_i[t] + v_i[t], \\ v_i[t+1] &= v_i[t] + u_i[t], \end{aligned} \tag{6.9}$$

where the norm of all controls $u_i[t]$, $i \in \{1, \dots, n\}$, $t \in \mathbb{N}_0$, is upper-bounded by $r_{\text{ctr}} \in \mathbb{R}_+$. The communication model is the following. The processor of each agent has access to the agent location and velocity. Each agent can transmit information to other agents within a distance $r_{\text{cmm}} \in \mathbb{R}_+$. We remark that the control bound r_{ctr} and the communication radius r_{cmm} are the same for all agents.

Remarks 6.5 (i) *Our network model assumes synchronous execution, although*

it would be important to consider more general asynchronous networks.

(ii) *We will not address here the correctness of our algorithms in the presence of measurement errors or communication quantization.* \square

We now state the control design problem of interest.

Problem 6.6 (Connectivity Maintenance) *Choose a state dependent graph $\mathcal{G}_{\text{target}}$ on \mathbb{R}^{2d} and design (state dependent) control constraints sets with the following property: if each agent's control takes values in the control constraint set, then the agents move in such a way that the number of connected components of $\mathcal{G}_{\text{target}}$ (evaluated at the agents' states) does not increase with time.* \square

This objective is to be achieved with the limited information available through message exchanges between agents. This problem was originally stated and solved for first-order agents in [33].

6.2.2 A known result for agents with first-order dynamics

In [33], a connectivity constraint was developed for a set of agents modeled by first-order discrete-time dynamics:

$$p_i[t + 1] = p_i[t] + u_i[t].$$

Here the graph whose connectivity is of interest, is the disk graph $\mathcal{G}_{\text{disk}}(r_{\text{cmm}})$ over the vertices $\{p_1[t], \dots, p_n[t]\}$. Network connectivity is maintained by restricting the allowable motion of each agent. In particular, it suffices to restrict the motion of each agent as follows. If agents i and j are neighbors in the r_{cmm} -disk graph

$\mathcal{G}_{\text{disk}}(r_{\text{cmm}})$ at time t , then their positions at time $t + 1$ are required to belong to $B\left(\frac{p_i[t]+p_j[t]}{2}, \frac{r_{\text{cmm}}}{2}\right)$. In other words, connectivity between i and j is maintained if

$$u_i[t] \in B\left(\frac{p_j[t] - p_i[t]}{2}, \frac{r_{\text{cmm}}}{2}\right),$$

$$u_j[t] \in B\left(\frac{p_i[t] - p_j[t]}{2}, \frac{r_{\text{cmm}}}{2}\right).$$

The constraint is illustrated in Figure 6.3.

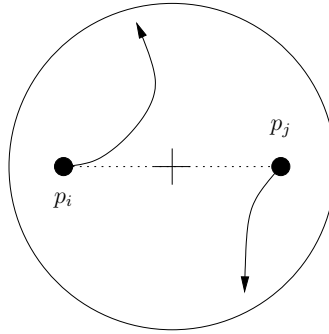


Figure 6.3: Starting from p_i and p_j , the agents are restricted to move inside the disk centered at $\frac{p_i+p_j}{2}$ with radius $\frac{r_{\text{cmm}}}{2}$.

Note that this constraint takes into account only the positions of the agents; this fact can be attributed to the *first-order dynamics* of the agents. We wish to construct a similar constraint for agents with second order dynamics. It is reasonable to expect that this new constraint will depend on positions as well as velocities of the neighboring agents.

6.2.3 An appropriate graph for the connectivity maintenance problem for agents with second-order dynamics

We begin working on the stated problem with a negative result regarding two candidate target graphs.

Lemma 6.4 (Unsuitable graphs) *Consider a network of n agents with double integrator dynamics (6.9) in \mathbb{R}^d . Let r_{cmm} be the communication range and let r_{ctr} be the control bound. Let $\mathcal{G}_{\text{target}}$ be either $\mathcal{G}_{\text{disk}}(r_{\text{cmm}})$ on \mathbb{R}^{2d} or $\mathcal{G}_{\text{di-disk}}(r_{\text{cmm}}, 2r_{\text{ctr}})$. There exist states $\{(p_i, v_i)\}_{i \in \{1, \dots, n\}}$ such that*

- (i) *the graph $\mathcal{G}_{\text{target}}$ at $\{(p_i, v_i)\}_{i \in \{1, \dots, n\}}$ is connected, and*
- (ii) *for all $\{u_i\}_{i \in \{1, \dots, n\}} \subseteq B(0_d, r_{\text{ctr}})$, the graph $\mathcal{G}_{\text{target}}$ at $\{(p_i + v_i, v_i + u_i)\}_{i \in \{1, \dots, n\}}$, is disconnected.*

Proof. The proof of the statement for $\mathcal{G}_{\text{target}} = \mathcal{G}_{\text{disk}}(r_{\text{cmm}})$ is straightforward. Consider two agents whose relative position and velocity belong to $\mathcal{A}_0^d \setminus \mathcal{A}_1^d$. Then, after one time step, the two agents will not be connected in $\mathcal{G}_{\text{disk}}(r_{\text{cmm}})$ no matter what their controls are. Next, consider the case $\mathcal{G}_{\text{target}} = \mathcal{G}_{\text{di-disk}}(r_{\text{cmm}}, 2r_{\text{ctr}})$. For $d = 1$, let \bar{v} be the maximal velocity in $\mathcal{A}^1(r_{\text{cmm}}, 2r_{\text{ctr}})$ at $p = 0$, that is, $\bar{v} = \min\{r_{\text{cmm}}/m + (m - 1)r_{\text{ctr}} \mid m \in \mathbb{N}\}$. Take three agents with positions $p_1 = p_2 = p_3 = 0$ and velocities $v_1 = -\bar{v}$, $v_2 = 0$, and $v_3 = \bar{v}$. At this configuration, the graph $\mathcal{G}_{\text{di-disk}}(r_{\text{cmm}}, 2r_{\text{ctr}})$ contains two edges: between agent 1 and 2 and between agent 2 and 3. Connectivity is preserved after one time step if agent 2

remains connected to both agents 1 and 3 after one time step. However, to remain connected with agent 1, its control u_2 must be equal to $-r_{\text{ctr}}$ and, analogously, to remain connected with agent 3, its control u_2 must be equal to $+r_{\text{ctr}}$. Clearly this is impossible. \blacksquare

Remarks 6.7 (i) *The result in Lemma 6.4 on the double integrator graph has the following interpretation. Assume that agent i has two neighbors j and k in the graph $\mathcal{G}_{\text{di-disk}}(r_{\text{cmm}}, r_{\text{ctr}})$. By definition of the neighboring law for this graph, we know that there exists bounded controls for i and j to maintain the $((p_i, v_i), (p_j, v_j))$ link and that there exists bounded controls for i and k to maintain the $((p_i, v_i), (p_k, v_k))$ link. The lemma states that, for some states of the agents i , j , and k , there might not exist controls that maintain both links simultaneously.*

(ii) *In other words, Lemma 6.4 shows how the disk graph $\mathcal{G}_{\text{disk}}(r_{\text{cmm}})$ and the double integrator disk graph $\mathcal{G}_{\text{di-disk}}(r_{\text{cmm}}, 2r_{\text{ctr}})$ are not appropriate choices for the connectivity maintenance problem. \square*

The following theorem suggests that an appropriate scaling of the control bound is helpful in identifying a suitable state dependent graph for Problem 6.6.

Theorem 6.8 (A scaled double-integrator disk graph is suitable) *Consider a network of n agents with double integrator dynamics (6.9) in \mathbb{R}^d . Let r_{cmm} be the communication range and let r_{ctr} be the control bound. For $k \in \{1, \dots, n-1\}$, define*

$$\nu(k) = \frac{2}{k\sqrt{d}}.$$

Assume that $k \in \{1, \dots, n-1\}$ and the state $\{(p_i, v_i)\}_{i \in \{1, \dots, n\}}$ together have the property that the graph $\mathcal{G}_{\text{di-disk}}(r_{\text{cmm}}, \nu(k)r_{\text{ctr}})$ at $\{(p_i, v_i)\}_{i \in \{1, \dots, n\}}$ contains a spanning tree T with diameter at most k . Then there exists $\{u_i\}_{i \in \{1, \dots, n\}} \subseteq B(0_d, r_{\text{ctr}})$ such that if $((p_i, v_i), (p_j, v_j))$ is an edge of T , then $((p_i + v_i, v_i + u_i), (p_j + v_j, v_j + u_j))$ is an edge of $\mathcal{G}_{\text{di-disk}}(r_{\text{cmm}}, \nu(k)r_{\text{ctr}})$ at $\{(p_i + v_i, v_i + u_i)\}_{i \in \{1, \dots, n\}}$.

These results are based upon Shostak's Theory for systems of inequalities, as exposed in [48]. We provide the proof in Appendix C. The following results are immediate consequences of this theorem.

Corollary 6.1 (Simple sufficient condition) *With the same notation in Theorem 6.8, define $\nu_{\min} = \frac{2}{(n-1)\sqrt{d}}$. Assume that the state $\{(p_i, v_i)\}_{i \in \{1, \dots, n\}}$ has the property that the graph $\mathcal{G}_{\text{di-disk}}(r_{\text{cmm}}, \nu_{\min}r_{\text{ctr}})$ is connected at $\{(p_i, v_i)\}_{i \in \{1, \dots, n\}}$. Then*

- (i) *there exists $\{u_i\}_{i \in \{1, \dots, n\}} \subseteq B(0_d, r_{\text{ctr}})$, such that the graph $\mathcal{G}_{\text{di-disk}}(r_{\text{cmm}}, \nu_{\min}r_{\text{ctr}})$ is also connected at $\{(p_i + v_i, v_i + u_i)\}_{i \in \{1, \dots, n\}}$; and*
- (ii) *if T is a spanning tree of $\mathcal{G}_{\text{di-disk}}(r_{\text{cmm}}, \nu_{\min}r_{\text{ctr}})$ at $\{(p_i, v_i)\}_{i \in \{1, \dots, n\}}$, then there exists $\{u_i\}_{i \in \{1, \dots, n\}} \subseteq B(0_d, r_{\text{ctr}})$, such that, for all edges $((p_i, v_i), (p_j, v_j))$ of T , it holds that $((p_i + v_i, v_i + u_i), (p_j + v_j, v_j + u_j))$ is an edge of $\mathcal{G}_{\text{di-disk}}(r_{\text{cmm}}, \nu_{\min}r_{\text{ctr}})$ at $\{(p_i + v_i, v_i + u_i)\}_{i \in \{1, \dots, n\}}$.*

Remark 6.9 (Scaling of ν_{\min} with n) *The condition $\nu_{\min} = \frac{2}{\sqrt{d(n-1)}}$ implies that according to the sufficient conditions in Corollary 6.1, as the number of*

agents grows, the velocities of the agents must be closer and closer in order for the agents to be able to remain connected.

If $\mathcal{G}_{\text{di-disk}}(r_{\text{cmm}}, \nu(k)r_{\text{ctr}})$ at $\{(p_i, v_i)\}_{i \in \{1, \dots, n\}}$ is not connected for some k , then Theorem 6.8 applies to its connected components. In what follows we fix k and without loss of generality assume the graph $\mathcal{G}_{\text{di-disk}}(r_{\text{cmm}}, \nu(k)r_{\text{ctr}})$ at $\{(p_i, v_i)\}_{i \in \{1, \dots, n\}}$ to be connected. \square

Remark 6.10 (*Distributed computation of connectivity and of spanning trees*)
Each agent can compute its neighbors in the graph $\mathcal{G}_{\text{di-disk}}(r_{\text{cmm}}, \nu(k)r_{\text{ctr}})$ just by communicating with its neighbors in $\mathcal{G}_{\text{disk}}(r_{\text{cmm}})$ and exchanging with them position and velocity information. Alternatively, this computation may also be performed if each agent may sense relative position and velocity with all other agents at a distance no larger than r_{cmm} .

It is possible to compute spanning trees in networks via standard depth-first search distributed algorithms. It is also possible [49] to distributively compute a minimum diameter spanning tree in a network. \square

6.2.4 The control constraint set and its polytopic representation

We now concentrate on two agents with indices i and j . For $t \in \mathbb{N}_0$, we define the relative position, velocity and control by $p_{ij}[t] = p_i[t] - p_j[t]$, $v_{ij}[t] = v_i[t] - v_j[t]$

and $u_{ij}[t] = u_i[t] - u_j[t]$, respectively. It is easy to see that

$$\begin{aligned} p_{ij}[t+1] &= p_{ij}[t] + v_{ij}[t], \\ v_{ij}[t+1] &= v_{ij}[t] + u_{ij}[t]. \end{aligned}$$

Assume that agents i, j are connected in $\mathcal{G}_{\text{di-disk}}(r_{\text{cmm}}, \nu(k)r_{\text{ctr}})$ at time t . By definition, this means that the relative state $(p_{ij}[t], v_{ij}[t])$ belongs to $\mathcal{A}^d(r_{\text{cmm}}, \nu(k)r_{\text{ctr}})$. If this connection is to be maintained at time $t+1$, then the relative control at time t must satisfy

$$u_i[t] - u_j[t] \in \mathcal{U}^d(r_{\text{cmm}}, \nu(k)r_{\text{ctr}}) \cdot (p_{ij}[t], v_{ij}[t]). \quad (6.10)$$

Also, implicit are the following bounds on individual control inputs $u_i[t]$ and $u_j[t]$:

$$u_i[t] \in B(0_d, r_{\text{ctr}}), \quad u_j[t] \in B(0_d, r_{\text{ctr}}). \quad (6.11)$$

This discussion motivates the following definition.

Definition 6.1 *Given $r_{\text{cmm}}, r_{\text{ctr}}, \nu(k) \in \mathbb{R}_+$ and given a set E of edges in $\mathcal{G}_{\text{di-disk}}(r_{\text{cmm}}, \nu(k)r_{\text{ctr}})$ at $\{(p_i, v_i)\}_{i \in \{1, \dots, n\}}$, the control constraint set is defined by*

$$\begin{aligned} &\mathcal{U}_E^d(r_{\text{cmm}}, r_{\text{ctr}}, \nu(k)) \cdot (\{p_i, v_i\}_{i \in \{1, \dots, n\}}) \\ &= \{(u_1, \dots, u_n) \in B(0_d, r_{\text{ctr}})^n \mid \forall ((p_i, v_i), (p_j, v_j)) \in E, \\ &\quad u_i - u_j \in \mathcal{U}^d(r_{\text{cmm}}, \nu(k)r_{\text{ctr}}) \cdot (p_i - p_j, v_i - v_j)\}. \end{aligned}$$

In other words, the control constraint set for an edge set E is the set of controls for each agent with the property that all edges in E will be maintained in one time step.

Remark 6.11 *We can now interpret the results in Theorem 6.8 as follows.*

- (i) To maintain connectivity between any pair of connected agents, we should simultaneously handle constraints corresponding to all edges of $\mathcal{G}_{\text{di-disk}}(r_{\text{cmm}}, \nu(k)r_{\text{ctr}})$. This might render the control constraint set empty.
- (ii) However, if we only consider constraints corresponding to edges belonging to a spanning tree T of $\mathcal{G}_{\text{di-disk}}(r_{\text{cmm}}, \nu(k)r_{\text{ctr}})$, then the set $\mathcal{U}_T^d(r_{\text{cmm}}, \nu(k)r_{\text{ctr}}) \cdot (\{p_i, v_i\}_{i \in \{1, \dots, n\}})$ is guaranteed to be nonempty. \square

Let us now provide a concrete representation of the control constraint set. Given a pair i, j of connected agents, the admissible control set $\mathcal{U}^d(r_{\text{cmm}}, \nu(k)r_{\text{ctr}}) \cdot (p_{ij}, v_{ij})$ is convex and compact (Lemma 6.1). Hence, we can fit a polytope with N_{poly} sides inside it. This approximating polytope leads to the following tighter version of the constraint in (6.10):

$$(C_{ij}^\eta)^T (u_i - u_j) \leq w_{ij}^\eta, \quad \eta \in \{1, \dots, N_{\text{poly}}\}, \quad (6.12)$$

for some appropriate vector $C_{ij}^\eta \in \mathbb{R}^d$ and scalar $w_{ij}^\eta \in \mathbb{R}$. Similarly, one can compute an inner polytopic approximation of the closed ball $B(0_d, r_{\text{ctr}})$ and write the following linear vector inequalities:

$$(C_{i\theta}^\eta)^T u_i \leq w_{i\theta}^\eta, \quad \eta \in \{1, \dots, N_{\text{poly}}\}, \quad (6.13)$$

where the symbol θ has the interpretation of a fictional agent. In this way, we have cast the original problem of finding a set of feasible control inputs into a satisfiability problem for a set of linear inequalities.

Remark 6.12 *Rather than a network-wide control constraint set, one might like to obtain decoupled constraint sets for each individual agent. However, (1) it is*

not clear how to design a distributed algorithm to perform this computation, (2) such an algorithm will likely have large communication requirements, and (3) such a calculation might lead to a very conservative estimate for the decoupled control constraint sets. Therefore, rather than explicitly decoupling the control constraint sets, we next focus on a distributed algorithm to search the control constraint set for feasible controls that are optimal according to some criterion. \square

6.3 Distributed computation of optimal controls

In this section we formulate and solve the following optimization problem: given an array of desired control inputs $U_{\text{des}} = (u_{\text{des},1}, \dots, u_{\text{des},n})^T \in (\mathbb{R}^d)^n$, find, via local computation, the array $U = (u_1, \dots, u_n)$ belonging to the control constraint set, that is *closest* to the desired array U_{des} . To formulate this problem precisely, we need some additional notations. Let E be a set of edges in the undirected graph $\mathcal{G}_{\text{di-disk}}(r_{\text{cmm}}, \nu(k)r_{\text{ctr}})$ at $\{(p_i, v_i)\}_{i \in \{1, \dots, n\}}$. To deal with the linear inequalities of the form (6.12) and (6.13) associated to each edge of E , we introduce an appropriate *multigraph*. A *multigraph* (or *multiple edge graph*) is, roughly speaking, a graph with multiple edges between the same vertices. More formally, a multigraph is a pair $(V_{\text{mult}}, E_{\text{mult}})$, where V_{mult} is the vertex set and the edge set E_{mult} contains numbered edges of the form (i, j, η) , for $i, j \in V$ and $\eta \in \mathbb{N}$, and where E_{mult} has the property that if $(i, j, \eta) \in E_{\text{mult}}$ and $\eta > 1$, then also $(i, j, \eta - 1) \in E_{\text{mult}}$. In what follows, we let G_{mult} denote the multigraph with vertex set $\{1, \dots, n\}$ and with edge set $E_{\text{mult}} = \{(i, j, \eta) \in \{1, \dots, n\}^2 \times \{1, \dots, N_{\text{poly}}\} \mid ((p_i, v_i), (p_j, v_j)) \in E, i > j\}$. Note that to each element $(i, j, \eta) \in E_{\text{mult}}$ is associated the inequality $(C_{ij}^\eta)^T(u_i - u_j) \leq w_{ij}^\eta$. We

are now ready to formally state the optimization problem at hand in the form of the following quadratic programming problem:

$$\begin{aligned}
& \text{minimize} && \frac{1}{2} \sum_{i=1}^n \|u_i - u_{\text{des},i}\|^2, \\
& \text{subj. to} && (C_{ij}^\eta)^T (u_i - u_j) \leq w_{ij}^\eta, \quad \text{for } (i, j, \eta) \in E_{\text{mult}}, \\
& && (C_{i\theta}^\eta)^T u_i \leq w_{i\theta}^\eta, \quad \text{for } i \in \{1, \dots, n\}, \eta \in \{1, \dots, N_{\text{poly}}\}.
\end{aligned} \tag{6.14}$$

Here, somehow arbitrarily, we have adopted the 2-norm to define the cost function.

Remark 6.13 (Feasibility) *If E is a spanning tree of $\mathcal{G}_{\text{di-disk}}(r_{\text{cmm}}, \nu r_{\text{ctr}})$ at a connected configuration $\{(p_i, v_i)\}_{i \in \{1, \dots, n\}}$, then the control constraint set $\mathcal{U}_E^d(r_{\text{cmm}}, r_{\text{ctr}}, \nu(k)) \cdot \{(p_i, v_i)\}_{i \in \{1, \dots, n\}}$ is guaranteed to be non-empty by Theorem 6.8. In turn, this implies that the optimization problem (6.14) is feasible.*

□

6.3.1 Solution via duality: the projected Jacobi method

The problem (6.14) can be written in a compact form as:

$$\begin{aligned}
& \text{minimize} && \frac{1}{2} \|U - U_{\text{des}}\|^2, \\
& \text{subj. to} && B_{\text{mult}}^T U \preceq w,
\end{aligned}$$

for appropriately defined matrix B_{mult} and vector w . A dual “projected Jacobi method” algorithm for the solution of this standard quadratic program is described in Appendix B. According to this algorithm, let λ^* be the value of Lagrange multipliers at optimality. Then the global minimum for U is achieved at

$$U^* = U_{\text{des}} - B_{\text{mult}} \lambda^*. \tag{6.15}$$

The projected Jacobi iteration for each component of λ is given by

$$\lambda_\alpha(t+1) = \max \left\{ 0, \lambda_\alpha(t) - \frac{\tau}{(B_{\text{mult}}^T B_{\text{mult}})_{\alpha\alpha}} \left((w - B_{\text{mult}}^T U_{\text{des}})_\alpha + \sum_{\beta=1}^{N_{\text{poly}}(e+n)} (B_{\text{mult}}^T B_{\text{mult}})_{\alpha\beta} \lambda_\beta(t) \right) \right\}, \quad (6.16)$$

where $\alpha \in \{1, \dots, N_{\text{poly}}(e+n)\}$ and τ is the step size parameter. We can select $\tau = \frac{1}{N_{\text{poly}}(e+n)}$ to guarantee convergence.

6.3.2 A distributed implementation of the dual algorithm

Because of the particular structure of the matrix $B_{\text{mult}}^T B_{\text{mult}}$, the iterations (6.16) can be implemented in a distributed way over the original graph G . To highlight the distributed structure of the iteration we denote the components of λ by referring to the nodes that they share and the inequality they are related to. In particular for each edge in G_{mult} , the corresponding Lagrange multiplier will be denoted as λ_{ij}^η if the edge goes from node i to node j , $i > j$, and the edge is associated to the inequality constraint $C_{ij}^\eta(u_i - u_j) \leq w_{ij}^\eta$. This makes up the first $N_{\text{poly}}e$ entries of the vector λ . To be consistent with this notation, the next $N_{\text{poly}}n$ entries will be denoted $\lambda_{1\theta}^1, \dots, \lambda_{1\theta}^{N_{\text{poly}}}, \dots, \lambda_{n\theta}^1, \dots, \lambda_{n\theta}^{N_{\text{poly}}}$. Additionally, define $\mathcal{N}(i) = \{j \in \{1, \dots, n\} \mid \{(p_i, v_i), (p_j, v_j)\} \in E\} \cup \{\theta\}$. The symbol θ has the interpretation of a fictional node.

Defining $\lambda_{ij}^\eta := \lambda_{ji}^\eta$ and $C_{ij}^\eta := -C_{ji}^\eta$ for $i < j$, we can write equations (6.15) and (6.16) in components as follows. Equation (6.15) reads, for $i \in \{1, \dots, n\}$,

$$u_i^* = u_{\text{des},i} - \sum_{k \in \mathcal{N}(i)} \sum_{\eta=1}^{N_{\text{poly}}} C_{ik}^\eta \lambda_{ik}^\eta.$$

One can easily work an explicit expression for matrix product $B_{\text{mult}}^T B_{\text{mult}}$ in (6.16).

Then, equation (6.16) reads, for $(i, j, \eta) \in E_{\text{mult}}$,

$$\lambda_{ij}^\eta(t+1) = \max \left\{ 0, \lambda_{ij}^\eta(t) - \frac{\tau}{2(C_{ij}^\eta)^T C_{ij}^\eta} \cdot \left(\sum_{k \in \mathcal{N}(i)} \sum_{\sigma=1}^{N_{\text{poly}}} \left((C_{ij}^\eta)^T C_{ik}^\sigma \lambda_{ik}^\sigma \right) + \sum_{k \in \mathcal{N}(j)} \sum_{\sigma=1}^{N_{\text{poly}}} \left((C_{ji}^\eta)^T C_{jk}^\sigma \lambda_{jk}^\sigma \right) + w_{ij}^\eta - (C_{ij}^\eta)^T (u_{\text{des},i} - u_{\text{des},j}) \right) \right\},$$

together with, for $i \in \{1, \dots, n\}$, $\eta \in \{1, \dots, N_{\text{poly}}\}$,

$$\lambda_{i\theta}^\eta(t+1) = \max \left\{ 0, \lambda_{i\theta}^\eta(t) - \frac{\tau}{(C_{i\theta}^\eta)^T C_{i\theta}^\eta} \left(\sum_{k \in \mathcal{N}(i)} \sum_{\sigma=1}^{N_{\text{poly}}} \left((C_{i\theta}^\eta)^T C_{ik}^\sigma \lambda_{ik}^\sigma \right) + w_{i\theta}^\eta - (C_{i\theta}^\eta)^T u_{\text{des},i} \right) \right\}.$$

We distribute the task of running iterations for these $N_{\text{poly}}(e+n)$ Lagrange multipliers among the n agents as follows: an agent i carries out the updates for all quantities $\lambda_{i\theta}^\eta$ and all λ_{ij}^η for which $i > j$. By means of this partition and by means of iterated one-hop communication among agents, it is possible to compute the global solution for the optimization problem (6.14) in a distributed fashion over the double integrator disk graph.

6.4 Simulations

To illustrate our analysis we focus on the following scenario. For the two dimensional setting, i.e., for $d = 2$, we assume that there are $n = 5$ agents with (randomly chosen) initial condition and such that they are connected according

to $\mathcal{G}_{\text{di-disk}}$. The bound for the control input is $r_{\text{ctr}} = 2$ and the communication radius is $r_{\text{cmm}} = 10$.

We assigned to one of the agents a derivative feedback control $u_x[p, v] = (v_x - 2)$, $u_y[p, v] = (v_y - 5)$ as desired input. For the other agents the desired input is set to zero. We show the agent trajectories in Figure 6.4a, the velocities of the agents with respect to time in Figure 6.4b, and the distances between agents which are neighbors in the spanning tree in Figure 6.4c. Notice that the agents move with approximately identical velocity reaching a configuration in which all of them are at the limit distance $r_{\text{cmm}} = 10$. The interesting aspect of this simulation is that the maintenance of connectivity leads to the accomplishment of apparently unrelated coordination tasks as velocity alignment and cohesiveness. This numerical result illustrate how our connectivity maintenance approach might indeed be a starting point for novel investigations into the problem of flocking with connectivity.

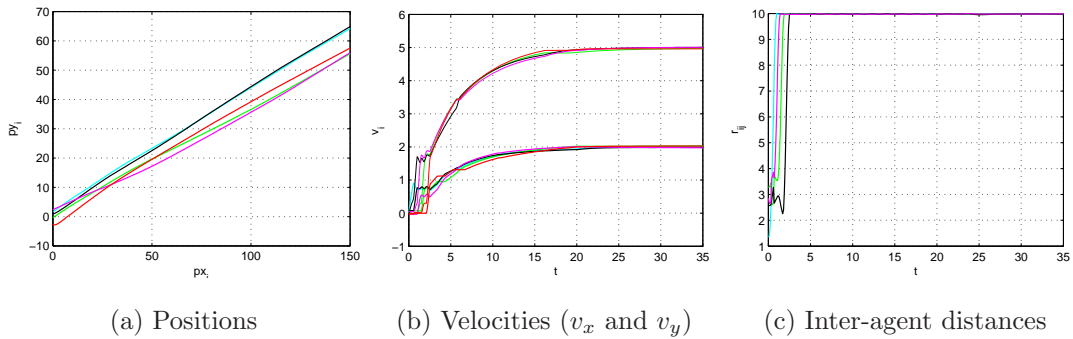


Figure 6.4: Velocity alignment and cohesiveness for 5 agents in the plane ($d = 2$)

6.5 Summary

We provided some distributed algorithms to enforce connectivity among networks of agents with double-integrator dynamics. Future directions of research include (i) evaluating the communication complexity of the proposed distributed dual algorithm and possibly designing faster ones, (ii) studying the relationship between the connectivity maintenance problem and the platooning and mesh stability problem, and (iii) investigating the flocking phenomenon and designing flocking algorithms which do not rely on a blanket assumption of connectivity.

Chapter 7

Conclusions

In the context of DTSP, future directions of research include finding a *single* algorithm which would provide constant factor approximation to the DTSP for the worst case *as well as* the stochastic setting. It is also interesting to consider the *non-uniform* stochastic DTSP when the points to be serviced are sampled according to a non-uniform probability distribution. Other avenues of future research are to use the tools developed in this paper to study Traveling Salesperson Problems for other dynamical vehicles, study decentralized versions of the DTRP and general task assignment and surveillance problems for multi-Dubins (and other dynamical) vehicles. Another set of interesting problems arise when the environment is non-convex (e.g., environment with obstacles) and/or we consider TSP problems without target location information, i.e., search problems. Another variation of the problems to be considered is when vehicles have finite "servicing footprints".

An immediate extension of the results for the coverage problem would be to

consider teams with non-uniform team composition. Studying loitering patterns with different notions of cost functions, like *average* cost instead of the *worst-case* cost, would also be interesting. Designing loitering patterns over more general class of curves (instead of only *circular* curves) is also a possible avenue of future research.

The connectivity maintenance problem also gives rise to many other exciting problems. An immediate task would be to evaluate the communication complexity of the proposed distributed dual algorithm and possibly designing faster ones. It would be interesting to study the relationship between the connectivity maintenance problem and the platooning and mesh stability problem. It is also interesting to investigate the flocking phenomenon and designing flocking algorithms which do not rely on a blanket assumption of connectivity. Finally, it would be exciting to extend this framework to more general notions of connectivity.

In this dissertation, we dealt mainly with the motion coordination aspects of multi-UAV systems. One can envision future UAV systems equipped with heterogeneous sensors like radars, acoustic transducers and collectively performing various cooperative tasks like target identification, estimation and tracking. The possibility to control sensor modalities (e.g., waveform selection, beam steering) and mobility of sensor platforms (UAVs) gives the possibility to increase the performance of conventional systems by orders of magnitude. At the same time, it gives rise to challenging problems in sensor management, distributed estimation and signal processing, data fusion and decentralized motion planning. Solving these fundamental scientific problems is essential to extract the maximum out of the emergent UAV technology.

Bibliography

- [1] J. Cortés and F. Bullo, “Coordination and geometric optimization via distributed dynamical systems,” *SIAM Journal on Control and Optimization*, vol. 44, no. 5, pp. 1543–1574, 2005.
- [2] K. B. Ariyur, P. Lommel, and D. F. Enns, “Reactive inflight obstacle avoidance via radar feedback,” in *American Control Conference*, (Portland, OR), pp. 2978–2982, 2005.
- [3] C. Tomlin, I. Mitchell, and R. Ghosh, “Safety verification of conflict resolution manoeuvres,” *IEEE Transactions on Intelligent Transportation Systems*, vol. 2, no. 2, pp. 110–120, 2001.
- [4] S. M. LaValle, *Planning Algorithms*. Cambridge, UK: Cambridge University Press, 2006.
- [5] U. Boscain and B. Piccoli, *Optimal Syntheses for Control Systems on 2-D Manifolds*. Mathématiques et Applications, New York: Springer Verlag, 2004.
- [6] P. R. Chandler, M. Pachter, D. Swaroop, J. M. Fowler, J. K. Howlett, S. Rasmussen, C. Schumacher, and K. Nygard, “Complexity in UAV cooperative

- control,” in *American Control Conference*, (Anchorage, AK), pp. 1831–1836, 2002.
- [7] Z. Tang and Ü. Özgüner, “Motion planning for multi-target surveillance with mobile sensor agents,” *IEEE Transactions on Robotics*, vol. 21, no. 5, pp. 898–908, 2005.
- [8] R. W. Beard, T. W. McLain, M. A. Goodrich, and E. P. Anderson, “Coordinated target assignment and intercept for unmanned air vehicles,” *IEEE Transactions on Robotics and Automation*, vol. 18, no. 6, pp. 911–922, 2002.
- [9] S. Rathinam, R. Sengupta, and S. Darbha, “A resource allocation algorithm for multi-vehicle systems with non holonomic constraints,” *IEEE Transactions on Automation Sciences and Engineering*, 2006. To appear.
- [10] E. Frazzoli and F. Bullo, “Decentralized algorithms for vehicle routing in a stochastic time-varying environment,” in *IEEE Conf. on Decision and Control*, (Paradise Island, Bahamas), pp. 3357–3363, Dec. 2004.
- [11] A. E. Gil, K. M. Passino, and A. Sparks, “Cooperative scheduling of tasks for networked uninhabited autonomous vehicles,” in *IEEE Conf. on Decision and Control*, (Maui, Hawaii), pp. 522–527, Dec. 2003.
- [12] A. Richards, J. Bellingham, M. Tillerson, and J. How, “Coordination and control of multiple UAVs,” in *AIAA Conf. on Guidance, Navigation and Control*, (Monterey, CA), Aug. 2002.
- [13] A. A. Markov, “Some examples of the solution of a special kind problem on greatest and least quantities,” *Soobshch. Kharkovsk. Mat. Obshch.*, vol. 1, pp. 250–276, 1887. (in Russian).

- [14] L. E. Dubins, “On curves of minimal length with a constraint on average curvature and with prescribed initial and terminal positions and tangents,” *American Journal of Mathematics*, vol. 79, pp. 497–516, 1957.
- [15] J.-D. Boissonnat, A. Cérézo, and J. Leblond, “Shortest paths of bounded curvature in the plane,” *Journal of Intelligent and Robotic Systems*, vol. 11, pp. 5–20, 1994.
- [16] A. M. Shkel and V. J. Lumelsky, “Classification of the Dubins set,” *Robotics and Autonomous Systems*, vol. 34, pp. 179–202, 2001.
- [17] J.-D. Boissonnat and S. Lazard, “A polynomial-time algorithm for computing a shortest path of bounded curvature amidst moderate obstacles,” *International Journal of Computational Geometry & Applications*, vol. 13, pp. 189–229, 2003.
- [18] J. Beardwood, J. Halton, and J. Hammersly, “The shortest path through many points,” in *Proceedings of the Cambridge Philosophy Society*, vol. 55, pp. 299–327, 1959.
- [19] J. M. Steele, “Probabilistic and worst case analyses of classical problems of combinatorial optimization in Euclidean space,” *Mathematics of Operations Research*, vol. 15, no. 4, p. 749, 1990.
- [20] D. Applegate, R. Bixby, V. Chvátal, and W. Cook, “On the solution of traveling salesman problems,” in *Documenta Mathematica, Journal der Deutschen Mathematiker-Vereinigung*, (Berlin, Germany), pp. 645–656, Aug. 1998. Proceedings of the International Congress of Mathematicians, Extra Volume ICM III.

- [21] S. Arora, “Nearly linear time approximation scheme for Euclidean TSP and other geometric problems,” in *IEEE Symposium on Foundations of Computer Science*, (Miami Beach, FL), pp. 554–563, Oct. 1997.
- [22] S. Lin and B. W. Kernighan, “An effective heuristic algorithm for the traveling-salesman problem,” *Operations Research*, vol. 21, pp. 498–516, 1973.
- [23] A. Aggarwal, D. Coppersmith, S. Khanna, R. Motwani, and B. Schieber, “The angular-metric traveling salesman problem,” *SIAM Journal on Computing*, vol. 29, no. 3, pp. 697–711, 1999.
- [24] D. J. Bertsimas and G. J. van Ryzin, “A stochastic and dynamic vehicle routing problem in the Euclidean plane,” *Operations Research*, vol. 39, pp. 601–615, 1991.
- [25] K. Savla, E. Frazzoli, and F. Bullo, “On the point-to-point and traveling salesperson problems for Dubins’ vehicle,” in *American Control Conference*, (Portland, OR), pp. 786–791, June 2005.
- [26] J. Le Ny and E. Feron, “An approximation algorithm for the curvature-constrained traveling salesman problem,” in *Allerton Conference on Communications, Control and Computing*, (Monticello, IL), Sept. 2005.
- [27] S. Darbha, “Combinatorial motion planning for a collection of Reeds-Shepp vehicles,” tech. rep., ASEE/AFOSR SFFP, AFRL, Eglin, Aug. 2005.
- [28] K. Savla, F. Bullo, and E. Frazzoli, “On traveling salesperson problems for Dubins’ vehicle: stochastic and dynamic environments,” in *IEEE Conf. on*

- Decision and Control and European Control Conference*, (Seville, Spain), pp. 4530–4535, Dec. 2005.
- [29] S. Itani and M. A. Dahleh, “On the average length of the stochastic TSP with Dubins’ metric,” tech. rep., LIDS, Massachusetts Institute of Technology, 2005.
- [30] K. Savla, E. Frazzoli, and F. Bullo, “On the Dubins Traveling Salesperson Problems: Novel approximation algorithms,” in *Robotics: Science and Systems II*, Cambridge, MA: MIT Press, 2007.
- [31] C. Schumacher, P. R. Chandler, S. J. Rasmussen, and D. Walker, “Task allocation for wide area search munitions with variable path length,” in *American Control Conference*, (Denver, CO), pp. 3472–3477, 2003.
- [32] J. Cortés, S. Martínez, T. Karatas, and F. Bullo, “Coverage control for mobile sensing networks,” *IEEE Transactions on Robotics and Automation*, vol. 20, no. 2, pp. 243–255, 2004.
- [33] H. Ando, Y. Oasa, I. Suzuki, and M. Yamashita, “Distributed memoryless point convergence algorithm for mobile robots with limited visibility,” *IEEE Transactions on Robotics and Automation*, vol. 15, no. 5, pp. 818–828, 1999.
- [34] J. Lin, A. S. Morse, and B. D. O. Anderson, “The multi-agent rendezvous problem,” in *IEEE Conf. on Decision and Control*, (Maui, HI), pp. 1508–1513, Dec. 2003.
- [35] J. Cortés, S. Martínez, and F. Bullo, “Robust rendezvous for mobile autonomous agents via proximity graphs in arbitrary dimensions,” *IEEE Transactions on Automatic Control*, vol. 51, no. 8, pp. 1289–1298, 2006.

- [36] A. Ganguli, J. Cortés, and F. Bullo, “On rendezvous for visually-guided agents in a nonconvex polygon,” in *IEEE Conf. on Decision and Control and European Control Conference*, (Seville, Spain), pp. 5686–5691, Dec. 2005.
- [37] D. P. Spanos and R. M. Murray, “Motion planning with wireless network constraints,” in *American Control Conference*, (Portland, OR), pp. 87–92, June 2005.
- [38] M. M. Zavlanos and G. J. Pappas, “Controlling connectivity of dynamic graphs,” in *IEEE Conf. on Decision and Control and European Control Conference*, (Seville, Spain), pp. 6388–6393, Dec. 2005.
- [39] G. Percus and O. C. Martin, “Finite size and dimensional dependence of the Euclidean traveling salesman problem,” *Physical Review Letters*, vol. 76, no. 8, pp. 1188–1191, 1996.
- [40] J. J. Enright and E. Frazzoli, “UAV routing in a stochastic time-varying environment,” in *IFAC World Congress*, (Prague, Czech Republic), July 2005. Electronic Proceedings.
- [41] R. Motwani and P. Raghavan, *Randomized Algorithms*. Cambridge, UK: Cambridge University Press, 1995.
- [42] Y. Azar, A. Z. Broder, A. R. Karlin, and E. Upfal, “Balanced allocations,” *SIAM Journal on Computing*, vol. 29, no. 1, pp. 180–200, 1999.
- [43] L. Kleinrock, *Queueing Systems. Volume I: Theory*. New York: John Wiley, 1975.
- [44] J. J. Enright, E. Frazzoli, K. Savla, and F. Bullo, “On multiple UAV routing with stochastic targets: performance bounds and algorithms,” in *AIAA*

- Conf. on Guidance, Navigation and Control*, Aug. 2005. Electronic Proceedings.
- [45] J. Lawrence, *A catalog of special plane curves*. New York: Dover Publications, 1972.
- [46] R. Kershner, “The number of circles covering a set,” *American Journal of Mathematics*, vol. 61, no. 3, pp. 665–671, 1939.
- [47] Z. Gao, “On discrete time optimal control: A closed-form solution,” in *American Control Conference*, (Boston, MA), pp. 52–58, 2004.
- [48] B. Aspvall and Y. Shiloach, “A polynomial time algorithm for solving systems of linear inequalities with two variables per inequality,” *SIAM Journal on Computing*, vol. 9, no. 4, pp. 827–845, 1980.
- [49] M. Bui, F. Butelle, and C. Lavault, “A distributed algorithm for constructing a minimum diameter spanning tree,” *Journal of Parallel and Distributed Computing*, vol. 64, pp. 571–577, 2004.
- [50] D. P. Bertsekas and J. N. Tsitsiklis, *Parallel and Distributed Computation: Numerical Methods*. Belmont, MA: Athena Scientific, 1997.

Appendix A

On the proof of Theorem 2.4

A.1 Dubins classification of optimal curves

Following [14], the minimum length feasible curve for the Dubins vehicle is either (i) an arc of a circle of radius ρ , followed by a line segment, followed by an arc of a circle of radius ρ , or (ii) a sequence of three arcs of circles of radius ρ , or (iii) a subpath of a path of path type (i) or (ii). To specify the *type* of these minimum length feasible curves for the Dubins path we follow the notations used in [16]. Three elementary motions are considered: turning to the left, turning to the right (both along a circle of radius ρ), and straight line motion S . Three operators are introduced: L_v (for left/counterclockwise turn of length $v > 0$), R_v (for right/clockwise turn of length $v > 0$), S_v (for straight motion of length $v > 0$). The operators L_v , R_v , and S_v , transform an arbitrary configuration

$(x, y, \psi) \in \text{SE}(2)$ into its corresponding image point in $\text{SE}(2)$ by

$$\begin{aligned} & (x + \sin(\psi + v) - \sin \psi, y - \cos(\psi + v) + \cos \psi, \psi + v), \\ & (x - \sin(\psi - v) + \sin \psi, y + \cos(\psi - v) - \cos \psi, \psi - v), \\ & (x + v \cos \psi, y + v \sin \psi, \psi), \end{aligned}$$

respectively. Thus, the *Dubins set* \mathcal{D} which is the domain for the type of the minimum length feasible curve for a Dubins vehicle between a given initial and final configuration is given by $\mathcal{D} = \{LSL, RSR, RSL, LSR, RLR, LRL\}$. One may refer to [14] for a detailed discussion on the construction of these path types between a given initial and final configuration. One may note that there are sets of initial and final configurations for which all the path types may not be feasible between those configurations.

In the remaining part of the chapter we will need to frequently use the curves of type *LRL* and *RLR* starting with the initial configuration $(0, 0, 0)$ and the final configuration $(0, 0, \psi)$. We introduce some additional notations to facilitate presentation of the same. We introduce notations for the path type *LRL*. For $\psi \neq 0$, let $C_{p_1}(\psi)$ be a circle with center $O_{C_{p_1}} := (0, \rho)$ and radius ρ , and let $C_{p_2}(\psi)$ be a circle with center $O_{C_{p_2}} := (-\rho \sin \psi, \rho \cos \psi)$ and radius ρ . Note that $\psi \neq 0$ implies that $C_{p_1}(\psi) \cap C_{p_2}(\psi)$ is either a point or 2 points. Then let $C_{m_1}(\psi)$ and $C_{m_2}(\psi)$ be two circles with radius ρ that are tangent to both $C_{p_1}(\psi)$ and $C_{p_2}(\psi)$, see Figure A.1 and Figure A.2.

By construction, $C_{p_1}(\psi)$ intersects $C_{m_1}(\psi)$ and $C_{m_2}(\psi)$ at one point each: let $P_1(\psi)$ be the first of these two points that is reached moving left from the origin O along $C_{p_1}(\psi)$. Without loss of generality, assume $P_1(\psi) \in C_{m_1}(\psi)$. Let $O_{C_{m_1}}$ be the center of C_{m_1} . Let $P_2(\psi) = C_{m_1}(\psi) \cap C_{p_2}(\psi)$. In order to remove ambiguity,

A.2 Proof of Theorem 2.4

We begin with some preliminary results.

Lemma A.1 (*Length of LRL and RLR curves returning to the origin*) Given $\psi \in]0, 2\pi[$ and $\rho > 0$, then

$$(i) \text{ Length}(LRL_O(\psi)) = \rho\psi + 4\rho \cos^{-1}\left(\frac{\sin(\psi/2)}{2}\right), \text{ and}$$

$$(ii) \text{ Length}(RLR_O(\psi)) = \rho(2\pi - \psi) + 4\rho \cos^{-1}\left(\frac{\sin(\psi/2)}{2}\right).$$

Proof. Let us prove part (i); part (ii) is proved by symmetry. We first consider the case where $\psi \in]0, \pi]$. It is immediate from the definition of t_1, t_2, t_3 and from Figure A.1 that

$$\text{Length}(LRL_O(\psi)) = t_1 + t_2 + t_3 = 2t_1 + t_2, \quad t_1 = \phi - \delta, \quad t_2 = \pi + 2\phi. \quad (\text{A.1})$$

Some elementary calculations lead to

$$\cos \phi = \frac{\|O_{C_{p_2}} - O_{C_{p_1}}\|}{4\rho}, \quad \cos \delta = \frac{\|O_{C_{p_2}} - O_{C_{p_1}}\|}{2\rho}, \quad \|O_{C_{p_2}} - O_{C_{p_1}}\| = 2\rho \sin\left(\frac{\psi}{2}\right).$$

Therefore, we have

$$\cos \phi = \sin(\psi/2)/2, \quad \cos \delta = \sin(\psi/2) \quad \implies \quad \delta = \pi/2 - \psi/2. \quad (\text{A.2})$$

From the expressions in equation (A.1), for $\psi \in]0, \pi]$, we have

$$\text{Length}(LRL_O(\psi)) = \rho\psi + 4\rho \cos^{-1}\left(\frac{\sin(\psi/2)}{2}\right). \quad (\text{A.3})$$

We now consider the case where $\psi \in]\pi, 2\pi[$. For this case, one can verify from Figure A.2 that the expressions for t_2 and ϕ are same as in (A.1) and (A.2),

respectively. However, following on similar lines as in the case when $\psi \in]0, \pi]$ and referring to Figure A.2, the expressions for t_1 and δ are now given by $t_1 = \phi + \delta$, and $\delta = \psi/2 - \pi/2$. Therefore, for $\psi \in]\pi, 2\pi]$, we have

$$\text{Length}(LRL_O(\psi)) = \rho\psi + 4\rho \cos^{-1} \left(\frac{\sin(\psi/2)}{2} \right).$$

The final result follows by combining the latter equation with (A.3). ■

This Lemma A.1 has the following direct consequence.

Lemma A.2 (*Upper bound on the length of shortest curves returning to the origin*) For all $\psi \in [0, 2\pi[$ and $\rho > 0$

$$\mathcal{C}_\rho(0, 0, \psi) \leq \mathcal{C}_\rho(0, 0, \pi) = \frac{7}{3}\pi\rho.$$

Next, we start to analyze the general case where $(x, y) \neq (0, 0)$. In what follows, we let $(d, \theta) = \text{polar}(x, y)$ be the polar coordinates of $(x, y) \neq (0, 0)$ and, with a slight abuse of notation, we let $\mathcal{C}_\rho(d, \theta, \psi) = \mathcal{C}_\rho(x, y, \psi)$.

Lemma A.3 *Upper bound on the optimal length via LRL_O and RLR_O* For $\psi \in]0, 2\pi[$, and $(d, \theta) = \text{polar}(x, y)$,

$$(i) \text{ if } (x, y) \in V_1^c(\psi), \text{ then } \mathcal{C}_\rho(d, \theta, \psi) \leq d + \text{Length}(LRL_O(\psi)),$$

$$(ii) \text{ if } (x, y) \in V_2^c(\psi), \text{ then } \mathcal{C}_\rho(d, \theta, \psi) \leq d + \text{Length}(RLR_O(\psi)).$$

Proof. Let us prove part (i); part (ii) is proved by similar considerations. We recall the construction used for $LRL_O(\psi)$ curves. We define two additional circles

\bar{C}_{m_1} and \bar{C}_{p_1} of radiuses ρ and whose respective centers $O_{\bar{C}_{m_1}}$ and $O_{\bar{C}_{p_2}}$ are given by

$$O_{\bar{C}_{m_1}} = O_{C_{m_1}} + (d \cos \theta, d \sin \theta), \quad O_{\bar{C}_{p_2}} = O_{C_{p_2}} + (d \cos \theta, d \sin \theta).$$

Let \bar{C}_{m_1} be oriented clockwise and let \bar{C}_{p_2} be oriented counter-clockwise. Then, there always exists an oriented segment, say M , tangent to C_{m_1} and \bar{C}_{m_1} with the property that a Dubins vehicle can make transition from C_{m_1} to \bar{C}_{m_1} through M . Let $P_3 = M \cap C_{m_1}$, $\bar{P}_3 = M \cap \bar{C}_{m_1}$, $\bar{P}_2 = P_2 + (d \cos \theta, d \sin \theta)$ and $\bar{O} = O + (d \cos \theta, d \sin \theta)$. It is easy to see from the construction that, provided the point P_3 lies in the clockwise arc P_1P_2 along the circle C_{m_1} , the path consisting of (in order) OP_1 along C_{p_1} , P_1P_3 along C_{m_1} , $P_3\bar{P}_3$ along M , $\bar{P}_3\bar{P}_2$ along \bar{C}_{m_1} , $\bar{P}_2\bar{O}$ along \bar{C}_{p_2} is a feasible curve for the Dubins vehicle from O to \bar{O} , see Figure A.3. With a slight abuse of notation, we shall denote this curve as $LRL_{\bar{O}}(d, \theta, \psi)$. The condition that P_3 lies along the arc P_1P_2 along the circle C_{m_1} holds true when the orientation of the segment $M = P_3\bar{P}_3$ does not lie between the orientations of the tangents to C_{m_1} at P_1 and P_2 . In summary, we have:

$$\text{orientation of } M = \text{orientation of } P_3\bar{P}_3 = \theta,$$

$$\text{orientation of tangent to } C_{m_1} \text{ at } P_1 = \psi/2 - \pi/2 + \cos^{-1}(\sin(\psi/2)/2),$$

$$\text{orientation of tangent to } C_{m_1} \text{ at } P_2 = \psi/2 + \pi/2 - \cos^{-1}(\sin(\psi/2)/2).$$

Therefore, the above condition is satisfied when

$$\theta \notin]\psi/2 - \pi/2 + \cos^{-1}(\sin(\psi/2)/2), \psi/2 + \pi/2 - \cos^{-1}(\sin(\psi/2)/2)[.$$

It follows from the definition of $V_1(\psi)$ that this is true *if and only if* $(x, y) \in V_1^c(\psi)$.

Because $LRL_{\overline{O}}(d, \theta, \psi)$ is a suboptimal path, for $\psi \in]0, 2\pi[$, $(x, y) \in V_1^c(\psi)$ and $(d, \theta) = \text{polar}(x, y)$, we have

$$\mathcal{C}_\rho(d, \theta, \psi) \leq \text{Length}(LRL_{\overline{O}}(d, \theta, \psi)). \quad (\text{A.4})$$

From Figure A.1 and Figure A.3,

$$\text{Length}(LRL_{\overline{O}}(d, \theta, \psi)) = d + \text{Length}(LRL_O(\psi)). \quad (\text{A.5})$$

Combining (A.4) and (A.5) we get the final result. ■

One can prove that for $d = 0$, the minimal length feasible curve for the Dubins vehicle is of type LRL or RLR . This, along with Lemma A.1, leads us to our next lemma which we state without any proof.

Lemma A.4 *Optimal path length returning to the origin* Let $d = 0$ and $\theta \in [0, 2\pi[$.

(i) if $\psi \in]0, \pi]$, then $LRL_O(\psi)$ is the optimal path and $\mathcal{C}_\rho(0, \theta, \psi) = \rho\psi + 4\rho \cos^{-1}\left(\frac{\sin(\psi/2)}{2}\right)$,

(ii) if $\psi \in]\pi, 2\pi[$, then $RLR_O(\psi)$ is the optimal path and $\mathcal{C}_\rho(0, \theta, \psi) = \rho(2\pi - \psi) + 4\rho \cos^{-1}\left(\frac{\sin(\psi/2)}{2}\right)$.

Let

$$U_1 = \bigcup_{\psi \in]0, \pi]} V_1^c(\psi), \quad U_2 = \bigcup_{\psi \in]\pi, 2\pi[} V_2^c(\psi).$$

Lemma A.5 *Relation between $\mathcal{C}_\rho(d, \theta, \psi)$ and $\mathcal{C}_\rho(0, \theta, \psi)$* For $(d, \theta) = \text{polar}(x, y)$ and $(x, y) \in U_1 \cup U_2$,

$$\mathcal{C}_\rho(d, \theta, \psi) \leq d + \mathcal{C}_\rho(0, \theta, \psi),$$

and, therefore, $\mathcal{C}_\rho(d, \theta, \psi) \leq d + \frac{7}{3}\pi\rho$.

Proof. The proof follows from Lemmas A.3 and A.4; the second statement follows from Lemma A.2. ■

It now remains to obtain a bound on $C_r(d, \theta, \psi)$ when $(x, y) \in V_1(\psi)$ or $(x, y) \in V_2(\psi)$ where $(d, \theta) = \text{polar}(x, y)$. To this effect, let the vehicle start moving at time $t = 0$ at unit speed along C_{p_1} in the counterclockwise direction and keep updating the parameters d, θ, ψ as if the coordinate system was moving along with the vehicle. Consequently $V_1(\psi)$ keeps shrinking and there is a time instant $t = t^*$ when the final configuration is such that $(x, y) \notin V_1(\psi)$. The following lemma and its proof contain the details of this constructions and its implications.

Lemma A.6 *For $\psi \in]0, \pi[$, $(x, y) \in V_1(\psi)$, $(d, \theta) = \text{polar}(x, y)$ and $r > 0$,*

$$C_\rho(d, \theta, \psi) \leq d + \rho F_1(\psi).$$

Proof. Let Ω_0 be a fixed coordinate frame. We define a moving coordinate frame $\Omega(t)$, $t \in \overline{\mathbb{R}}_+$, where $\Omega(0) = \Omega_0$. The origin of $\Omega(t)$, denoted as $O_{\Omega(t)}$ is defined by $O_{\Omega(t)} := [(\rho \sin t, \rho - \rho \cos t)]_{\Omega_0}$, where we use the notation $[a]_B$ to mean that the quantity a is to be interpreted in the B frame of reference. Along similar lines we define the unit vectors along the X and Y direction as:

$$\hat{x}_{\Omega(t)} = [\hat{x} \cos t + \hat{y} \sin t]_{\Omega_0}, \quad \hat{y}_{\Omega(t)} = [-\hat{x} \sin t + \hat{y} \cos t]_{\Omega_0},$$

where \hat{x} and \hat{y} are the unit vectors along the X and Y directions respectively in Ω_0 . We introduce the additional notations to interpret the quantities $(d, \theta) =$

polar(x, y) and ψ in different frames of reference.

$$\begin{aligned} x &= x_0 = [x]_{\Omega_0}, & x(t) &= [x]_{\Omega(t)}, & y &= y_0 = [y]_{\Omega_0}, & y(t) &= [y]_{\Omega(t)}, \\ d &= d_0 = [d]_{\Omega_0}, & d(t) &= [d]_{\Omega(t)}, & \theta &= \theta_0 = [\theta]_{\Omega_0}, & \theta(t) &= [\theta]_{\Omega(t)}, \\ \psi &= \psi_0 = [\psi]_{\Omega_0}, & \psi(t) &= [\psi]_{\Omega(t)}. \end{aligned}$$

Also, with a slight abuse of notations, let

$$\begin{aligned} V_1(\psi)_0 &= [V_1(\psi_0)]_{\Omega_0}, & V_1(\psi)(t) &= [V_1(\psi(t))]_{\Omega(t)}, \\ V_2(\psi)_0 &= [V_1(\psi_0)]_{\Omega_0}, & V_2(\psi)(t) &= [V_2(\psi(t))]_{\Omega(t)}. \end{aligned}$$

Let t^* be the first instant such that $(x(t^*), y(t^*)) \notin V_1(\psi)(t^*)$. Note that t^* is a function of θ_0 and ψ_0 , but we drop the arguments for convenience. From the definition it follows that

$$\psi(t) = \psi_0 - t, \quad \theta(t) = \theta_0 - t. \quad (\text{A.6})$$

Therefore,

$$\theta(t^*) = \frac{\psi(t^*)}{2} - \frac{\pi}{2} + \cos^{-1} \left(\frac{\sin(\psi(t^*)/2)}{2} \right). \quad (\text{A.7})$$

Solving equations (A.6) and (A.7), we get

$$\tan \left(\frac{t^*}{2} \right) = \frac{\sin(\psi_0/2) - 2 \sin(\psi_0/2 - \theta_0)}{\cos(\psi_0/2) + 2 \cos(\psi_0/2 - \theta_0)}.$$

Now $\psi_0 \in]0, \pi[$ implies that $\theta(t^*) > 0$ and $t^* \in]0, \pi[$, and in turn that $t^* = F_0(\psi_0, \theta_0)$, where F_0 is as defined before Theorem 2.4. Since $(x(t^*), y(t^*)) \notin V_1(\psi)(t^*)$, for $\psi_0 \in]0, \pi[$, it follows from Lemmas A.4 and A.5 that

$$\mathcal{C}_\rho(d(t^*), \theta(t^*), \psi(t^*)) \leq d(t^*) + \rho\psi(t^*) + 4\rho \cos^{-1} \left(\frac{\sin(\psi(t^*)/2)}{2} \right).$$

Also, it follows from the construction that $\mathcal{C}_\rho(d, \theta, \psi) = \mathcal{C}_\rho(d_0, \theta_0, \psi_0) \leq \rho t^* + \mathcal{C}_\rho(d(t^*), \theta(t^*), \psi(t^*))$. The triangle inequality implies $d(t^*) \leq d_0 + 2\rho \sin(t^*/2)$.

From these last equations and equations (A.6), we have

$$\mathcal{C}_\rho(d, \theta, \psi) = \mathcal{C}_\rho(d_0, \theta_0, \psi_0) \leq d_0 + \rho\psi_0 + 2\rho \sin\left(\frac{t^*}{2}\right) + 4\rho \cos^{-1}\left(\frac{\sin((\psi_0 - t^*)/2)}{2}\right).$$

Now, note that, for $t^* = F_0(\psi_0, \theta_0)$ and for $\alpha(\psi_0)$ being the half angle of $V_1(\psi)_0$, the supremum of

$$\psi_0 + 2 \sin\left(\frac{t^*}{2}\right) + 4 \cos^{-1}\left(\frac{\sin((\psi_0 - t^*)/2)}{2}\right)$$

over $\theta_0 \in]\frac{\psi_0}{2} - \alpha(\psi_0), \frac{\psi_0}{2} + \alpha(\psi_0)[$ is achieved at $\theta_0 = \frac{\psi_0}{2} - \alpha(\psi_0)$ and is equal to $F_1(\psi_0)$ as defined before Theorem 2.4. Since we are interested in the case when $(x_0, y_0) \in V_1(\psi)_0$, for $(d_0, \theta_0) = \text{polar}(x_0, y_0)$ we have

$$\sup_{(x_0, y_0) \in V_1(\psi)_0} \mathcal{C}_\rho(d_0, \theta_0, \psi_0) \leq d_0 + \rho F_1(\psi_0).$$

Reverting back to the original notations, i.e., $\psi_0 = \psi$ etc., we obtain the desired result. ■

From the definition, it follows that for $(x, y) \neq (0, 0)$, $(x, y) \in V_1(\psi)$ implies $(x, y) \in V_2^c(\psi)$. This observation along with part (ii) of Lemma A.3 and part (ii) of Lemma A.1 leads to the next lemma that we state without proof.

Lemma A.7 *For $\psi \in]0, \pi]$, $(x, y) \in V_1(\psi)$, $(d, \theta) = \text{polar}(x, y)$ and $\rho > 0$,*

$$\mathcal{C}_\rho(d, \theta, \psi) \leq d + \rho F_2(\psi).$$

Lemma A.8 *For $\psi \in]0, \pi[$, $(x, y) \in V_1(\psi)$, $(d, \theta) = \text{polar}(x, y)$ and $\rho > 0$,*

$$\mathcal{C}_\rho(d, \theta, \psi) \leq d + \rho \min\{F_1(\psi), F_2(\psi)\}.$$

Therefore, for $\psi \in]0, \pi]$, $(x, y) \in V_1(\psi)$, $(d, \theta) = \text{polar}(x, y)$ and $\rho > 0$,

$$\mathcal{C}_\rho(d, \theta, \psi) \leq d + \rho \max\{F_2(\pi), \sup_{\psi \in]0, \pi[} \min\{F_1(\psi), F_2(\psi)\}\} = d + \kappa\pi\rho.$$

Proof. The first statement follows from Lemma A.6 and Lemma A.7. This along with the consideration for the case of $\psi = \pi$ easily leads one to the second statement. ■

Similarly, one can prove that for $\psi \in]\pi, 2\pi[$, $(x, y) \in V_2(\psi)$, $(d, \theta) = \text{polar}(x, y)$ and $\rho > 0$, $\mathcal{C}_\rho(d, \theta, \psi) \leq d + \kappa\rho$. Combining this with Lemma A.5 and the last statement of Lemma A.8, we can state that for $\psi \in]0, 2\pi[$, $(x, y) \in \mathbb{R}^2$, $(d, \theta) = \text{polar}(x, y)$ and $\rho > 0$

$$\mathcal{C}_\rho(d, \theta, \psi) \leq d + \kappa\rho. \tag{A.8}$$

It now remains to prove a similar bound on $\mathcal{C}_\rho(d, \theta, 0)$ for which we state the following lemma.

Lemma A.9 For $(x, y) \in \mathbb{R}^2$, $(d, \theta) = \text{polar}(x, y)$ and $\rho > 0$,

$$\mathcal{C}_\rho(d, \theta, 0) \leq d + 2\pi\rho.$$

Proof. We recall the setup used for the proof of Lemma A.6. In accordance with that setup,

$$\mathcal{C}_\rho(d_0, \theta_0, 0) \leq d_0 + 2\rho \sin\left(\frac{\Delta t}{2}\right) + 4\rho \cos^{-1}\left(\frac{\sin(-\Delta t/2)}{2}\right),$$

where $\Delta t > 0$. The result follows by taking the limit as $\Delta t \rightarrow 0^+$ and reverting back to the original notations. ■

Lemma A.9 combined with equation (A.8) gives the proof for Theorem 2.4. It is easy to check that for $\psi \in]0, \pi[$, $F_1(\psi)$ is a monotonically increasing function of ψ and $F_2(\psi)$ is a monotonically decreasing function of ψ . Therefore, there exists a unique ψ^* such that $F_1(\psi^*) = F_2(\psi^*)$. By numerical calculations one can find that $\kappa \simeq 2.6575$.

A.3 Numerical Results

The length of the optimal Dubins path, $\mathcal{C}_\rho(d, \theta, \psi)$, was calculated for numerous sets of final configurations (d, θ, ψ) starting with an initial configuration of $(0, 0, 0)$ and a corresponding parameter k was evaluated for each of the instances according to the relation: $\mathcal{C}_\rho(d, \theta, \psi) = d + k\pi\rho$. The results suggest that the value of k is bounded by a quantity, say κ_{num} whose value is equal to $\frac{7}{3}$. Moreover, it appears that k achieves the value of κ_{num} only when the Dubins vehicle makes a transition from a state of the form $(0, 0, 0)$ to a state of the form $(0, 0, \pi)$ according to our setup. Hence, though we do not have an analytical proof to establish these empirical results exactly, our analysis gives a fairly good estimate of κ_{num} .

Appendix B

Projected Jacobi method

We briefly review here a parallel algorithm for the solution of a quadratic optimization problem. The technique is known as the *projected Jacobi method* in the literature on network flow control problems ([50], Section 3.4).

Consider the quadratic programming problem

$$\begin{aligned} & \text{minimize } \frac{1}{2}x^T Qx - b^T x, \\ & \text{subj. to } Ax \preceq c, \end{aligned}$$

where Q is a given $n \times n$ symmetric positive definite matrix, A is a given $m \times n$ matrix, and $b \in \mathbb{R}^n$ and $c \in \mathbb{R}^m$ are given vectors. The dual problem is

$$\begin{aligned} & \text{minimize } \frac{1}{2}y^T Fy + s^T y, \\ & \text{subj. to } y \succeq 0, \end{aligned}$$

for $F = AQ^{-1}A^T$ and $s = c - AQ^{-1}b$. If y^* solves the dual problem, then $x^* = Q^{-1}(b - A^T y^*)$ solves the primal problem.

For a step size parameter $\tau > 0$ and for $j \in \{1, \dots, n\}$, the projected Jacobi

iteration, when the j^{th} coordinate is updated, has the form

$$y_j(t+1) = \max \left\{ 0, y_j(t) - \frac{\tau}{f_{jj}} \left(s_j + \sum_{k=1}^m f_{jk} y_k(t) \right) \right\}, \quad (\text{B.1})$$

where f_{jk} is the j, k^{th} element of the matrix F . As discussed in [50], this algorithm converges to the global solution of the dual problem if the step size τ is chosen sufficiently small; in particular, convergence is guaranteed for $\tau = 1/m$.

Appendix C

On the Shostak's test

This section provides a proof for Theorem 6.8. The proof amounts to showing that if E is the edge set of a spanning tree T in $\mathcal{G}_{\text{di-disk}}(r_{\text{cmm}}, \nu(k)r_{\text{ctr}})$ at $\{(p_i, v_i)\}_{i \in \{1, \dots, n\}}$, then the control constraint set $\mathcal{U}_E^d(r_{\text{cmm}}, r_{\text{ctr}}, \nu(k)) \cdot \{(p_i, v_i)\}_{i \in \{1, \dots, n\}}$ is non-empty. We first consider a polytopic approximation of constraints (6.10) and (6.11). Among all possible choices, we use the conservative orthotope approximation that allows us to decouple the constraints into d independent sets of linear inequalities (one for each dimension). Then we use Shostak's theory to obtain sufficient conditions for the feasibility of these linear inequalities. For brevity, we drop the dependence of the quantities on t and we assume that the variables u_i are scalars, for all $i \in \{1, \dots, n\}$ and $t \geq 0$. The resulting sets of linear inequalities for one particular dimension are

$$\delta_{i,j}^l \leq u_i - u_j \leq \delta_{i,j}^u, \quad \text{and} \quad -\frac{r_{\text{ctr}}}{\sqrt{d}} \leq u_i \leq \frac{r_{\text{ctr}}}{\sqrt{d}}. \quad (\text{C.1})$$

where $-\nu(k)r_{\text{ctr}} \leq \delta_{i,j}^l \leq \delta_{i,j}^u \leq \nu(k)r_{\text{ctr}}$, for all $i, j \in \{1, \dots, n\}$ and $i \neq j$.

C.1 Shostak Theory

In this section we present Shostak's theory for feasibility of linear inequalities involving at most two variables, similar to the ones in (C.1). These ideas will then be used to prove Theorem 6.8. The notations used in [48] adapted to our case are presented next. Let u_0 be an auxiliary *zero variable* that always occurs with zero coefficient - the only variable that can do this. Without loss of generality, we can thus assume that all the inequalities in \mathcal{L} contain two variables. As a result of this, the inequalities in (C.1) can be succinctly written as

$$u_i - u_j \leq \delta_{i,j}, \quad \forall i, j \in \{0, \dots, n\}, \quad (\text{C.2})$$

where for all $i, j \in \{1, \dots, n\}$, $i \neq j$, $-\nu(k)r_{\text{ctr}} \leq \delta_{i,j} \leq \nu(k)r_{\text{ctr}}$ and for all $i \in \{1, \dots, n\}$, $\delta_{i,0} = \delta_{0,i} = \frac{r_{\text{ctr}}}{\sqrt{d}}$. Also implicit in this formulation is the relation that $\delta_{i,j} + \delta_{j,i} \geq 0$ for all $i, j \in \{0, \dots, n\}$ and $i \neq j$.

Let \mathcal{L} denote the system of inequalities in (C.2). We construct the graph $G(\mathcal{L})$ with $n + 1$ vertices and $2(2n - 1)$ edges as follows: (a) For each variable u_i occurring in \mathcal{L} , add a vertex i to $G(\mathcal{L})$. (b) For each inequality of the form $a_{i,j}u_i + b_{i,j}u_j \leq \delta_{i,j}$ in \mathcal{L} , add an undirected edge between i and j to $G(\mathcal{L})$, and label the edge with the inequality (see Figure C.1). It is easy to see the following relation between the spanning tree T in $\mathcal{G}_{\text{di-disk}}(r_{\text{cmm}}, \nu(k)r_{\text{ctr}})$ at $\{(p_i, v_i)\}_{i \in \{1, \dots, n\}}$ that is used to derive the constraints in the inequalities (C.2) and the graph $G(\mathcal{L})$: (a) The vertex set of $G(\mathcal{L})$ is the union of the vertex set of T and the auxiliary vertex 0 (b) For every edge $\{i, j\}$ in T , there are two edges between the vertices i and j in $G(\mathcal{L})$ (c) Additionally, $G(\mathcal{L})$ contains two edges between 0 and every other vertex i , for all $i \in \{1, \dots, n\}$.

To every edge represented by the inequality of the form $a_{i,j}u_i + b_{i,j}u_j \leq$

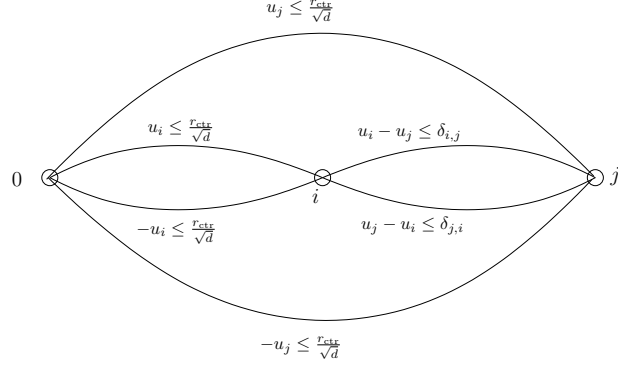


Figure C.1: Snippet of the graph $G(\mathcal{L})$ for the system of inequalities in (C.2)

$\delta_{i,j}$, we associate a triple $\langle a_{i,j}, b_{i,j}, \delta_{i,j} \rangle$. Note that $\langle b_{i,j}, a_{i,j}, \delta_{i,j} \rangle$ is also a triple associated with the same edge. Without loss of generality, consider a path of $G(\mathcal{L})$ determined by the vertices $\{1, 2, \dots, l+1\}$ and the edges $e_{1,2}, e_{2,3}, \dots, e_{l,l+1}$ between them. A triple sequence, P , associated with the path is defined as

$$\langle a_{1,2}, b_{1,2}, \delta_{1,2} \rangle, \langle a_{2,3}, b_{2,3}, \delta_{2,3} \rangle, \dots, \langle a_{l,l+1}, b_{l,l+1}, \delta_{l,l+1} \rangle,$$

where, for $1 \leq i \leq l$, $a_{i,i+1}u_i + b_{i,i+1}u_j \leq \delta_{i,i+1}$ is the inequality associated with the edge $e_{i,i+1}$. If $a_{i+1,i+2}$ and $b_{i,i+1}$ have opposite signs for $1 \leq i < l$, then P is called *admissible*.

Define $\langle a_P, b_P, \delta_P \rangle$, the *residue* of P , as

$$\langle a_P, b_P, \delta_P \rangle = \langle a_{1,2}, b_{1,2}, \delta_{1,2} \rangle \odot \langle a_{2,3}, b_{2,3}, \delta_{2,3} \rangle \odot \dots \odot \langle a_{l,l+1}, b_{l,l+1}, \delta_{l,l+1} \rangle,$$

where \odot is the associativity binary operator defined on triples by

$$\langle a, b, \delta \rangle \odot \langle a', b', \delta' \rangle = \langle \kappa a a', -\kappa b b', \kappa(\delta a' - \delta' b) \rangle,$$

$$\text{where } \kappa = a'/|a'|.$$

Intuitively, the operator \odot takes two inequalities and derives a new inequality by eliminating a common variable; e.g., $ax + by \leq \delta$ and $a'y + b'z \leq \delta'$ imply

$-aa'x + bb'z \leq -(\delta a' - \delta' b)$ if $a < 0$ and $b > 0$. Note that the signs of a_P and $a_{1,2}$ agree, as do the signs of b_P and $b_{1,2}$.

A path is called a *loop* if the initial and final vertices are identical. (A loop is not uniquely specified unless its initial vertex is given.) If all the intermediate vertices of a path are distinct, the path is *simple*. An admissible triple sequence P associated with a loop with initial vertex x is *infeasible* if its residue satisfies $a_P + b_P = 0$ and $\delta_P < 0$. A loop which contains an infeasible triple sequence is called an *infeasible loop*. Thus if $G(\mathcal{L})$ has an infeasible loop, the system of inequalities \mathcal{L} is unsatisfiable. However, the converse is not true in general. Next, we show how to extend \mathcal{L} to an equivalent system \mathcal{L}' such that $G(\mathcal{L}')$ has an infeasible simple loop if and only if \mathcal{L} is unsatisfiable.

For each vertex i of $G(\mathcal{L})$ and for each admissible triple sequence P with $a_P + b_P \neq 0$ associated with a simple loop of $G(\mathcal{L})$ and initial vertex i , add a new inequality $(a_P + b_P)u_i \leq \delta_P$ to \mathcal{L} . This new system \mathcal{L}' is referred to as the *Shostak extension* of \mathcal{L} . We now state the necessary and sufficient condition on the extended system of inequalities \mathcal{L}' for the satisfiability of the original system \mathcal{L} .

Theorem C.1 (Shostak's Theorem [48]) *Let \mathcal{L}' be the Shostak extension of \mathcal{L} . The system of inequalities \mathcal{L} is satisfiable if and only if $G(\mathcal{L}')$ contains no infeasible simple loop.*

C.2 Satisfiability test

In this section we use the Shostak criterion to derive conditions for the satisfiability of the inequalities in (C.2).

Lemma C.1 *Let \mathcal{L} be the system of inequalities of the form (C.2) obtained by considering pairwise neighbors in a spanning tree T in $\mathcal{G}_{\text{di-disk}}(r_{\text{cmm}}, \nu(k)r_{\text{ctr}})$ at $\{(p_i, v_i)\}_{i \in \{1, \dots, n\}}$. Then the Shostak extension of \mathcal{L} is itself.*

Proof. Consider a simple loop of $G(\mathcal{L})$ with the initial vertex $i \in \{0, 1, \dots, n\}$. Consider an admissible triple sequence P associated with the loop. Since $a_{i,j}, b_{i,j} \in \{-1, +1\}$, for all $i, j \in \{1, \dots, n\}, i \neq j$, and $a_{0,i}, a_{i,0}, b_{i,0}, b_{0,i} \in \{-1, 0, +1\}$, for all $i \in \{1, \dots, n\}$, the residue of P , $\langle a_P, b_P, \delta_P \rangle$, is such that $a_p + b_p = 0$. Hence, no new inequality must be added to obtain the Shostak extension of \mathcal{L} . ■

Lemma C.2 *Let \mathcal{L} be the system of inequalities of the form (C.2) obtained by considering pairwise neighbors in a spanning tree T of depth at most k in $\mathcal{G}_{\text{di-disk}}(r_{\text{cmm}}, \nu(k)r_{\text{ctr}})$ at $\{(p_i, v_i)\}_{i \in \{1, \dots, n\}}$. If $\nu(k) = \frac{2}{k\sqrt{d}}$, then there is no infeasible simple loop in $G(\mathcal{L})$.*

Proof. Looking at figure C.1 it is clear that there are two types of simple loops with admissible triple sequences in $G(\mathcal{L})$:

- (i) $\langle +1, -1, \delta_{i,j} \rangle, \langle +1, -1, \delta_{j,i} \rangle$ or $\langle -1, +1, \delta_{i,j} \rangle, \langle -1, +1, \delta_{j,i} \rangle$,
 where $i, j \in \{0, \dots, n-1\}$ and $\{i, j\}$ is an edge in T .

$$(ii) \left\langle 0, -1, \frac{r_{\text{ctr}}}{\sqrt{d}} \right\rangle, \left\langle +1, -1, \delta_{i_1, i_2} \right\rangle, \dots, \left\langle +1, -1, \delta_{i_{l-1}, i_l} \right\rangle, \left\langle +1, 0, \frac{r_{\text{ctr}}}{\sqrt{d}} \right\rangle \text{ or}$$

$$\left\langle 0, +1, \frac{r_{\text{ctr}}}{\sqrt{d}} \right\rangle, \left\langle -1, +1, \delta_{i_2, i_1} \right\rangle, \dots, \left\langle -1, +1, \delta_{i_l, i_{l-1}} \right\rangle, \left\langle -1, 0, \frac{r_{\text{ctr}}}{\sqrt{d}} \right\rangle,$$

where $i_l \in \{1, \dots, \zeta\}$ for all $l \in \{1, \dots, \zeta\}$ and $\{i_l, i_{l+1}\}$ is an edge in T .

The residue for the first set of loops is $\langle +1, -1, \delta_{i,j} + \delta_{j,i} \rangle$ or $\langle -1, +1, \delta_{i,j} + \delta_{j,i} \rangle$.

The feasibility condition is trivially satisfied by construction since $\delta_{i,j} + \delta_{j,i} \geq 0$.

For the second set of loops, the residue is:

$$\left\langle 0, -1, \frac{r_{\text{ctr}}}{\sqrt{d}} \right\rangle \odot \left\langle +1, -1, \delta_{i_1, i_2} \right\rangle \odot \dots \odot \left\langle +1, -1, \delta_{i_{\zeta-1}, i_\zeta} \right\rangle \odot \left\langle +1, 0, \frac{r_{\text{ctr}}}{\sqrt{d}} \right\rangle$$

$$= \left\langle 0, 0, 2\frac{r_{\text{ctr}}}{\sqrt{d}} + \sum_{l=1}^{\zeta-1} \delta_{i_l, i_{l+1}} \right\rangle,$$

or

$$\left\langle 0, +1, \frac{r_{\text{ctr}}}{\sqrt{d}} \right\rangle \odot \left\langle -1, +1, \delta_{i_2, i_1} \right\rangle \odot \dots \odot \left\langle -1, +1, \delta_{i_\zeta, i_{\zeta-1}} \right\rangle \odot \left\langle -1, 0, \frac{r_{\text{ctr}}}{\sqrt{d}} \right\rangle$$

$$= \left\langle 0, 0, 2\frac{r_{\text{ctr}}}{\sqrt{d}} + \sum_{l=1}^{\zeta-1} \delta_{i_l, i_{l+1}} \right\rangle.$$

In order to guarantee the feasibility of the second set of loops, we need that $2\frac{r_{\text{ctr}}}{\sqrt{d}} + \sum_{l=1}^{\zeta-1} \delta_{i_l, i_{l+1}} \geq 0$. We derive conditions for the worst case which occurs when the loop is written for the longest path in T , i.e., when $\zeta = k + 1$ and when $\delta_{i_l, i_{l+1}} = -\nu(k)r_{\text{ctr}}$, for all $l \in \{1, \dots, k\}$. In this case, there is no infeasible simple loop if and only if

$$2\frac{r_{\text{ctr}}}{\sqrt{d}} - k\nu(k)r_{\text{ctr}} \geq 0,$$

that is, if and only if $\nu(k) = \frac{2}{k\sqrt{d}}$. ■

Finally, the proof of Theorem 6.8 follows from Theorem C.1, Lemma C.1 and Lemma C.2.